SAPIENZA
UNIVERSITÀ DI ROMA

Ph.D. in Environmental and Evolutionary Biology
XXXIII Cycle

Macroecology of Global Alpine Vegetation

Candidate:
Riccardo Testolin

Tutors:
Fabio Attorre
Borja Jiménez-Alfaro

Faculty of Mathematical, Physical and Natural Sciences
Department of Environmental Biology
Curriculum in Botany

Sapienza University of Rome
Faculty of Mathematical, Physical and Natural Sciences
Department of Environmental Biology
Ph.D. in Environmental and Evolutionary Biology
Curriculum in Botany
XXXIII Cycle

MACROECOLOGY OF GLOBAL ALPINE VEGETATION

Riccardo Testolin

Tutors:
Fabio Attorre
Sapienza University of Rome, Italy
Borja Jiménez-Alfaro
University of Oviedo, Spain

Evaluators:
Manuela Winkler
University of Natural Resources and Life Sciences, Vienna, Austria
Manuel Steinbauer
University of Bayreuth, Germany

Cover: *Alexander von Humboldt, Mount Chimborazo, Vues des Cordillères, c. 1816.*

Table of contents

Summary

Alpine ecosystems, namely high-elevation habitats above the climatic treeline, are essential to human livelihoods and are among the environments with the highest vulnerability to anthropogenic climate change. Despite the overall agreement on the distribution and ecological features of terrestrial biomes, the actual extent and bioclimatic characteristics of alpine ecosystems worldwide are still uncertain. Furthermore, the patterns and drivers of plant diversity and functioning in alpine ecosystems are largely unknown at the global scale. This work represents a novel contribution to the delineation of macroecological patterns of global alpine biomes.

First, I created a map of global alpine areas by modelling regional treeline elevations at high spatial resolution using global forest cover data. I used this map in combination with global digital datasets to assess the climatic characteristics of alpine ecosystems and to evaluate patterns of primary productivity. Second, I assessed the global patterns of plant species richness in alpine ecosystems and the relative effect of environmental, geographical and historical factors at different spatial scales. To do so, I compiled a global dataset of alpine vegetation consisting of more than 8,900 plots, evaluated latitudinal patterns of regional and community richness and modelled them against different predictors estimated using global raster layers. Third, I assessed the functional variation of alpine vegetation and its relationship with evolutionary history and macroclimate. I filtered the abovementioned dataset of alpine vegetation plots based on the availability of functional trait and phylogenetic data. I assessed the functional trade-offs of alpine plant species and the functional dissimilarity of alpine vegetation across large geographic units with different dominant lowland vegetation, macroclimate, and evolutionary history. Finally, I modelled functional dissimilarity against environmental and phylogenetic dissimilarity.

I found that alpine biomes cover almost 3% of land outside Antarctica. Despite temperature differences across latitudes, these ecosystems converge below a sharp threshold of 5.9 °C and towards the colder end of the global climatic space. Below that temperature threshold, alpine ecosystems are influenced by a latitudinal gradient of mean annual temperature and are climatically differentiated by seasonality and continentality. This gradient delineates a climatic envelope of global alpine biomes. Although alpine biomes are similarly dominated by poorly vegetated areas, world ecoregions show strong differences in the productivity of their alpine belt irrespectively of major climate zones. Furthermore, in contrast with the well-known latitudinal diversity gradient, plant species richness of some temperate alpine regions in Eurasia is comparable to that of hyper-diverse tropical alpine ecosystems. This pattern is mainly explained by the current and past alpine area, isolation, and variation in soil pH among regions, while community richness depends on local environmental factors. Finally, plant species in alpine areas seemingly reflect the global variation of plant function and are mainly differentiated for their resource-use

strategies. The current macroclimate exerts a limited effect on alpine vegetation, mostly acting at the community level in combination with evolutionary history. Alpine vegetation is also functionally independent from the vegetation zones in which it is embedded, exhibiting strong functional convergence at the global scale.

Overall, despite their global distribution and apparent heterogeneity, alpine environments form a distinct group of functionally convergent biomes, strongly decoupled from lowland environments, and with a varied biogeographic history, whose legacy can still be observed on current diversity patterns which are locally refined by fine-scale factors.

Riassunto

Gli ecosistemi alpini, ossia gli habitat di alta quota al di sopra della linea degli alberi, sono essenziali per il sostentamento umano e sono tra gli ambienti più minacciati dal cambiamento climatico di origine antropica. Nonostante il consenso generale sulla distribuzione e le caratteristiche ecologiche dei biomi terrestri, l'effettiva estensione e le caratteristiche bioclimatiche degli ecosistemi alpini globali sono ancora incerte. Inoltre, i pattern e le cause della diversità vegetale e del funzionamento degli ecosistemi alpini globali sono in gran parte sconosciuti. Questo lavoro rappresenta un punto di partenza per la delineazione dei pattern macroecologici dei biomi alpini globali.

In primo luogo, ho creato una mappa delle aree alpine globali modellando le quote altimetriche regionali della linea degli alberi ad alta risoluzione spaziale, utilizzando dataset globali di copertura forestale. Ho usato questa mappa in combinazione con altri dataset digitali per valutare le caratteristiche climatiche degli ecosistemi alpini e determinarne i pattern di produttività primaria. In secondo luogo, ho analizzato i pattern globali di ricchezza delle specie vegetali negli ecosistemi alpini e l'influenza di fattori ambientali, geografici e storici a diverse scale spaziali. Per fare ciò, ho messo insieme un dataset globale della vegetazione alpina composto da oltre 8.900 plot, ho valutato i pattern latitudinali di ricchezza regionale e a livello di singole comunità vegetali, e li ho modellati rispetto a diversi predittori, stimati utilizzando raster globali. Infine, ho analizzato la variazione funzionale della vegetazione alpina in rapporto alla storia evolutiva e al macroclima. Per fare ciò, ho ulteriormente selezionato il suddetto dataset di plot di vegetazione alpina in base alla disponibilità di tratti funzionali e dati filogenetici. Ho valutato le strategie funzionali delle diverse specie di piante alpine e la dissimilarità funzionale della vegetazione tra grandi unità geografiche caratterizzate da diversa vegetazione planiziale dominante, macroclima e storia evolutiva. Infine, ho modellato la dissimilarità funzionale rispetto alle dissimilarità ambientale e filogenetica.

Dalle analisi effettuate, è emerso che i biomi alpini coprono quasi il 3% delle terre emerse al di fuori dell'Antartide. Nonostante le differenze di temperatura tra le diverse latitudini, questi ecosistemi convergono al di sotto di una soglia di 5,9 °C di temperatura media annua e verso l'estremità più fredda dello spazio climatico globale. Al di sotto di tale soglia di temperatura, gli ecosistemi alpini sono influenzati da un gradiente latitudinale di temperatura media annua e sono differenziati dal punto di vista climatico per stagionalità e continentalità. Questo gradiente distingue lo spazio climatico dei biomi alpini globali da quello dei biomi temperati, boreali e della tundra. Sebbene i biomi alpini siano similmente caratterizzati da aree scarsamente vegetate, le ecoregioni mondiali mostrano forti differenze nella produttività della loro fascia alpina indipendentemente dalle principali zone climatiche. Inoltre, in contrasto con il ben noto gradiente di diversità latitudinale, la ricchezza di specie vegetali alpine di alcune regioni temperate dell'Eurasia è paragonabile

a quella degli ecosistemi alpini tropicali. Questo pattern è principalmente spiegato dall'estensione attuale e passata delle aree alpine, dall'isolamento e dalla variazione del pH del suolo tra le diverse regioni, mentre la ricchezza delle comunità vegetali dipende da fattori ambientali locali. Infine, le specie vegetali delle aree alpine sembrano riflettere la variazione funzionale globale di tutte le piante e sono principalmente differenziate per le loro strategie di utilizzo delle risorse. Il macroclima attuale esercita un effetto limitato sulla vegetazione alpina, agendo per lo più a livello delle singole comunità vegetali e in combinazione con la storia evolutiva. Inoltre, la vegetazione alpina globale è funzionalmente indipendente dalle zone di vegetazione in cui è integrata, mostrando una forte convergenza funzionale.

Nel complesso, nonostante la loro distribuzione globale e l'apparente eterogeneità, gli ambienti alpini formano un gruppo distinto di biomi funzionalmente convergenti, fortemente disaccoppiati dagli ambienti di pianura e con una storia biogeografica varia, la cui eredità può ancora essere osservata sugli attuali pattern di diversità che sono ulteriormente rifiniti da fattori locali.

Background

Ecosystems in peril

In a special report published in 2019, the Intergovernmental Panel on Climate Change (IPCC) warned about the threats that the current climate crisis is posing to high mountain areas worldwide (IPCC 2019). Located above the elevational treeline, these ecosystems are home to more than 10,000 plant species, many of which are endemics (Körner 2003), and are already impacted by land use change (Nagy and Grabherr 2009). High mountain areas also supply fresh water to more than half of the human population (Goulden and Bales 2014, Pomeroy 2015) and may stock up to 1% of the global terrestrial carbon pool (Körner 1995). The melting of glaciers, disruption of snowfall patterns and thawing of permafrost triggered by climate change have already induced range shifts of plant communities (Morueta-Holme et al. 2015, Evangelista et al. 2016, Freeman et al. 2018, Liang et al. 2018, You et al. 2018, He et al. 2019), bringing high mountain specialists on the brink of local extinction (Panetta et al. 2018). If global warming exceeds 1.5 °C relative to preindustrial levels – which might happen by 2024 (WMO 2020) – it will have major repercussions on the vegetation in high mountain areas (Hoegh-Guldberg et al. 2018) affecting several ecosystem services and threatening regional and global biodiversity (IPCC 2019). Therefore, understanding the patterns of plant diversity in high mountain environments is key to planning conservation initiatives aimed at mitigating adverse effects of global change on these ecosystems and support the livelihoods of human mountain populations.

A mountain of words

In this thesis, I use the word *alpine* to indicate areas above the natural elevational treeline (Körner 2003). Although the term was coined after the European Alps, alpine ecosystems extend well beyond these mountains to encompass boreal, temperate and tropical mountain ranges worldwide (Körner 2003, Quinn 2008, Nagy and Grabherr 2009).

Therefore, the word *alpine* may sound simplistic or even inappropriate to describe such a diverse set of mountain environments, characterised by different climates and vegetation formations (Faber-Langendoen et al. 2016). Furthermore, it has been suggested that using the name of a European mountain range to describe such far-apart areas in different continents might reinforce the feeling of a Eurocentric perspective of the natural world, which is an ongoing issue in current ecology (Baker et al. 2019).

Several authors proposed alternative terms to describe global environments above the treeline, but new terms are still far from being widely accepted. One example is *páramo*, used to define high mountain habitats in the Northern Andes – also called *high Andean* (Simpson 1983) – or tropical montane vegetation above the treeline in general (Walter 1973, Lauer 1981, Monasterio 1986). However, this word is strictly bound to intertropical regions and thus not suited to describe high mountain vegetation globally. Moreover, *páramo* is still a term of European origin as it was employed by Spanish tribes to identify flat plains in Castilian open ecosystems, and then applied to Northern Andean environments by early Spanish explorers (Luteyn 1999). Other terms are too broad in concept – e.g. *oreophytic* (Agakhanjanz and Breckle 1995) – and could be mistakenly used to describe mountain vegetation in general, while alternative wordings that refer to the elevational characteristics of naturally treeless mountain areas (e.g. *high-altitude, -elevation, -mountain, -montane*) would fail to represent low elevation treeless areas found at higher latitudes (Körner 2003, Quinn 2008, Nagy and Grabherr 2009).

In defence of the use of *alpine*, one could recall its etymology. Indeed, the word has a pre-Roman origin, with *alp* or *alb* indicating mountain in general (Körner 2003), that predates the Latin *Alpes* after which the European range is named (Quinn 2008). Therefore, while acknowledging that global ecosystems above the elevational treeline can be climatically and physiognomically different from those of the European Alps, naming them *alpine* seems an acceptable compromise to avoid misinterpretations and allow meaningful comparisons.

Open issues in global alpine research

The following paragraphs outline the main knowledge gaps in global alpine vegetation research, that have been addressed in Chapters 1, 2 and 3 of this thesis.

Extent and bioclimatic characteristics of alpine ecosystems

Globally, terrestrial biomes have traditionally been defined based on their dominant vegetation and macroclimate (Mucina 2019). Alpine environments, where trees and tall shrubs are replaced by prostrate growth forms in response to low temperatures and low soil nutrients (Körner 2003, Körner and Paulsen 2004, Paulsen and Körner 2014), form a

continuum of grassland and dwarf-shrubland habitats occurring above the natural treeline in all continents except Antarctica. The treeline itself represents one of the most abrupt ecological transitions in plant form (Körner 2003), and can be clearly identified in most non-arid mountains ranges.

Despite the widespread distribution of alpine environments, their placement among global biomes is still uncertain. First classifications of alpine ecosystems often related them to other pre-defined biomes. For instance, Holdridge (1947) developed a temperature-based system equating alpine and nival environments to frigid and polar areas, thus pooling together arctic and alpine tundra. However, despite the apparent analogies between arctic and alpine environments (e.g. low mean annual temperatures, absence of trees and abundance of rocky habitats), differences outnumber similarities. As arctic areas are cast into complete darkness or daylight for several months per year, their daily temperature amplitudes are narrow, while seasonal variations in temperature and incoming solar radiation are much greater than in alpine areas, especially if compared to the tropical ones (Körner 2003, Quinn 2008). Moreover, alpine areas lack the continuous, thick layer of permafrost typical of arctic environments, which prevents soil drainage favouring the greater abundance of wet meadows at higher latitudes (Quinn 2008). Due to their complex topography, alpine areas are also characterised by a variety of microclimates while flat arctic environments are more homogeneous in this respect (Quinn 2008). Finally, alpine areas at high elevation are characterised by lower CO_2 and O_2 concentrations than lowland arctic environments, with effects on plant physiological adaptations (Körner 2003, Quinn 2008).

Almost thirty years after Holdridge, Whittaker described arctic and alpine biome types in his characterisation of world biomes (Whittaker 1975), distinguishing latitudinal and elevational ecoclines in the transition from forests to tundra environments. In a similar way, Walter (Walter and Box 1976) separated latitudinal *zonobiomes* from elevational alpine *orobiomes*, although it failed to recognise the analogies among different alpine regions. Indeed, as per the authors, alpine orobiomes are simply members of the total sequence of altitudinal belts and, in mountains located in different climate zones, "alpine belts are just as distinct as the alpine belt is from other altitudinal belts" (p.77, Walter and Box 1976). Later, Olson et al. (2001) identified the *montane grasslands and shrublands* habitat type, which included tropical and subtropical mountains but excluded most of temperate and boreal alpine regions, that were encompassed by other habitat types. For example, the European Alps were entirely classified as *temperate conifer forests*, while the Scandes were included in the *tundra* habitat type together with Northern Siberia and Arctic islands. Recently, Faber-Langendoen et al. (2016) distinguished arctic and alpine vegetation formations and split the latter into *tropical high montane scrub and grassland* and *temperate and boreal alpine vegetation*. However, the authors did not classify páramo and puna vegetation as alpine and instead included them in the *tropical montane grassland and shrubland* formation, due to the greater abundance of mesomorphic grasses and higher

vegetation cover in these environments (Faber-Langendoen et al. 2016). Yet, the same authors called for a review of the placement of páramo and puna within the formations system to achieve consistency in the definition of global alpine zones (Faber-Langendoen et al. 2016). In the second edition of the global ecosystem typology recently published by the International Union for Conservation of Nature (IUCN), global alpine ecosystems are also distinguished between tropical and temperate, although boreal and temperate alpine deserts are equated to polar environments (Keith et al. 2020).

Due to these inconsistencies in the definition of global alpine ecosystems, an empirical characterisation of their ecological properties and their relationships with other terrestrial biomes is still missing. Indeed, most studies aimed at describing alpine bioclimate are limited to continental (Körner et al. 2003) or regional scales (Noroozi and Körner 2018) while current estimates of the global alpine area are either based on average regional treeline elevations and expert evaluation (Körner 2003) or coarse-resolution delineations of altitudinal belts using on global climatic datasets (Körner et al. 2011). This knowledge gap has so far hindered any comparative analysis of global alpine ecosystems in relation to their bioclimatic patterns.

Patterns of vascular plant taxonomic diversity

Current efforts in alpine research are mainly oriented at monitoring the response of alpine plant communities to climate change (Gottfried et al. 2012, Pauli et al. 2012, Steinbauer et al. 2018). Notably, the Global Observation Research Initiative in Alpine environments (GLORIA) is aimed at quantifying the changes in vegetation patterns of mountain summits worldwide through the establishment and long-term observation of permanent plots, following a standardised sampling protocol (Pauli et al. 2015). Albeit ideal to monitor temporal dynamics at localised spots, this approach is not aimed at capturing the diversity of vegetation types characterizing different alpine regions, but mountain summits alone. Thus, due to the current lack of a comprehensive database of global alpine biodiversity and methodological limitations posed by the use of published floras (Körner 1995, Muellner-Riehl et al. 2019) a global representation of vascular plant diversity in alpine habitats is still missing, and so is the knowledge of its global drivers.

Species diversity patterns are known to reflect the complex interplay of historical and contemporary factors acting on speciation, extinction and colonisation rates (Chase 2012, Graham et al. 2014). One of the most acknowledged global biodiversity pattern is the latitudinal diversity gradient (Hillebrand 2004), according to which species diversity increases from the poles to the equator. Among the possible explanations to such pattern, the species-energy hypothesis states that the greater available metabolic energy in tropical areas can sustain larger populations, thus reducing extinction rates (Wang et al. 2009, Lomolino et al. 2017). A similar diversity pattern is assumed to emerge in global alpine areas (Körner 1995). However, this assumption is based on a handful of regional alpine

floras (Körner 1995) and could hardly be explained by a larger energy input around the equator, which is in fact rather uniform across global alpine areas regardless of latitude (Körner 2003).

Recent studies have shown that, besides variation in current climate and topography, other forces determine diversity pattern in mountains, including geology, climatic fluctuations and biogeographic factors (Antonelli et al. 2018, Muellner-Riehl et al. 2019, Rahbek et al. 2019a). These drivers represent a *historical sieve* that constrains species pools at large spatial scales, and is also expected to affect global patterns of alpine plant diversity (Körner 1995). Current alpine floras represent a mixture of species originated by the upward movements and evolution of taxa from adjacent lowland floras, new evolutionary lines from allopatric speciation, and long-distance migrations through habitat corridors during past glaciations (Billings 1974, Körner 2003, Hörandl and Emadzade 2011). Previous studies have shown that periodical expansions and contractions of alpine areas during Pleistocene glacial cycles affected the diversity of plant species in alpine regions (Hewitt 2000, McGlone et al. 2001, Harris 2007, Flantua et al. 2019), in a similar fashion to vascular plant species in global oceanic islands (Weigelt et al. 2016). Indeed, alpine areas form fragmented archipelagos of *sky islands* surrounded by lowland environments that could prevent the dispersal of alpine plants (McCormack et al. 2009). According to the ecological principles of the species-area relationship (Lomolino 2000) and of the theory of island biogeography (MacArthur and Wilson 1967), the extent and isolation of alpine habitats – together with their changes with glacial cycles (Fernández-Palacios et al. 2016) – could have affected current patterns of plant diversity through differential rates of colonisation, speciation and extinction of plants (Heaney 2000, Steinbauer et al. 2016). However, whether these assumptions apply to global diversity patterns of alpine vegetation, is still debated (Nagy and Grabherr 2009).

Functional variation in alpine vegetation

The functioning of plants, through resource acquisition and transformation, determines the quality and quantity of habitats available to other organisms and plays a key role in regulating the Earth's climate (Lenton et al. 2012, Garnier et al. 2016). Understanding these functions, their drivers and the way they are combined across different spatial scales represents one of the challenges of modern ecology (Garnier et al. 2016) and can assist our understanding of the impacts of global changes on ecosystem functions and services (Bruelheide et al. 2018).

The spectrum of plant adaptations can be quantified using functional traits, defined as measurable features affecting the performance of species in their environment (McGill et al. 2006, Garnier et al. 2016). A small set of traits can be used to explain different aspects of plant life (Grime 1974, Díaz et al. 2016, Bruelheide et al. 2018). At large spatial scales, macroclimate selects the species pools that are further refined at the regional and

community level by local abiotic and biotic factors (Zobel 2016, Mucina 2019). As a consequence, the total set of functional traits in a given climatic region, is subject to environmental filtering and biotic interactions that select local species assemblages with favourable combinations of traits (Mucina 2019).

Despite the global distribution of alpine ecosystems and their floristic differences, the functional characteristics of their dominant vegetation appear to converge throughout world mountains (Körner 2003). Indeed, alpine vegetation is mainly represented by stress-tolerant species with resource-conservative trait syndromes (Körner et al. 1989, Stanisci et al. 2020). The most common growth forms in alpine ecosystems are short stature plants forming dwarf shrublands near the treeline, followed by graminoids at higher elevations (Poaceae, Cyperaceae, Juncaceae), and sparse prostrate vegetation in proximity of mountain tops (Körner 2020). These growth forms reflect the functional adaptations to the environmental characteristics of global alpine environments, characterised by low temperatures, short growing season and limited nutrient availability (Körner 2003, 2020, Stanisci et al. 2020). Yet, at the global scale, alpine vegetation shows a certain degree of functional divergence, with some growth forms disproportionally abundant in certain regions (e.g. evergreen dwarf shrubs in boreal ranges or sclerophyllous species in Mediterranean mountains) or unique to specific alpine areas, such as giant rosettes in tropical mountains (e.g. *Espeletia* and *Dendrosenecio*) (Nagy et al. 2003). One possible explanation is that evolutionary processes, constrained by long-term isolation of major landforms (Chaboureau et al. 2014), created biogeographic realms with shared history in terms of phylogenetic origin (Holt et al. 2013, Daru et al. 2017, 2018) which, in combination with macroclimate, defined the functional characteristics of vegetation. Similar processes may apply to global mountain ecosystems, as they are embedded in different vegetation zones (Walter and Box 1976), which are in turn characterised by distinct evolutionary history and species pools (Mucina 2019). Yet, the extent to which functional adaptations of alpine vegetation reflect the historical legacy of different alpine regions is unknown, and so is its overall degree of functional variation.

Aim of the thesis

Despite their ubiquity and relevance to global biodiversity, we still lack empirical evidence of the spatial distribution of global alpine ecosystems and their bioclimatic characteristics. Furthermore, although countless researchers have contributed to collecting plant species data all over the world, a comprehensive representation of the global patterns and drivers of alpine vascular plant diversity is still missing. This thesis combines a wealth of field data collected in situ with remote sensing data and information from functional traits databases to provide a first overview of the global patterns of alpine ecosystems by answering the following questions:

1) What is the spatial distribution and extent of alpine ecosystems worldwide? How are alpine ecosystems related to major lowland biomes as for their bioclimatic patterns? How do alpine ecosystems compare to one another as for their primary productivity? (Chapter 1; page 20).
2) What are the global latitudinal patterns of alpine plant species richness? What is the relative influence of environmental, geographical and historical factors in driving such patterns? How do these patterns and drivers change across different spatial scales? (Chapter 2; page 36).
3) What are the functional trade-offs of vascular plant species in global alpine ecosystems? How does functional variation change in different vegetation zones, climatic groups and biogeographic realms? What is the relative contribution of macroclimate and evolutionary history in shaping the functional variation of alpine plant communities? (Chapter 3; page 54).

Chapter 1
Global distribution and bioclimatic characterisation of alpine biomes

Testolin R., Attorre A., Jiménez-Alfaro B. 2020. Global distribution and bioclimatic characterization of alpine biomes. *Ecography* 43: 779–788.
https://doi.org/10.1111/ecog.05012

Abstract

Although there is a general consensus on the distribution and ecological features of terrestrial biomes, the allocation of alpine ecosystems in the global biogeographic system is still unclear. Here, we delineate a global map of alpine areas above the treeline by modelling regional treeline elevation at 30 m resolution, using global forest cover data and quantile regression. We then used global datasets to 1) assess the climatic characteristics of alpine ecosystems using principal component analysis, 2) define bioclimatic groups by an optimised cluster analysis and 3) evaluate patterns of primary productivity based on the normalised difference vegetation index. As defined here, alpine biomes cover 3.56 Mkm2 or 2.64% of land outside Antarctica. Despite temperature differences across latitude, these ecosystems converge below a sharp threshold of 5.9 °C and towards the colder end of the global climatic space. Below that temperature threshold, alpine ecosystems are influenced by a latitudinal gradient of mean annual temperature and they are climatically differentiated by seasonality and continentality. This gradient delineates a climatic envelope of global alpine biomes around temperate, boreal and tundra biomes as defined in Whittaker's scheme. Although alpine biomes are similarly dominated by poorly vegetated areas, world ecoregions show strong differences in the productivity of their alpine belt irrespectively of major climate zones. These results suggest that vegetation structure and function of alpine ecosystems are driven by regional and local contingencies in addition to macroclimatic factors.

Introduction

The knowledge of the extent and climatic characteristics of terrestrial biomes, further linked to their functional aspects (e.g. productivity), is key to understanding ecological and biogeographical phenomena (Mucina 2019). Among terrestrial environments, alpine ecosystems (i.e. high-elevation habitats above the climatic treeline) are the only biogeographic unit represented across all continents and latitudes (Körner 2003); they are characterised by a varied history of climatic changes and strong microhabitat differentiation (Körner 2003); they also contain global biodiversity hotspots – e.g. the tropical Andes (Myers et al. 2000) – and support about 10 000 plant species as a whole, many of which are endemics (Körner 2003). Alpine ecosystems supply fresh water to more than half of the human population (Pomeroy 2015) and may stock up to 1% of the global terrestrial carbon pool (Körner 1995); they are also home to the habitats most threatened by land use (Nagy and Grabherr 2009) and anthropogenic climate change (Hughes 2000).

Despite the relevance of alpine ecosystems to global biodiversity, their biogeographic delineation in the biome system is still unclear. The definition of world biomes has been traditionally based on vegetation physiognomy and macroclimate for grouping areas with similar dominant ecosystems (Mucina 2019). Alpine ecosystems, which are characterised by the absence of trees in response to low temperatures, form a continuum of shrubland and grassland habitats occurring above the climatic treeline across latitudes. First attempts of characterizing alpine ecosystems were based on their relationships with pre-defined biomes. For example, the temperature-based system of Holdridge (1947) linked the alpine and nival altitudinal belts to the frigid and polar zones, encompassing all that is widely known as arctic and alpine tundra. In his influential characterisation of world biomes, Whittaker (1975) acknowledged the differences between arctic and alpine biome types by identifying two temperature-related ecoclines (i.e. latitudinal and altitudinal) involved in the transition from forest to treeless tundra. Similarly, Walter's classification of terrestrial ecosystems (Walter and Box 1976) separated latitudinal zonobiomes from alpine orobiomes. In a different biogeographical context, Olson et al. (2001) identified the *montane grasslands and shrublands* habitat type encompassing tropical and subtropical mountain ranges. Yet, this classification is not based on vegetation patterns and left out temperate and boreal alpine regions of the northern hemisphere, that were either included in forest biomes or arctic tundra. Similarly, Faber-Langendoen et al. (2016) defined *tropical montane and high montane grasslands and shrublands* in a recent classification of world vegetation formations, separating these areas from the non-tropical alpine tundra.

Despite large divergences in the interpretation of alpine ecosystems, an empirical characterisation of the ecological or functional properties of the global alpine belt and its relationships with terrestrial biomes is missing. Most studies are limited to continental (Körner et al. 2003) or regional scales (Noroozi and Körner 2018) while current estimates of the global alpine area are either based on average regional treeline elevations and expert

evaluation (Körner 2003) or coarse resolution delineation of altitudinal belts (Körner et al. 2011). This knowledge gap has so far hindered any comparative analysis of alpine ecosystems in relation to their biogeographical patterns, despite their well-known similarities in dominant vegetation (Körner 2003). Recent developments in publicly accessible cloud computing platforms like Google Earth Engine (Gorelick et al. 2017) and the increasing availability of large-scale datasets are facilitating the exploration of natural patterns at the global scale (Hansen et al. 2013, Bastin et al. 2017, 2019), allowing us to answer long standing questions about the biogeography of alpine ecosystems.

Here, we developed a method for estimating the global extent of alpine areas based on empirical data and a high-resolution map of their distribution. We then characterised alpine ecosystems to assess their bioclimatic and productivity patterns through global climatic variables and the normalised difference vegetation index (NDVI) from global to regional scales. Our first aim was to re-evaluate prevailing questions about the distribution of alpine ecosystems, such as 1) what is the spatial distribution and extent of alpine ecosystems worldwide? 2) How are alpine ecosystems related to major lowland biomes as for their bioclimatic and productivity patterns? By producing the first empirical dataset of global alpine biomes, our second aim was to advance their comparative ecology and to provide a spatial tool that will assist future mountain research across disciplines.

Material and methods

Study area

Our study focuses on global mountain regions with an alpine zone, i.e. a vegetation belt above the climatic treeline (Körner et al. 2011). Arctic or subarctic regions dominated by treeless vegetation (Baffin Island, Greenland, Iceland, Svalbard and Novaya Zemlya) were excluded because the arctic tundra, although analogous to the alpine zone, is not defined by elevational gradients (Quinn 2008) and represents a different zonobiome (Walter and Box 1976). We used a global inventory of mountain areas based on topographic ruggedness (Körner et al. 2017) and a raster of climatic belts (Körner et al. 2011) to obtain a preliminary GIS layer of mountain polygons that contained the *upper montane* belt and at least one pixel of the *alpine* belt. The workflow is illustrated in Appendix 1 Figure A1.1. This step excluded mountain polygons where the alpine belt is absent or scarcely represented, which was necessary to optimise our workflow. Nevertheless, we verified that our study area encompasses the majority of known alpine areas in all continents. Our working dataset included 345 mountain regions covering nearly 11 Mkm2 representing mid- to high-altitude mountain areas worldwide, thus ranging from mountain forests to the highest unforested summits.

Identification of alpine areas

We used the Google Earth Engine computing platform (Gorelick et al. 2017) to select alpine areas within the mountain polygons. First, we deleted forest areas as they were mapped at the global scale using satellite images from the year 2015 at 30 m spatial resolution (Hansen et al. 2013) (Appendix 1 Figure A1.1). All pixels with forest cover $>$ 0% were removed. As the resulting mask contained many scattered unforested pixels, we applied a low pass filter to reduce high frequency information by performing a linear convolution using 11 × 11 pixels moving window. We then upscaled the image to 50 m spatial resolution, to reduce its size while keeping most of the detail, and considerably speed up the following operations. The resulting raster, representing unforested mountain areas, was vectorised. At this spatial resolution, we were not able to isolate any unforested area in Mont Cameroun (Cameroon), Virunga Mountains (Democratic Republic of the Congo, Rwanda and Uganda), Hidaka-sanmyaku (Japan) and Kaimanawa Mountains (New Zealand) (Appendix 1 Figure A1.2), despite being included in the initial dataset. Thus, the following operations have been carried out on a set of 341 mountain regions. We also removed unforested area polygons smaller than 5 km2 to avoid the inclusion of many scattered patches of alpine and sub-alpine habitats in large mountain ranges that would have considerably increased computation time, with the only exception of Mount Meru (Tanzania) and Ruwenzori (Democratic Republic of the Congo, Uganda), whose unforested areas were kept despite all being smaller than 5 km2.

At this point the dataset consisted of unforested areas within and above the upper montane belt that may include, besides the alpine zone delimited by the climatic treeline, other mountain areas where the original forest was suppressed either by anthropogenic disturbance, local environmental or topographic conditions (Holtmeier 2009). To retain alpine areas only, we modelled regional treeline elevation with linear quantile regression using R software (R Core Team) and the *quantreg* package (Koenker 2018), based on equally spaced points sampled every 5 km along the unforested polygon boundaries using QGIS 2.18 (Development 2016) (Appendix 1 Figure A1.1). For each point we extracted elevation and northness (cosine of aspect) from the SRTM-3 global digital elevation model (DEM) (Farr et al. 2007, NASA and JPL 2013). In mountains located above 60° latitude, thus not covered by the SRTM-3 DEM, elevation and northness values were derived from the ASTER-2 global DEM (NASA/METI/AIST/Japan Spacesystems and U.S./Japan ASTER Science Team 2009). For each mountain range we modelled the 99th percentile of the distribution of forest border elevation values measured at the point locations, controlling for northness. We opted for the 99th percentile by analogy with the concept of treeline, defined as the line that connects the highest patches of forest – in our case forest pixels – within a series of slopes of similar exposure (Körner 2003). In mountain ranges spanning more than 5 degrees in latitude, latitude was also included in the model. We chose 5 degrees as a reasonable interval at which latitudinal changes of treeline elevation likely override possible disturbance-induced treeline shifts. To avoid singularities

and ensure model convergence, we added random noise constrained between −0.5 and 0.5 m to elevation values.

Our methodology relies on the assumption that, within each mountain region, the remaining traces of the climatic treeline can be used to model its elevation across the whole region. However, some arid mountain ranges naturally lack a treeline because low water availability prevents the establishment of trees regardless of temperature (Körner 2012). In our dataset, this was the case for some ranges in the driest parts of South America (21 ranges) and central Asia (34 ranges). To consistently identify the potential treeline elevation in these regions and ensure the continuity of alpine areas extent across adjacent mountains, we applied the treeline elevation quantile regression models derived from the closest neighbouring mountain range, controlling for local northness and latitude. As an example, we used the model for Himalaya to estimate the treeline elevation of the surrounding treeless mountains by applying it to each DEM, accounting for the difference in latitude. Similarly, for the arid central Andean mountains, treeline elevation was estimated by applying a hybrid model fitted using the points sampled along the unforested areas polygons of the closest surrounding mountain ranges (Cordillera Oriental Peru Bolivia Chile and the Cordillera Frontal) thus assuming a linear decrease in treeline elevation between the two. A complete list of the treeless mountain ranges for which such procedure was applied, together with the corresponding neighbouring ranges whose treeline model was used, is reported in Appendix 1 Table A1.1.

Finally, we extracted the area above the modelled treeline elevation within each mountain range, obtaining an estimate of the global extent of alpine ecosystems (Appendix 1 Figure A1.1). Given the high spatial resolution of the obtained alpine layer, we again filtered out polygons smaller than 5 km2 to reduce graininess and streamline further operations. To visualise the global patterns of the estimated treeline elevations, we calculated their mean for each mountain range by sampling equally spaced points every 20 km along the alpine polygons' boundaries and extracting their elevation in Google Earth Engine using the same DEMs described above. We applied a weighted loess fit with span = 0.4 to the mean values of treeline elevation along latitudes to describe the global pattern and to allow visual comparison with the treeline model compiled by Körner (2003) using worldwide field observations. To account for the uneven latitudinal distribution of mountain ranges (i.e. nonequal variance of treeline elevation along latitude), a greater weight was assigned to the mountains at under-represented latitudes. All distances were calculated in equidistant cylindrical Plate Carrée projection, while areas were calculated in equal area pseudo-cylindrical Eckert IV projection.

Bioclimatic characterisation

To outline the climatic space occupied by the mapped alpine ecosystems, we overlapped the values of mean annual temperature and annual precipitation with the widely

recognised Whittaker's biomes classification (Whittaker 1975), using the global climatic dataset CHELSA (Karger et al. 2017) at 30 arc-sec spatial resolution. At each pixel location, we also extracted elevation values from SRTM-3 and ASTER-2 global digital elevation models upscaled to 30 arc-sec resolution. To evaluate the climatic differences among different alpine ecosystems, we ran a principal component analysis (PCA) on 19 centred and scaled bioclimatic variables (Karger et al. 2017). The variables with the greatest factor loadings were used to interpret the PCA axes. To describe the climatic variation among global alpine ecosystems and delineate alpine regions of similar climatic conditions, we performed a cluster analysis based on the first four PCA axes, which captured almost 90% of the variance. We used Euclidean distances on PCA axes to overcome the strong multicollinearity of some of the original environmental variables and exploit their orthogonal properties (Weigelt et al. 2013). Prior to clustering, PCA axes were multiplied by the square root of their eigenvalues to weight their influence on the classification outcome according to their importance.

We employed the clustering large applications (CLARA) algorithm (Kaufman and Rousseeuw 1990), an extension of the k-medoids method for large datasets, using the *clara* function in the R package *cluster* (Maechler et al. 2018). This method considers a subset of the data with fixed size and applies the k-medoids algorithm to generate an optimal set of medoids for the sample. The quality of the resulting medoids is measured by the average dissimilarity between every object in the entire data set and the medoid of its cluster. The sampling and clustering process are then repeated for a fixed number of subsets of the entire dataset and the final clustering results correspond to the set of medoids with the lowest average dissimilarity. This method requires a specified number of clusters (k) in advance. For this, we explored a limited number of clusters, from 2 to 10, to facilitate presentation and interpretation of results. Given the size of our dataset (almost 6 million records), we adopted a heuristic approach for the choice of the best k. We ran the *clara* function on 100 random subsets of 1000 cells for each k and replicated the process 100 times. Each time, the best k was based on the highest average silhouette width. Finally, among the runs with k = best k, we chose the one with the greatest average silhouette width.

To further assess the reliability of the k-medoids-based clustering, we performed a hierarchical clustering using the first four weighted PC axes of a subset of 30 000 records. To make sure that the sample captured most of the climatic variability of alpine ecosystems, we stratified it equally among three latitudinal belts in each hemisphere: tropical (0–23.5°), temperate (23.5–50°) and subpolar ($>$ 50°). The clustering was performed using the *hclust* function of the *fastcluster* package (Müllner 2013), with the Ward2 clustering method. To assess the best number of k using this method, we repeated the process for 100 subsets and recorded the average silhouette width when cutting the

tree from 2 to 10 clusters. Then, we cut the dendrogram in order to get k = best k. Finally, we compared the two clustering outcomes using PC biplots and an alluvial plot.

Primary productivity

We estimated the primary productivity of alpine ecosystems based on the normalised difference vegetation index (NDVI), an indirect measure of vegetation cover and biomass related to the physical properties of plants (Cihlar et al. 1991, Pettorelli et al. 2005). Despite its limitations, the NDVI has been widely used as a proxy for ecosystem properties including global grassland productivity (Gao et al. 2016) and above ground biomass in the alpine belt (Liu et al. 2017). To minimise the problems related to single-date remote sensing studies of vegetation (Holben 1986), we calculated the maximum NDVI value at each pixel of 30 × 30 m using Landsat 8 Annual Greenest-Pixel images (from 2013 to 2018) in Google Earth Engine. The resulting NDVI values reflect the maximum productivity of each pixel during the growing season in recent times, independently of within-or between-year climatic variation. However, the length of the growing season could change at different latitudes and so would the total annual productivity, which remains undetectable using this methodology. Nevertheless, this allows us to interpret the relative proportion of ecosystems ranging from the smallest (rocky habitats) to the greatest (shrubby habitats) peak productivity across the study regions. The final composite was upscaled to 30 arc-sec resolution. We then removed artefact NDVI values that were negative or >1. To investigate the relationships between productivity, climate and dominant vegetation types, we compared the distributions of NDVI values among clusters and ecoregions (Olson et al. 2001) using kernel density plots. We also fitted a generalised additive model to NDVI data using the *bam* function in the R package *mgcv* (Wood 2011), assuming a Gamma distributed conditional response, with smooth terms for the first four PC axes described above, as a proxy of the alpine climatic space. To reduce the effect of spatial autocorrelation, we sampled 100 000 random points and fit the model on this subset, including also a smooth term for geographic coordinates. To assess the influence of macroclimate in vegetated areas only, we also ran a model on a subset of 100 000 points with NDVI values > 0.1.

Results

Despite the presence of a few outliers, treeline elevation shows an increasing trend toward the tropics and decreases again close to the equator, almost symmetrically in both hemispheres (Figure 1.1b). Based on regional treeline models, we isolated alpine ecosystems above the climatic treeline worldwide (Figure 1.1a) and estimated their extent to 3.56 Mkm^2, corresponding to 2.64% of total land area outside Antarctica. Asia hosts almost three fourths of the global alpine area with 2.59 Mkm^2, followed by South America

(15%; 0.55 Mkm^2), North America (9%; 0.32 Mkm^2) and Europe (2%; 0.08 Mkm^2), while Oceania and Africa together contribute to only 1% of the global alpine area (Figure 1.1c). The distribution of maximum NDVI values above the treeline peaks at 0.1, reaching a median value at 0.2 and with a decreasing frequency of higher values (Figure 1.1d).

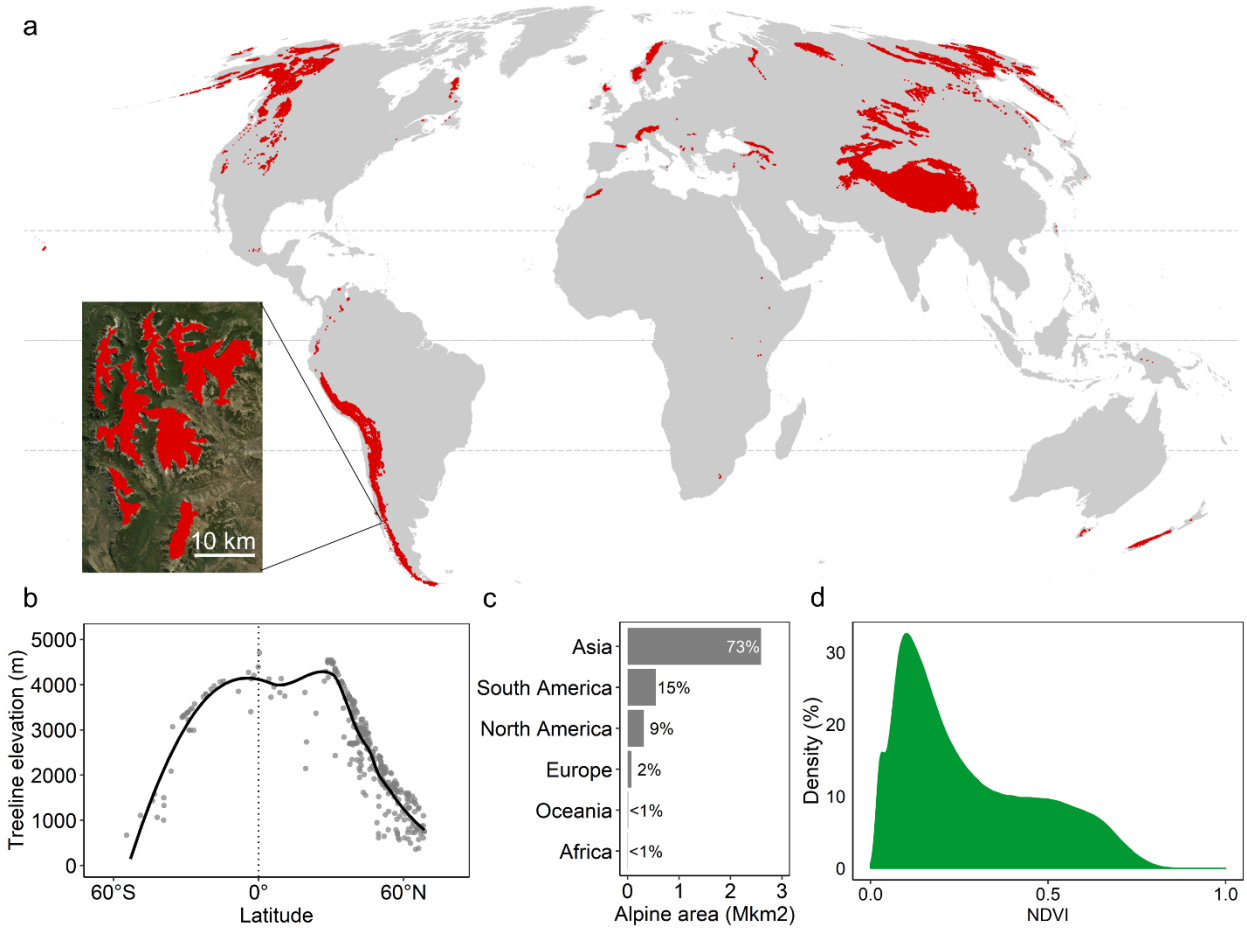

Figure 1.1. Extent and distribution of global alpine areas. (a) Spatial distribution of alpine areas based on a 30 m spatial resolution map. Dashed lines represent the equator and the tropics. (b) Distribution of treeline elevation values along latitude for 326 mountain ranges worldwide. Each dot represents the mean elevation and latitude for a mountain range. The black line represents a weighted loess fit. (c) Alpine areas extent and share for each continent. (d) Density plot of NDVI values above the treeline.

The mapped alpine ecosystems are grouped toward the colder end of the global climatic space (Figure 1.2), with 99% of the grid cells situated below a mean annual temperature of 5.9 °C and tropical alpine ecosystems lying on this threshold. The first two axes of the PCA of the 19 bioclimatic variables explained 66% of the global variation of the alpine climate and correspond to differences in seasonality and continentality of global alpine ecosystems (Figure 1.3). Clustering the whole dataset of alpine regions using the CLARA

algorithm with the first four weighted PCA axes highlighted the presence of four groups (best k = 4 in 95% of iterations; max average silhouette width = 0.40) (Appendix 1 Figure A1.3a), that were interpreted as 1) oceanic, 2) hemiboreal, 3) continental and 4) subtropical alpine ecosystems (Figure 1.3, Figure 1.4a).

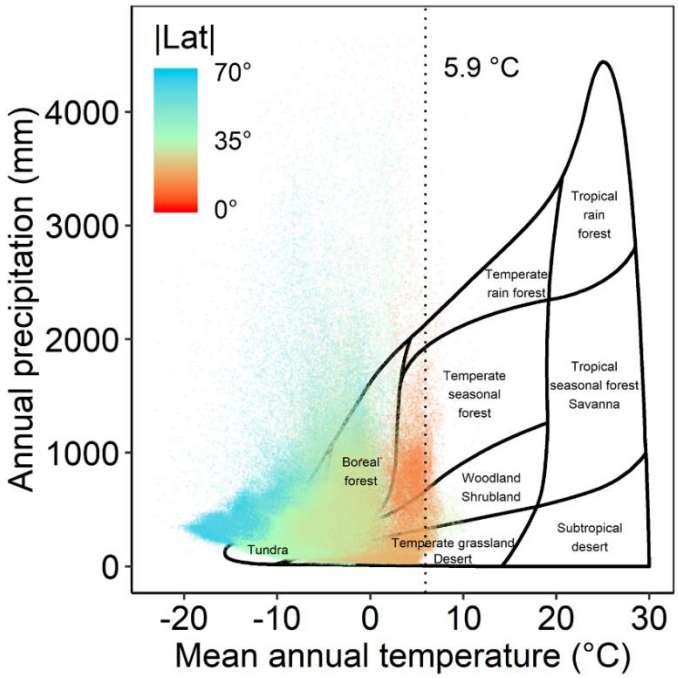

Figure 1.2. Values of temperatures and precipitation in alpine areas overlaid to Whittaker's biome plot. The dotted line represents the 99th percentile of the distribution of temperature values. Points are coloured according to their distance from the equator (|Lat|). To improve readability, the figure is based on a random subset of 500,000 30 arc-second cells in alpine areas.

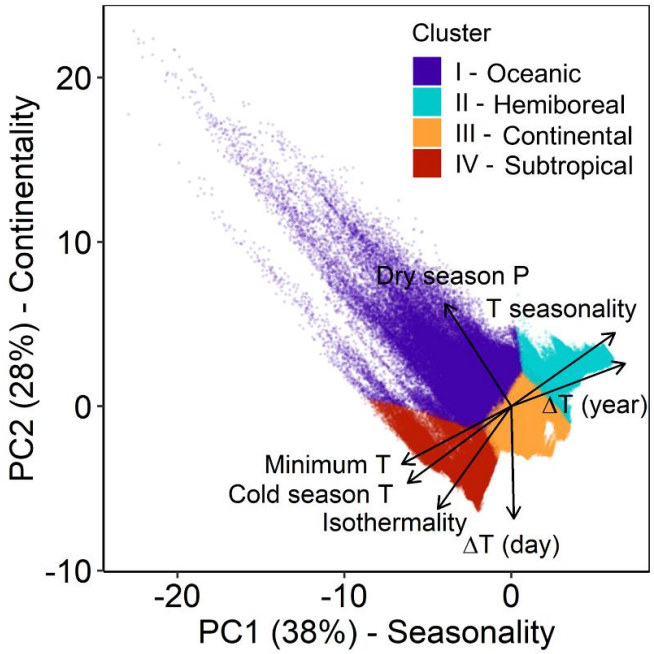

Figure 1.3. Biplot of principal component analysis of 19 climatic variables in alpine areas. The arrows indicate the loadings of selected climatic variables (correlation > 0.3 with one of the two axes). Points are coloured according to climatic clusters. Variables names' abbreviations and symbols (P: precipitation, T: temperature, Δ: difference). To improve readability, the figures are based on a random subset of 500,000 30 arc-second cells in alpine areas.

The hierarchical clustering based on the 30,000 records subset highlighted only two groups (best k = 2 in 100% of iterations; mean average silhouette width = 0.42) (Appendix 1 Figure A1.3b), with the first encompassing most of the continental, hemiboreal and subtropical groups, while the second taking up most of the oceanic cluster (Appendix 1 Figure A1.4a–c).

The four alpine clusters obtained by CLARA have similar NDVI values distribution (Figure 1.4a) and they are comparable to the pattern observed at the global level (Figure 1.1d). Nevertheless, this concordance disappears at the ecoregion scale, where the distribution of NDVI values, hence primary productivity, varies remarkably even within the same climatic cluster (Figure 1.4b). The generalised additive model of NDVI using the PC climatic axes values as predictors explained 58% of the deviance, with highly significant parametric coefficients and smooth terms ($p < 0.001$). Similarly, the model fit to a subset of pixels representing vegetated areas (NDVI > 0.1) explained 53% of the deviance.

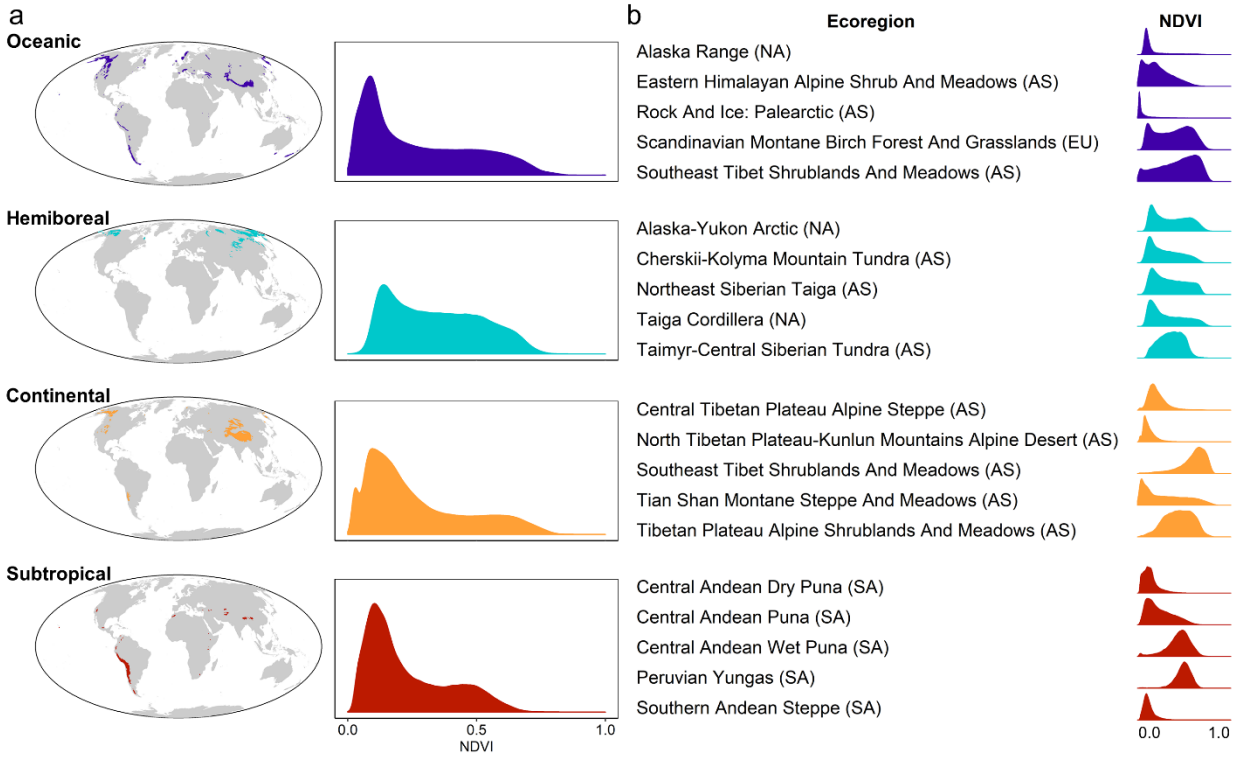

Figure 1.4. Distribution of climatic groups and NDVI values. (a) Global distribution of the four alpine climatic clusters and density plots of their NDVI values estimated using multitemporal Landsat eight Greenest Pixel imagery in the four alpine clusters. Y-axes are scaled to the same values. (b) Distribution of NDVI values of the alpine belt for the five largest ecoregions in each cluster. Continents are coded and reported in brackets (AS: Asia; EU: Europe; NA: North America; SA: South America). Y-axes of NDVI density plots are not scaled.

Discussion

Spatial distribution and extent of alpine ecosystems

This study provides, for the first time, a global map of alpine ecosystems at 30 m spatial resolution obtained through the analysis of global data sources on land cover and remote sensing. Our estimate of global alpine areas (3.56 Mkm^2) is very close to the 3.55 Mkm^2 reported by a previous study based on topography and broad climatic models (Körner et al. 2011). However, the two figures are not entirely comparable, since those authors included arctic mountain regions and excluded large parts of alpine plateaus (e.g. the Tibetan Plateau) which nonetheless may host alpine vegetation as defined here. In contrast, we based our approach on the presence of treeless vegetation thriving above the treeline, thus focusing on vegetation patterns rather than topography. For this reason (i.e. lying above the potential modelled treeline elevation, regardless of local terrain ruggedness) the flat Tibetan Plateau contributes to the total global alpine area in our map, while large portions of the Andean Altiplano were not included. Likewise, Arctic mountain regions and the rest of the Arctic tundra were excluded because they are located above the latitudinal treeline independently from elevational gradients.

We note that our estimation of treeline elevation is based on empirical forest cover data that consider as trees any vegetation taller than 5 m (Hansen et al. 2013). Although our map may include high-mountain forests with low (< 5 m) trees, the trends of the NDVI suggest that this effect is not relevant, or at least such forests have low cover and are mostly located in disrupted subalpine zones. In many mountain regions of the world, the treeline has been lowered by thousands of years of human activity (Holtmeier 2009) but some remnants of the climatic treeline usually survive on the least accessible slopes, even in very exploited regions like the European Alps (Holtmeier 2009). Through the analysis of a high-resolution map, we assume that our quantile regression was mainly based on the few remaining forest patches at the climatic treeline. Indeed, the resulting pattern of global treeline elevation closely resembles previous observations derived by field measurements (Körner 2003), showing well known patterns like the higher elevation of southern hemisphere treelines, when compared to the northern at the same distance from the equator (Cieraad et al. 2014, Karger et al. 2019). It also shows the general decreasing trend in treeline elevation close to the equator already reported by Körner (2003), despite some unexpectedly high afroalpine treelines (e.g. Ruwenzori: 4706 ± 49 m; Mount Kenia: 4390 ± 6 m). However, these values could have arisen from a misinterpretation of the local *Dendrosenecio* woodlands vegetation in the original forest cover map. Indeed, afroalpine vegetation is characterised by the presence of these giant rosettes forming open groves above the treeline (Shugart 2005) that might have accounted for tree cover in Hansen et al. (2013). Furthermore, some treelines were higher than expected also at mid latitudes, especially in large, longitudinally stretching ranges like the European Alps (2360 ± 19 m). This is probably due to the mass elevation effect that, combined with lower wind speeds, leads to higher treeline elevations approaching the centre of large mountain

ranges (Holtmeier 2009). As we did not account for these factors in our analyses, in some large mountain regions treelines may be skewed toward the upper values of their potential range, providing a rather conservative estimate of the alpine areas' extent. Likewise, the initial exclusion of some mountain regions that reportedly host an alpine belt, e.g. Iberian Peninsula mountains (Barrio et al. 2013) and Alborz mountains (Noroozi and Körner 2018), as well as the removal of smaller patches of alpine areas during the dataset cleaning process, were carried out for the sake of conservativeness. Despite the acknowledged contribution of small, isolated and endemics-rich patches of lower alpine habitats and isolated regions to the overall alpine biodiversity (Körner 2003), their removal likely had negligible effects on the estimation of the global alpine area.

Climatic and productivity patterns of global alpine biomes

Since our definition of alpine ecosystems is based on land cover data rather than a-priori assumptions about climate-treeline relationships, it allowed us to perform a climatic characterisation without risk of circularity (Peters 1976). Plotting the climatic envelope of the mapped alpine ecosystems in the classic representation of Whittaker's world biomes, we found a mean annual temperature threshold of 5.9 °C adjacent to tropical alpine regions. Although this temperature corresponds to global climatic models at 1 km resolution, it is in line with previous studies based on field measurements that found mean annual temperatures at the treeline in tropical mountains between 5 °C and 6 °C (Holtmeier 2009). Below this temperature threshold, the bioclimatic space of alpine ecosystems is driven by a major latitudinal temperature gradient that mainly overlaps with the position of tundra and boreal biomes in the Whittaker's scheme (Whittaker 1975). As mountain ranges approach the equator, the alpine belt from tropical and subtropical biomes decouples from the climatic space occupied by the corresponding lowland zones (Figure 1.2, Appendix 1 Figure A1.5). This reflects the outstanding compression of life zones (Körner 2003) that is found in tropical mountains where, within a few thousand meters difference in elevation, the diversity of habitats spans from the lowland rainforest to the glaciated mountain tops (Körner and Spehn 2019). In contrast, alpine biomes at the highest latitudes are centred on the environmental space of tundra, hence climatically close to their reference biome. They are also located at lower elevations (Appendix 1 Figure A1.5), making an exclusively climate-based distinction between arctic tundra and alpine tundra particularly challenging.

We also found that the climatic variation within global alpine biomes is mainly linked to seasonality and continentality, and less to temperature. This finding agrees with predictions on the primary role of seasonality and humidity gradients in defining alpine regions (Whittaker 1975, Nagy and Grabherr 2009), which had not been confirmed yet at the global scale due to the lack of global data. Since we had a rather complete sample of global alpine areas, we chose the CLARA algorithm to highlight the presence of main

clusters with the whole dataset, in accordance with previous studies that used semi-quantitative approaches for choosing the number of clusters (Metzger et al. 2013, Weigelt et al. 2013). The optimal classification in four clusters provided a meaningful biogeographic interpretation, in comparison with the two groups suggested by hierarchical clustering with a stratified subset. Although different clustering approaches usually lead to contrasting results, especially when applied to environmental data (Weigelt et al. 2013), the results provided in the two classifications were still comparable. Oceanic alpine regions were clearly differentiated in both cases; they are distributed across all continents and latitudes, encompassing mountain ranges characterised by an oceanic influence in terms of higher precipitation and relative temperature stability. Oceanic regions include the whole alpine belt of Europe and Oceania and large parts of North American ranges and the Andes, together with the Himalayas, at the interface between the seasonal humid, tropical climate of the Indian subcontinent and the cold mountain desert of the Tibetan Plateau. The other three groups defined by the CLARA algorithm were aggregated in the hierarchical clustering with the most continental subset of the oceanic group, but still suggesting a clear differentiation in the climatic space. Continental alpine regions are subject to much lower precipitation rates and greater daily temperature variability, including most of central Asian mountains and the driest portion of Rocky Mountains and central Andes, which are isolated from the influence of the Pacific Ocean. Interestingly, these oceanic and continental regions often occur in close vicinity within the same mountain range, sometimes even the same ecoregion (e.g. Southeast Tibet Shrubland and Meadows, Figure 1.4b). This happens because topography affects macroclimatic patterns, with the most exposed slopes forming a barrier to humid air streams, hence causing rainfalls on the one side and much drier conditions on the opposite. In contrast, hemiboreal alpine regions occur mainly at boreal latitudes of the northern hemisphere and have lower annual and seasonal temperature minima. They comprise most of the Siberian mountains and the northernmost ranges of North America, while subtropical alpine regions are mainly represented in the Andes and other tropical or subtropical regions that exhibit higher temperature minima and a much more stable climate throughout the year, despite marked diurnal variations. The latitudinal overlap of oceanic alpine regions with the others is in part an inherent consequence of the clustering approach. Indeed, the portion of oceanic alpine regions at higher latitudes is characterised by relatively greater seasonality than the one located closer to the equator. As a matter of fact, the oceanic group occupies a rather wide section of the global environmental space of alpine ecosystems. However, in a global perspective, oceanic regions as a whole are separated by hemiboreal and subtropical ones, forming a coherent, independent group. Furthermore, the spatial distribution and climatic characteristics of the oceanic alpine cluster are consistent with the oceanic group of the Köppen– Geiger climate classification (Köppen 1936). Oceanic climate is indeed characterised by relatively stable temperatures, the absence of a dry season and covers both coastland and inland areas of all continents, including mountain areas at subtropical latitudes like African mountains and parts of the Himalaya.

We also used global remote-sensing information to characterise alpine biomes using NDVI as a surrogate of photosynthetic activity and vegetation productivity (Whittaker 1975, Mucina 2019). In line with previous estimates (Bradley et al. 2017), the peak of the distribution of NDVI values in alpine ecosystems indicates dominance of bare or scarcely vegetated areas, while the lower frequencies of higher values represent the most productive vegetation found in these areas (i.e. grasslands and dwarf shrubs). Despite differences in temperature seasonality and amount of precipitation, alpine ecosystems grouped by climatic similarity show analogous patterns of NDVI variation, which in turn reflect a global system characterised by a large portion of poorly vegetated and low-productive areas. However, when looking at the NDVI values distribution among WWF ecoregions (Olson et al. 2001) within the same climatic group (i.e. comparing alpine ecosystems with similar climate across the globe), visible differences can be observed in all groups. These results suggest that, although macroclimate is able to explain 58% of the overall variation in NDVI, this is not the only factor shaping vegetation structure and function in the alpine belt, which may also differ strongly among regions. The growth of alpine plant species and the dominance of specific life forms also depend on regional and local factors like fine scale topography, disturbance and biogeographic history (Körner 2003, Jiménez-Alfaro et al. 2014), as additional factors explaining the heterogeneity of regional biodiversity across mountain regions. More studies are therefore needed to characterise the functional properties of alpine biomes, by combining remote-sensing indices with data collected on the ground from different vegetation types across regions.

Conclusions

This study provides a fine-scale estimate of the worldwide extent of alpine biomes and their bioclimatic characterisation. Rather than relying on temperature thresholds, our study provides an empirical view on this decades-old issue, using big data sources and a consistent definition of the study system. Although this study is based on a well-accepted definition of alpine ecosystems, we note that there could be different views on the interpretation of alpine versus arctic tundra, the inclusion or exclusion of rugged areas within the alpine zones, or the definition of world biomes under different frameworks. Our approach provides a conservative estimate of the extent of alpine areas, but our methodological framework had little effect on their bioclimatic characterisation. Indeed, our workflow can be easily applied from local to global scales and adjusted according to specific aims and conceptual assumptions.

By considering the assumptions of our approach, this study also provides the first spatial and bioclimatic characterisation of alpine biomes using a consistent, data-driven methodology. In general terms, we highlight that global alpine biomes occupy a relatively well-defined and continuous climatic space, which is geographically and climatically independent form other biomes regardless of latitude. Alpine biomes are mainly driven by

seasonality and continentality gradients, but major groups defined over this variation may be heterogenous in the structure and function of dominant vegetation, reflecting regional differences and the coexistence of multiple plant life-forms. Our findings are likely to be consistent under other assumptions on alpine biomes, given that we have analysed most alpine regions in the world, but less so for those approaches including arctic tundra into the same methodological framework, because this will add a new source of climatic variability. For the assessment of alpine biomes as defined here (i.e. high-elevation regions above the climatic treeline), our results may help in the evaluation of these relevant ecosystems at global and regional scales. The associated data sources of this study also provide useful tools for biodiversity assessment, ecological modelling, habitat monitoring or the analysis of climate change adaptation of different biota.

Chapter 2
Global patterns and drivers of alpine plant species richness

Testolin R., Attorre F., Borchardt P., Brand R.F., Bruelheide H., Chytrý M., De Sanctis M., Dolezal J., Finckh M., Haider S., Hemp A., Jandt U., Kessler M., Korolyuk A.Y., Lenoir J., Makunina N., Malanson G.P., Montesinos-Tubée D.B., Noroozi J., Nowak A., Peet R.K., Peyre G., Sabatini F.M., Šibík J., Sklenář P., Sylvester S.P., Vassilev K., Virtanen R., Willner W., Wiser S.K., Zibzeev E.G., Jiménez-Alfaro B. Global patterns and drivers of alpine plant species richness. *Global Ecology and Biogeography*. https://doi.org/10.1111/geb.13297

Abstract

Alpine ecosystems differ in area, macroenvironment and biogeographic history across the Earth, but the relationship between these factors and plant species richness is still unexplored. Here, we assess the global patterns of plant species richness in alpine ecosystems and their association with environmental, geographical and historical factors at regional and community scales. We used a dataset representative of global alpine vegetation, consisting of 8,928 plots sampled within 26 ecoregions and six biogeographic realms to estimate regional richness using sample-based rarefaction and extrapolation. Then, we evaluated latitudinal patterns of regional and community richness with generalized additive models. Using environmental, geographical and historical predictors from global raster layers, we modelled regional and community richness in a mixed-effect modelling framework. The latitudinal pattern of regional richness peaked around the equator and at mid-latitudes, in response to current and past alpine area, isolation, and variation in soil pH among regions. At the community level, species richness peaked at mid-latitudes of the northern hemisphere, despite a considerable within-region variation. Community richness was related to macroclimate and historical predictors, with strong effects of other spatially structured factors. In contrast with the well-known latitudinal

diversity gradient, the alpine plant species richness of some temperate regions in Eurasia was comparable to that of hyper-diverse tropical ecosystems, such as the páramo. The species richness of these putative hotspot regions is mainly explained by the extent of alpine area and their glacial history, while community richness depends on local environmental factors. Our results highlight hotspots of species richness at mid-latitudes, indicating that the diversity of alpine plants is linked to regional idiosyncrasies and to the historical prevalence of alpine ecosystems, rather than current macroclimatic gradients.

Introduction

More than two hundred years after Alexander von Humboldt's attempt to formulate a unified theory of the natural world, understanding the global patterns of diversity remains one of the greatest challenges in biogeography and macroecology (Kier et al. 2005, Kreft et al. 2008, Weigelt et al. 2016, Keil and Chase 2019, Brummitt et al. 2020). In particular, mountains have been revealed as centres of biodiversity with a disproportionately high species richness compared to their corresponding lowland regions (Antonelli et al. 2018, Muellner-Riehl et al. 2019, Rahbek et al. 2019a). Along the elevational gradient of mountains, the compression of life zones brings different biomes into proximity, with the alpine belt representing the outpost for plant life above the climatic treeline. Alpine ecosystems, governed by low-temperature regimes, cover about 3% of land outside Antarctica and are distributed across all continents and latitudes (Körner et al. 2011, Testolin et al. 2020). Despite ongoing efforts to monitor changes in the biota of mountain summits in the face of climate change (Gottfried et al. 2012, Pauli et al. 2012, Steinbauer et al. 2018), we still lack a global picture of the patterns of plant diversity in alpine habitats, let alone the understanding of its major drivers.

According to the general latitudinal diversity gradient, biodiversity is expected to peak at the equator (Hillebrand 2004). Among the possible explanations for this pattern (Lomolino et al. 2017), latitude is normally interpreted as a proxy for climatic conditions and available metabolic energy, which might have an effect on speciation rates (Wang et al. 2009). Whether this general rule also applies to alpine ecosystems, however, is still a matter of debate. Therefore, lowland and alpine thermal conditions from polar to equatorial latitudes are increasingly decoupled from one another (Testolin et al. 2020). Besides having a lower energy input compared to the lowlands, alpine ecosystems are also highly heterogeneous in their topoclimates (Quinn 2008), which might weaken the correlation between latitude and primary productivity (Testolin et al. 2020). For these reasons, plant diversity in alpine areas may decouple from major climatic gradients.

Alpine areas are also isolated from each other, forming fragmented systems of *sky islands* surrounded by lowland environments that limit species' dispersal (McCormack et al. 2009). Following the ecological principle of the species-area relationship (Lomolino 2000) and their application to the theory of island biogeography (MacArthur and Wilson 1967),

the extent of alpine habitats and their isolation could have affected rates of colonisation, speciation and extinction of plants (Heaney 2000, Steinbauer et al. 2016). These processes may have resulted in biodiversity patterns linked to the historical and current abundance of alpine habitats at the global scale. Although it has been widely reported that the biogeographical history of mountains has shaped diversity patterns of cold-adapted plant species in alpine regions (McGlone et al. 2001, Harris 2007, Sklenář et al. 2014, Flantua et al. 2019), a major unresolved question is the extent to which the interplay of ecological drivers and historical contingencies dictates the patterns of alpine plant diversity at the global level (Nagy and Grabherr 2009). The significance of these drivers may shift from global to local spatial scales, and can reveal new patterns and relationships that are not evident at regional scales at which alpine plant diversity patterns have been studied so far (Moser et al. 2005, Vonlanthen et al. 2006, Lenoir et al. 2010, Jiménez-Alfaro et al. 2014).

Here, we compiled a dataset of 8,928 vegetation plots with 5,325 vascular plant species sampled by botanical experts in alpine ecosystems over the past 100 years, and representative of global alpine vegetation. By analysing the data at both the regional and community level, we investigate (1) the global latitudinal patterns of alpine plant species richness and (2) the relative influence of environmental, geographical and historical factors in driving such patterns. We further evaluate how those patterns and drivers change between regional and community levels, and how they relate to hotspots of alpine plant diversity recognised at the global scale.

Material and methods

Study system and data collection

We considered as zonal alpine vegetation any plant community dominated by graminoids, forbs, and dwarf shrubs above the climatic treeline (Körner 2003). In addition to strictly zonal habitats, snow-patch vascular plant communities and vegetation on rocks and screes are also found ubiquitously in the alpine belt and were included in our study. We did not consider vegetation from polar climates due to the absence of elevational treelines and their distinct environments (Walter and Box 1976, Quinn 2008). Therefore, the alpine vegetation included in the present study corresponds to the *mid-latitude alpine tundra* and the *tropical alpine biome* groups as defined by (Quinn 2008).

We assembled vegetation-plot data of vascular plant communities sampled by the authors, compiled from the literature, or included in sPlot – the global vegetation database (Bruelheide et al. 2019) – with the aim of obtaining a representative sample of the global alpine vegetation. The plots were selected using habitat classifications of the data sources and then revised by data providers based on the scope of our study (Appendix 2 Table A2.1). Datasets from different sources were standardised by identifying a minimum

common set of plot attributes including size, elevation, and geographic coordinates. When the latter were missing for small, clearly delimited areas, we estimated plot locations from maps (i.e. Mount Jaya; Hope et al. 1976) or by randomly assigning the coordinates of raster cells with the same elevation (±10 m) as the plots in that area (i.e. Mount Wilhelm and Drakensberg; Wade & McVean 1969; Brand et al. 2015), using the SRTM-3 digital elevation model at 30 m resolution (Farr et al. 2007, NASA and JPL 2013). Species cover values with discrete scales were transformed to the mean value of the corresponding percentage interval. Species names were harmonised using the *Taxonomic Name Resolution Service* (Boyle et al. 2013) online tool (https://tnrs.biendata.org) with default settings, updating the names to the most recent nomenclature and merging subspecies and varieties to the species level by summing their respective cover values.

The initial dataset, consisting of 10,408 plots, was further filtered by removing plots with tree species or incomplete taxonomic identification. When taxa identified to the genus level or higher taxonomic rank represented ≥ 10% of the plot vegetation cover, the corresponding plot was discarded; otherwise we removed those taxa from the plot record (3,086 plots from which at least one taxon was removed; median number of taxa removed = 1). Each plot was then assigned to a region based on its location. Regions were defined based on the approximate extent of ecoregions (Olson et al. 2001), which represent an ecologically meaningful framework for identifying distinct geographic units at the global scale. As the names of some ecoregions did not reflect the presence of an alpine vegetation belt, we renamed these regions after the main mountain ranges where the plots were located, following Körner et al. (2017) (Appendix 2 Table A2.2). For the analyses, we retained only regions with at least 60 plots, and removed extremely small or large plots (<0.25 or >400 m2). To filter out compositional outliers, we performed a detrended correspondence analysis (DCA) on each regional dataset, excluding those plots whose score on the first axis (DCA1) was larger or smaller than 10 times the width of the interquartile range from the median. After removing the outliers, the gradient length of DCA1 ranged from 3.6 to 9.9 standard deviation units of species turnover within different regions (Appendix 2 Table A2.3), indicating different – yet high – degrees of regional beta diversity. Finally, to assess the representativeness of our dataset, we compared the climatic space of the plots against the climatic envelope of global alpine areas (Testolin et al. 2020) (Appendix 2 Figure A2.1). The final dataset consisted of 8,928 plots of alpine vascular vegetation along elevational gradients above the treeline in 26 regions belonging to six biogeographic realms (Keil and Chase 2019) (Figure 2.1a,b; Appendix 2 Table A2.3), distributed across all continents except Antarctica and sampled over a period of almost 100 years, between 1923 and 2019.

Diversity measures

As the number of samples differed considerably among regions, we estimated regional species richness using sample-based rarefaction and extrapolation (Chao et al. 2014) with the R software (R Core Team 2020) and the package *iNEXT* (Hsieh et al. 2016). This technique allows a statistically sound comparison of diversity across groups with different sample sizes through the construction of sampling curves for species richness. These curves can be rarefied (i.e. interpolated) to smaller sample sizes or extrapolated (i.e. predicted) to larger sample sizes (Chao et al. 2014, Hsieh et al. 2016). Here, we estimated regional richness for a unique sample size of 180 plots, corresponding to approximately three times the smallest regional sample (Figure 2.1b). We chose 180 plots as a trade-off between the loss of data in intensively sampled regions versus the inclusion of all regions in the analyses. As such, these estimates should not be interpreted as representing the total regional species pools, but rather as comparable estimates of regional richness. Since our global dataset comprised plots of different sizes, we evaluated the effect of plot size on the species richness estimates. To do this we compared the same estimates using three subsets of different plot sizes (small: $<$10 m2; medium: $\geq$10 and $<$100 m2; large: $\geq$100 m2). For those regions where at least 60 plots of each of the three different sizes were available (Alborz Mountains, Central and Eastern Alps, Colombian and Ecuadorian Andes, Eastern African Mountains, South Central Rocky Mountains and Western Carpathians), we compared richness estimates obtained from the different subsets. We found that, regardless of the subset used, the relative differences among regions were largely preserved, especially for those datasets comprising large numbers of plots (e.g. Central and Eastern Alps and Western Carpathians). An exception was the region of the Colombian and Ecuadorian Andes, where regional richness estimates were highly dependent on plot size (Appendix 2 Figure A2.2). However, that large and small plots both resulted in lower species richness estimates compared to medium-sized plots, suggesting that the differences are driven by different vegetation types being sampled with differently sized plots.

For each plot we calculated community richness as the total number of species. We evaluated latitudinal patterns of regional and community richness using generalised additive models (GAMs) with a smoothing term for latitude. Our alpine regions were characterized by very different extents, and plot size varied widely. To account for different regional extents and plot sizes in the evaluation of species richness patterns, we also fitted GAMs on the residuals from ordinary least square regressions of log(regional richness) as a function of log(current local alpine area) and log(community richness) as a function of log(plot size). The procedure for calculating local alpine area is described below.

Environmental predictors

To analyse the drivers of species richness, we retrieved a set of environmental variables linked to plant diversity in the alpine belt from online sources. We calculated several climatic predictors at the plot level using digital sources at ~1 km resolution. We used data from CHELSA (Karger et al. 2017) within the time frame of the growing season, defined as days with mean temperature > 0.9 °C (Paulsen and Körner 2014). As daily temperature data were not available, we estimated the growing season using monthly averages, including the months with a mean temperature > 0.9 °C. Although this may have resulted in a sharper delimitation of season lengths, it likely had little effect on our global analyses. We included the mean temperature, precipitation, growing degree days and mean potential evapotranspiration of the growing season, which have all been reported to have positive effects on photosynthetic activity and species richness in alpine areas (Körner 2003, Moser et al. 2005, Nagy and Grabherr 2009). Growing degree days (i.e. the sum of monthly temperatures > 0.9 °C multiplied by the total number of days in such months) were calculated using the *growingDegDays* function of the R package *envirem* (Title and Bemmels 2018). Mean potential evapotranspiration of the growing season was estimated with the *hargreaves* function of the R package *SPEI* (Beguería and Vicente-Serrano 2017), using maximum and minimum monthly values of temperature and monthly precipitation. The monthly values of potential evapotranspiration obtained were then averaged across months with a mean temperature > 0.9 °C. Together with climate, soil pH is known to be a significant driver of species richness in the alpine belt (Vonlanthen et al. 2006) and is a good surrogate for the dominant bedrock, effectively differentiating calcareous and siliceous substrates (Lenoir et al. 2010, Jiménez-Alfaro et al. 2014)j. We derived estimates of soil pH from the SoilGrids database, averaging the values estimated at 5 and 15 cm depths (Hengl et al. 2017). When the pH value was missing for a plot location (45 plots), we assigned the value of the closest pixel to the plot. Despite the limitations posed by the use of global datasets to estimate fine-scale soil properties (Hengl et al. 2017), the obtained values covered a wide span of soil pH variation in alpine environments (4.40 - 8.35) and were therefore useful to distinguish dominant bedrock types. In addition to climate and soil, topography also represents a major factor linked to plant diversity in alpine areas (Lenoir et al. 2010, Jiménez-Alfaro et al. 2014), as it creates a fine-scale mosaic of contrasting microclimates (Körner 2003, Nagy and Grabherr 2009, Rahbek et al. 2019a, b). As measures of topographic heterogeneity of the terrain surrounding each plot, we used the topographic position index and terrain ruggedness index (Amatulli et al. 2018). Regional values of the predictors computed at the plot level were then estimated as the average of all vegetation plots within a region. For climatic predictors and soil pH, we also calculated the standard deviation of the predictor to test for the effect of environmental heterogeneity.

Geographical and historical predictors

In addition to environmental variables, large-scale geographical factors like area and isolation are known to influence the current diversity of island-like ecosystems (MacArthur and Wilson 1967, Whittaker et al. 2008, 2017), and so do their historical changes caused by climatic fluctuations (Fernández-Palacios et al. 2016, Weigelt et al. 2016). We delimited alpine area as the portion of land with a mean temperature of the growing season between 3.5 °C and 6.4 °C, or with a length of the growing season between 1 and 3 months (Paulsen and Körner 2014). We did this both for current climatic conditions and considering climate during the Last Glacial Maximum (LGM) (Appendix 2 Figure A2.3). Alpine areas were calculated at two scales reflecting the spatial extents of each regional sample (local area) and the total continuous alpine area extending beyond the samples (total area). We defined the local area as the extent of the alpine area contained within the convex hull formed by all plots of each region. In some cases, the coarse resolution of the climatic datasets used to estimate the alpine areas failed to detect any alpine patch within the hulls. Therefore, we applied a 5 km buffer around each hull to include at least some alpine area patches for all regions. The total alpine area for each region was estimated as the continuous extent of all alpine patches intersected by the hulls, reflecting the total extent of alpine habitats available to species dispersal (Appendix 2 Figure A2.4). Calculating alpine areas at two scales also allowed us to estimate the completeness of the regional samples by calculating the percentage of the local alpine area encompassed by the samples over the total alpine area (Appendix 2 Table A2.3). As the local and total log-transformed areas were highly correlated (Pearson's $r > 0.8$), only the former was retained in the subsequent analyses.

In addition, we estimated the current and LGM isolation as the minimum distance from the centroid of each alpine region to the boundary of the nearest alpine area ≥1,000 km2. We set a threshold of 1,000 km2 to exclude smaller alpine patches that could still be part of the same alpine region, i.e. islands of the same archipelago (Steinbauer et al. 2016). If an alpine region had a total area ≥1,000 km2, isolation was set to zero. Current and LGM alpine areas and isolation were log-transformed. Since past climatic changes could have affected current diversity patterns (Graham et al. 2014), we also calculated the velocity of climate change since the LGM as a measure of regional climatic instability (Loarie et al. 2009, Sandel et al. 2011), using the $gVoCC$ function of the $VoCC$ package (García Molinos et al. 2019) with current and LGM mean annual temperatures. The latter was calculated as the average of the two PMIP3 climatic datasets derived using the CCSM4 and MIROC-ESM climate models (Sandel et al. 2011, Weigelt et al. 2013, 2016). Finally, we included biogeographical realms (Keil and Chase 2019) as a proxy for differences in evolutionary history. Due to the lack of regional data, we did not account for differences in the geological history of mountains. However, we acknowledge that this could influence speciation and partially explain species richness (Whittaker et al. 2008, 2017).

Statistical analyses

We tested the influence of environment, geography and history on estimated regional richness by fitting individual Poisson generalised linear mixed-effects models (GLMMs) to each predictor with the *glmer* function of the R package *lme4* (Bates et al. 2015). We first tested univariate relationships to select a set of significant variables to be used in subsequent multivariate modelling. To account for uncertainties in regional richness estimates, we weighted the observations by the inverse of their 95% confidence interval width. We also scaled the predictors by subtracting their mean and dividing by their standard deviation across the regions to ensure model convergence. To control for overdispersion and reduce the risk of type I errors, we added an observation level random effect (OLRE) to the models, i.e. a unique level of a random effect for each data point that models the extra-Poisson variation present in the data (Harrison 2014). The ratios between the sum of squared Pearson residuals and the residual degrees of freedom of the fitted models with OLRE indicated no additional overdispersion. Then, we analysed the correlations among significant predictors with the Pearson correlation coefficient. We found that some of our regional variables were strongly correlated to one another (Appendix 2 Figure A2.5), limiting our ability to distinguish partial contributions. However, we built alternative multivariate models by retaining only the significant, uncorrelated predictors. Finally, we checked for the presence of spatial autocorrelation in model residuals with the Moran's I test implemented in the *testSpatialAutocorrelation* function of the *DHARMa* package (Hartig 2020) and found none (Appendix 2 Table A2.4). We also fit a null (intercept-only) model to compare the goodness of the fits. Models were compared using the Akaike Information Criterion corrected for small sample sizes (AICc) as well as marginal and conditional R2 (mR2; cR2), calculated with the *r.squaredGLMM* function of the *MuMIn* package (Barton 2019). As the only random effect in the models was an OLRE, mR2 = cR2.

We modelled community richness by fitting Poisson GLMMs including the environmental, geographical, and historical predictors. Growing degree days and precipitation of the growing season were highly correlated to temperature and evapotranspiration of the growing season, respectively (Pearson's $r > 0.6$). Likewise, area and isolation-related variables were highly correlated to one another. Thus, to avoid multicollinearity issues, we retained temperature and evapotranspiration of the growing season, as well as current and LGM local areas, and excluded the other variables. We also accounted for different plot sizes by adding their log-transformed values to the model and controlled for overdispersion by adding an OLRE. As the plot-level predictors were derived from digital datasets at 1 km resolution, we randomly selected one plot for each 0.01-degree cell (~1 km). We repeated the process 999 times and obtained as many random subsets of 2,534 plots, i.e. one plot for each 0.01-degree cell. Before modelling, all predictor variables were scaled to ensure model convergence. We then fit the GLMMs to each of the 999 subsets. As the Moran's I tests highlighted strong spatial autocorrelation of the models' residuals,

we re-fit the models including random intercepts for 0.05 (≈ 5 km) and 0.1 (≈ 10 km) degree cells, which largely resolved the issue (Moran's I ≈ 0; $p > 0.05$ for 75% of model fits). We also tested for regional effects by fitting another model to the 999 subsets with an additional random intercept for regions. Finally, we averaged the fixed effect coefficients of the resulting models using weights based on their AICc with the *model.avg* function of the *MuMIn* package. The two resulting averaged models (with and without the random intercept for region) were compared using mean AICc, mR2 and cR2, obtained by calculating the weighted average of the respective indexes for the 999 fits.

Results

According to sample-based rarefaction and extrapolation of regional richness (estimated for 180 plots), the richest alpine regions in this study were the Colombian and Ecuadorian Andes (Neotropic; 543 species), followed by the Pamir Mountains (Eastern Palearctic; 497 species), and the Altai Mountains (Eastern Palearctic; 486 species). At intermediate species richness levels, we found the Central and Eastern Alps (Western Palearctic; 387 species), Sayan Mountains (Eastern Palearctic; 369 species), and Cordillera de Mérida (Neotropic; 350 species). On the other end of the gradient, the poorest regions were Mount Cameroon (Afrotropic; 120 species) and Northern Scandes (Western Palearctic; 98 species) (Figure 2.1b,c).

The latitudinal pattern of regional richness peaked around the equator and at mid-latitudes of the northern hemisphere, with low species richness values around the tropics and at high latitudes (Figure 2.2a). At the community level, we observed a single peak at mid-latitudes of the northern hemisphere but a wide range of species richness values across all regions (Figure 2.3a). The same patterns emerged even when different regional extents and plot sizes were accounted for, with an additional peak of regional richness at mid-latitudes of the southern hemisphere corresponding to the Drakensberg (Afrotropic) and the Australian Alps (Australasia) (Appendix 2 Figure A2.6a,b).

The null model of estimated regional richness had AICc = 67. The GLMMs of estimated species richness against individual predictors highlighted a positive significant effect of current area ($\hat{\beta} = 0.33 \pm 0.07$; AICc = 54), LGM area ($\hat{\beta} = 0.26 \pm 0.08$; AICc = 61) and soil pH variability ($\hat{\beta} = 0.24 \pm 0.08$; AICc = 61), while current isolation ($\hat{\beta} = -0.26 \pm 0.08$; AICc = 61) and LGM isolation ($\hat{\beta} = -0.20 \pm 0.09$; AICc = 65) had a negative effect (Figure 2.2b; Appendix 2 Table A2.4; Appendix 2 Figure A2.7). Among significant predictors, current area was correlated to soil pH variability ($r = 0.70$, $p < 0.001$) and to current isolation ($r = -0.76$, $p < 0.001$), while LGM area was correlated to LGM isolation ($r = -0.72$, $p < 0.001$) (Appendix 2 Figure A2.5). Multivariate Poisson GLMMs with uncorrelated significant predictors explained 67% (current isolation + LGM isolation;

AICc = 58) and 79% (current area + LGM area; AICc = 52) of the variance (Appendix 2 Table A2.4).

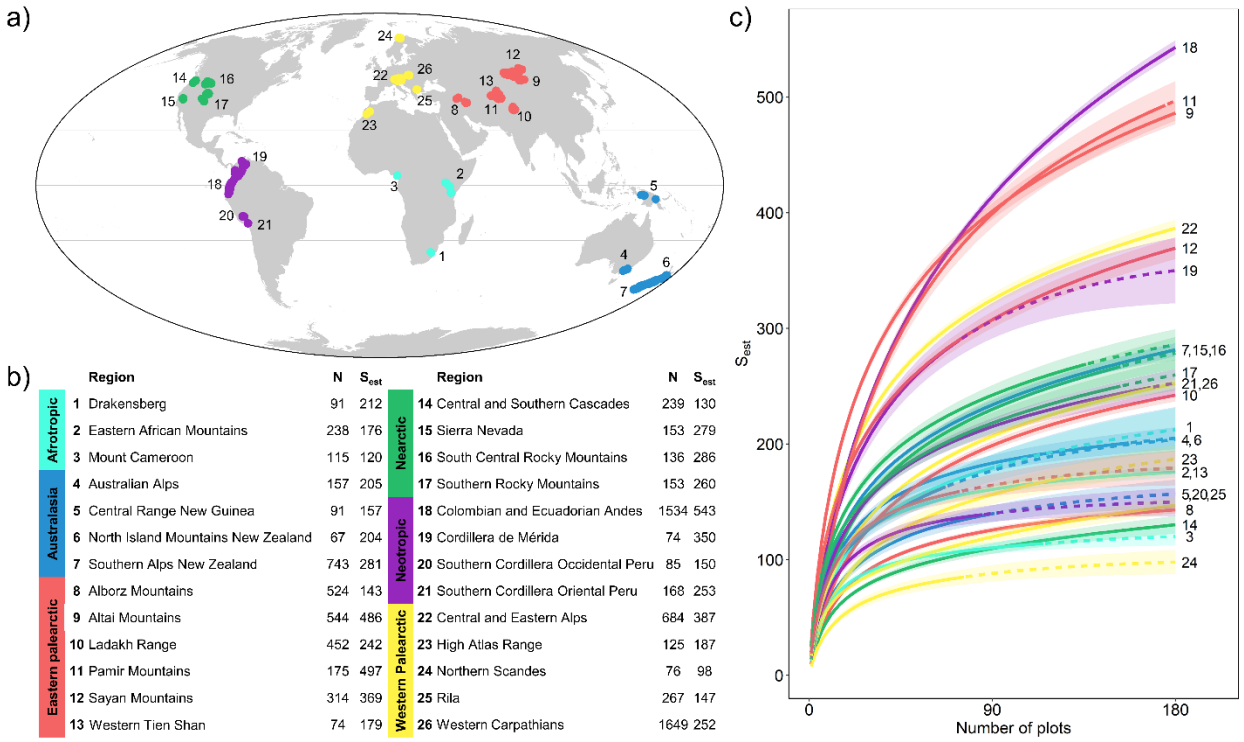

Figure 2.1. Overview of the global alpine vegetation dataset and regional species richness. a) Spatial distribution of alpine vegetation plots; b) Number of plots collected in this study (N) and estimated species richness (S_{est}) for 26 alpine regions in six biogeographic realms; c) Rarefaction curves of species richness for each region. Dashed lines indicate extrapolated values beyond the available number of plots. Continuous lines indicate that regional estimates were interpolated from larger sample sizes. The shaded areas represent the 95% bootstrap confidence intervals.

At the community scale, species richness was positively related to the evapotranspiration of the growing season ($\hat{\beta}$ = 0.13 ± 0.05; $p < 0.001$), velocity of climate change ($\hat{\beta}$ = 0.10 ± 0.05; $p < 0.001$), and LGM alpine area ($\hat{\beta}$ = 0.19 ± 0.05; $p < 0.001$), while it was negatively related to soil pH ($\hat{\beta}$ = -0.12 ± 0.05; $p < 0.001$). Nearctic plots were generally poorer in species than plots in other realms ($\hat{\beta}$ = -0.44 ± 0.22; $p < 0.001$) (Figure 2.3b; Appendix 2 Table A2.5). Overall, the fixed effects explained 22% of the variance, while the inclusion of the random effects controlling for the plots' spatial aggregation at 5 and 10 km increased the explained variance to 58%. The inclusion of regions as an additional random effect further increased the total explained variance to 65% and left as significant fixed effects the mean temperature of the growing season ($\hat{\beta}$ = 0.04 ± 0.03; $p < 0.05$) and soil pH ($\hat{\beta}$ = -0.07 ± 0.05; $p < 0.05$), which together explained 26% of the variance (Figure 2.3b; Appendix 2 Table A2.5).

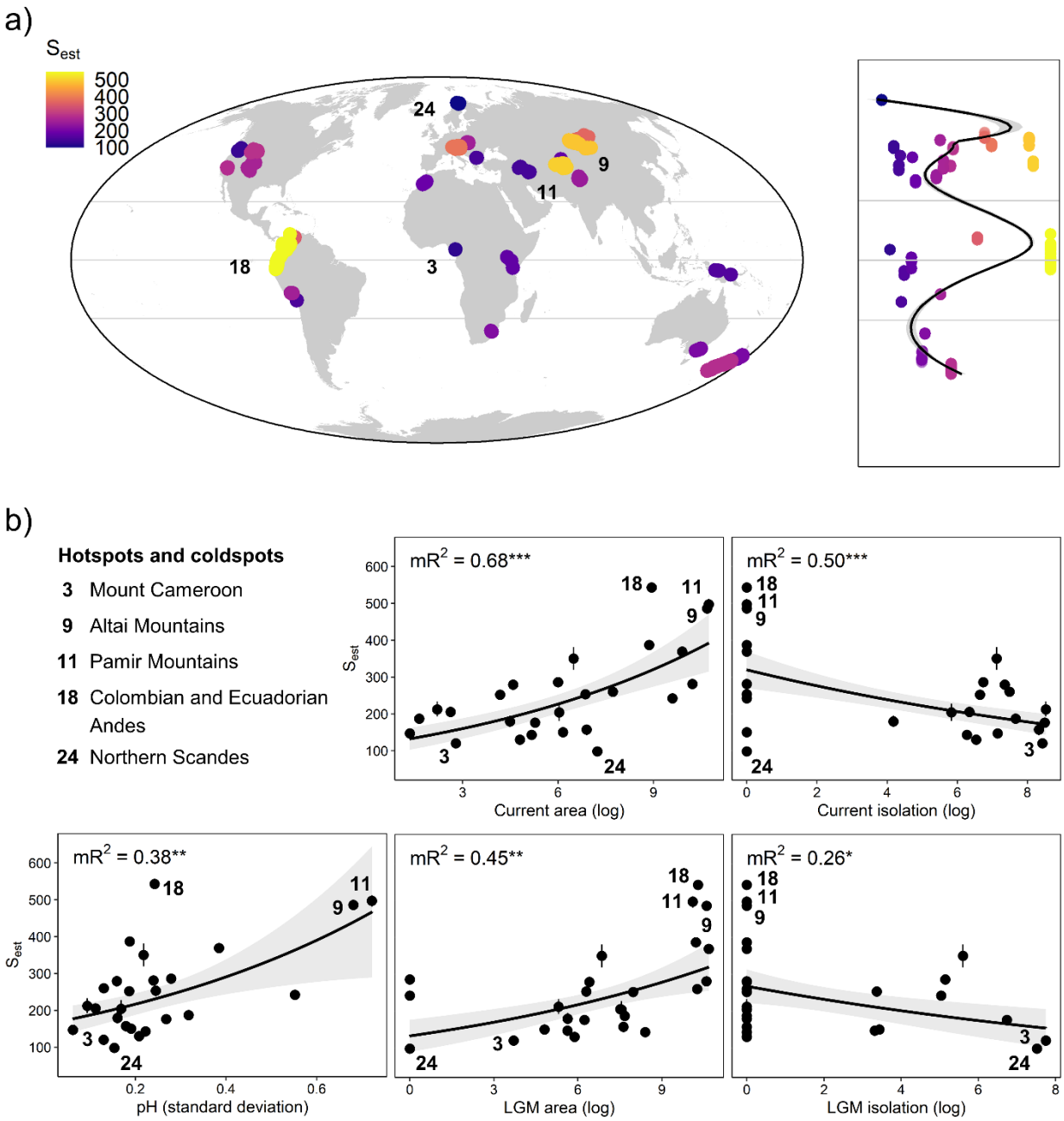

Figure 2.2. Latitudinal patterns and drivers of estimated regional species richness. a) Regional plant species richness estimated for 180 plots (S_{est}). The scatterplot on the right represents the latitudinal trend. The horizontal grey lines in the map and the scatterplot represent the equator and the tropics. The black line represents a GAM fit; b) Single-predictor models of regional species richness. The dots represent the regional plant species richness estimated for 180 plots (S_{est}). The error bars represent the 95% bootstrap confidence intervals of the richness estimates. Black lines represent the individual GLMM fits. The grey bands are the 95% bootstrap confidence intervals. Marginal R^2 (mR^2) and model significance are reported. Significance codes: < 0.001 (***); < 0.01 (**); < 0.05 (*). The numbers of the regions mentioned in the main text are reported according to Figure 2.1.

Discussion

Regional patterns and drivers

Our results, based on a representative sample of global alpine vegetation, showed a latitudinal pattern of plant species richness with peaks at mid-latitudes and around the equator. The highest estimate of regional richness was detected in the Colombian and Ecuadorian Andes (Neotropic). This region is home to the páramo ecosystem, a centre of plant diversity within the tropical biodiversity hotspot known to host the richest alpine flora in the world (Myers et al. 2000, Madriñán et al. 2013). At higher latitudes, we also found that the Pamir and Altai Mountains (Eastern Palearctic) exhibited regional richness comparable to the páramos, representing actual hotspots of alpine plant diversity outside the tropics. This is consistent with previous studies that highlighted the high plant diversity of the Altai, Pamir, as well as other Central Asian mountain systems (Agakhanjanz and Breckle 1995, Körner 1995, Kier et al. 2005, Xing and Ree 2017, Brummitt et al. 2020). Nevertheless, these putative mid-latitude alpine hotspots are generally excluded from global centres of biodiversity, despite their importance as refugia for cold-adapted plant species (Chytrý et al. 2019). When accounting for the extent of the local alpine area, the Drakensberg (Afrotropic) and the Australian Alps (Australasia) emerged as alpine plant richness centres of the southern hemisphere. Indeed, the high-elevation plateau of the Drakensberg has been widely recognised as a continental hotspot of botanical diversity (Brand et al. 2019, Carbutt 2019), and the Australian Alps have been listed among the main national areas of plant species richness (Crisp et al. 2001, Bell et al. 2018). Other regions showed lower species richness with no clear distinctions among different realms or latitudes. The lowest richness was found in Mount Cameroon (Afrotropic) and the Northern Scandes (Western Palearctic) which, interestingly, are located at the extremes of the latitudinal distribution of the global alpine biomes, one near the equator and the other at the arctic circle. Mount Cameroon represents the only isolated outpost of the alpine life zone in tropical Western Africa (Anthelme and Dangles 2012) and is an active volcano with eruptions that limit vegetation development (Nagy and Grabherr 2009). On the other hand, the Northern Scandes were completely glaciated during the Pleistocene glacial maxima and located far from the Southern European glacial refugia further south (Lenoir et al. 2010).

Our models showed that the regional richness of alpine ecosystems is mostly independent of macroclimatic gradients. An analogous decoupling pattern has also been reported for the global diversity of grasses as a response to biogeographic history and the adaptation of certain lineages to cold and arid environments (Visser et al. 2014). Indeed, global alpine areas are climatically constrained toward low-temperature conditions (Körner 2003, Nagy and Grabherr 2009, Paulsen and Körner 2014). Thus, despite alpine plants respond to changes in temperature and light because of topography, large-scale richness patterns of alpine vegetation seem to be largely independent of energy gradients that determine species diversity at lower elevations (Hillebrand 2004). On the other hand, global alpine

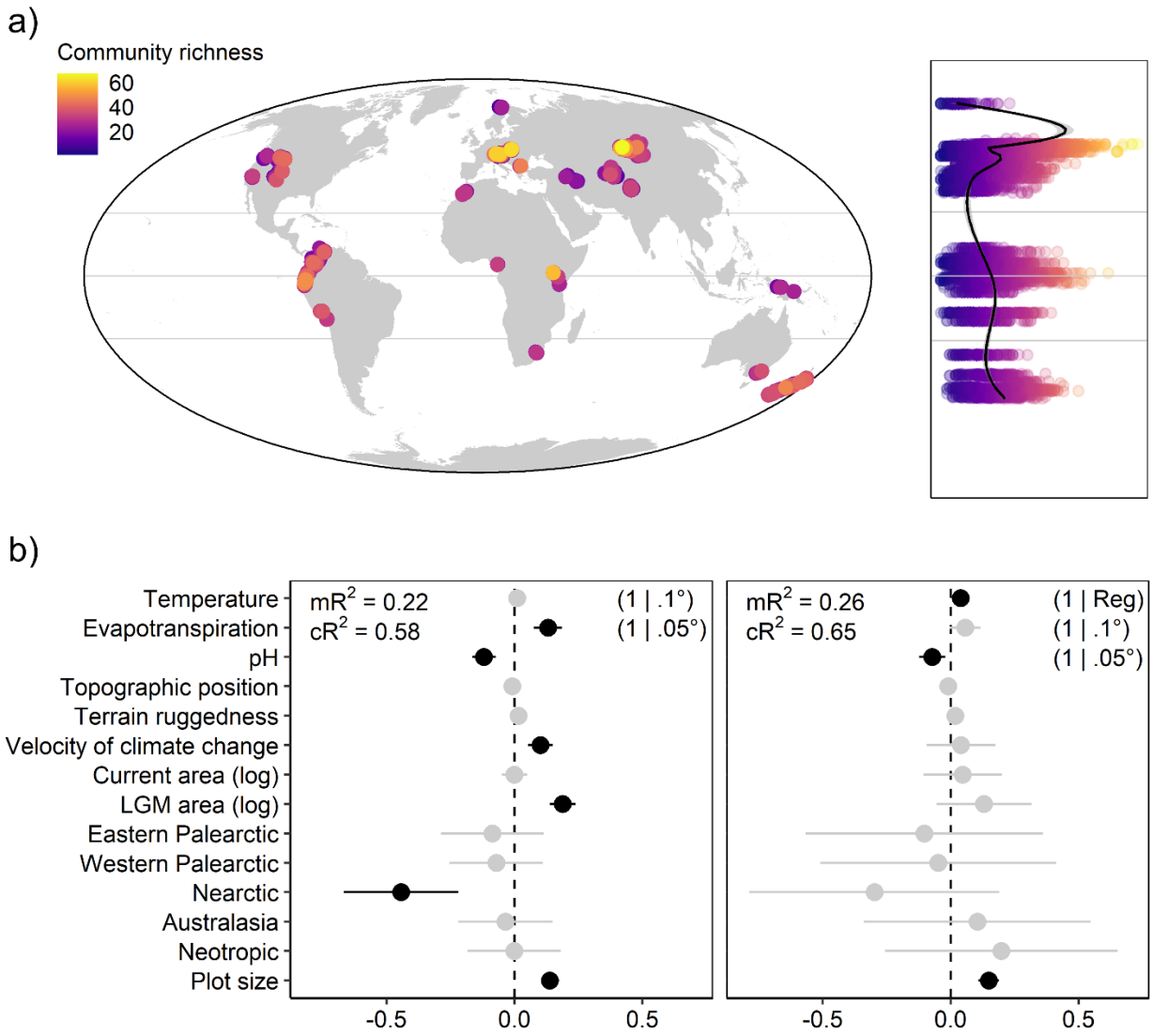

Figure 2.3. Latitudinal patterns and drivers of community species richness. a) Community plant species richness. The scatterplot on the right represents the latitudinal trend. The three horizontal grey lines in the map and the scatterplot represent the equator and the tropics. The black line represents a GAM fit; b) Standardised fixed-effect coefficients from model-averaged GLMMs of 999 sub-models of community species richness, based on 999 random subsets of 2534 plots. Temperature and evapotranspiration are the mean values calculated during the growing season. Random effects: (1 | .05°) and (1 | .1°) group plots belonging to the same 0.05- and 0.1-degree cell; (1 | Reg) groups plots belonging to the same region. Dots and bars represent the mean and the 95% confidence interval of the coefficients. Significant coefficients are drawn in black. Marginal (mR2) and conditional (cR2) R2 represent the weighted average of the corresponding measures across all sub-models.

areas are subjected to different amounts of precipitation and are differentiated along a gradient of humidity (Körner 2003, Nagy and Grabherr 2009, Testolin et al. 2020). Although our dataset encompasses a large portion of the variation in water availability of

global alpine areas (Appendix 2 Figure A2.1), the effect of precipitation on regional richness was not significant. This suggests that the association of water availability with plant species richness might be restricted to local scales and especially to arid regions, where precipitation is the main factor limiting plant growth (Palpurina et al. 2017).

Contrarily to macroclimate, we found a positive effect of the extent of current alpine area and a negative effect of isolation. The importance of these factors is consistent with the predictions of the theory of island biogeography (MacArthur and Wilson 1967) that posits that larger, less isolated islands are characterised by lower extinction rates and greater chances of being colonised by new species. Nevertheless, the historical legacy of the extent and isolation of alpine areas during the LGM also left a strong imprint on regional richness patterns that is independent of their current geographical characteristics. The extent of alpine areas during the LGM was the second strongest predictor of regional richness and, together with the current area, explained almost 80% of the variance. This is consistent with recent refinements of the theory of island biogeography that incorporate the effect of Late Quaternary climate oscillations on oceanic islands (Fernández-Palacios et al. 2016, Weigelt et al. 2016). Pleistocene glacial-interglacial cycles acted like a *historical sieve* (Körner 1995) on alpine plant diversity. During glacial periods, downslope shifts of the alpine belt resulted in increased surface area and connectivity of tropical alpine archipelagos, as well as colonisation and diversification processes in mid-latitude mountain ranges that favoured in situ speciation (Flantua et al. 2020). The high species richness found in the Andes is probably the result of multiple contingencies related to South American tropical diversity and strong past connectivity of these mountains (Flantua et al. 2019), which are not co-occurring in any other tropical region. On the other hand, in Central Asian mountains, the emergence of habitat corridors during glacial periods resulted in extensive, long-distance dispersal with the consequent admixture of previously isolated floras (Agakhanyantz and Lopatin 1978, Agakhanjanz and Breckle 1995). Indeed, the Pamir Mountains are a continental hub for floristic migrations (the Pamir Knot) that connects south-central Asian ranges to the northern Siberian mountains (Agakhanjanz and Breckle 1995), whereas the Altai Mountains connect diversity between Euro-Siberian and Central Asian floristic regions (Chytrý et al. 2012). Our results also show a positive relationship between regional richness and soil pH variability – a surrogate for bedrock heterogeneity – largely driven by the Pamir and Altai Mountains. This finding confirms the effect of habitat heterogeneity on species richness inherent to larger areas (Lomolino 2000) through the occurrence of more diverse bedrock types (Moser et al. 2005).

Community patterns and drivers

At the community scale, the latitudinal pattern of species richness was less pronounced than at the regional scale, with a single peak at mid-latitudes of the northern hemisphere but a wide range of values within all regions. While controlling for plot size, we found a

positive effect of evapotranspiration of the growing season and a negative effect of soil pH on community richness. The former is consistent with the species-energy hypothesis, which states that more productive communities (i.e. where higher temperatures and solar radiation support greater photosynthetic rates) are also richer in species (Wright 1983). The latter could be explained by the absence of strongly acidic soils (pH < 4) in our dataset. Furthermore, soils with high pH values may be linked to reduced nutrient availability in harsh conditions and the confounding effect of reduced precipitation (Chytrý et al. 2007, Palpurina et al. 2017), explaining the lower species richness in our dataset. Despite the underlying causes of these effects, our results are in line with the role of energy-driven processes and bedrock mineralogy as determinants of vascular plant species richness in alpine communities (Moser et al. 2005, Vonlanthen et al. 2006, Lenoir et al. 2010). Nevertheless, evolutionary and historical factors may also affect current patterns of community richness (Ricklefs and He 2016). The Nearctic realm exhibited lower community richness than any other biogeographical realm, possibly due to limited evolutionary radiation of the North American temperate flora (Qian and Ricklefs 2000). In addition, the velocity of climate change and the LGM extent of alpine area were both positively related to community richness, indicating that the greater availability of alpine habitats in the past influences plant species richness at the community scale (Pärtel and Zobel 1999).

Large-scale environmental factors, however, only explained a limited proportion of the variation in community richness compared to regional and sub-regional effects, suggesting that dispersal-related processes and other spatially structured factors strongly influence local richness patterns (Dormann et al. 2007). In alpine landscapes, these effects are regulated by elevational and meso-topographical gradients that affect microclimatic conditions and local plant diversity (Bruun et al. 2006, Scherrer and Körner 2011, Jiménez-Alfaro et al. 2014). A weak influence of global macroclimatic gradients on local communities has also been detected for functional diversity across plant formations (Bruelheide et al. 2018), but it had not been tested before on a single ecosystem. Our results therefore support the dominant role of within-region effects linked to postglacial spatial configuration and historical contingencies, rather than macroclimatic factors, when explaining the global variation of alpine local communities.

Data constraints and assumptions

Despite including several alpine regions across all continents and latitudes, our dataset lacked information about some outstanding centres of alpine plant diversity such as the Himalayas and Hengduan Mountains (Favre et al. 2015, Xing and Ree 2017, Muellner-Riehl et al. 2019, Ding et al. 2020) or the Caucasus (Agakhanjanz and Breckle 1995, Körner 1995), due to the limited availability of plot data from these areas. Therefore, our results related to the latitudinal patterns of regional and community richness could be

further refined by the future addition of data from currently missing regions. Yet, our aim was not to present a complete census of global alpine regions, but rather to assess their richness patterns and the corresponding drivers using a representative sample. In this respect, the collection of georeferenced vegetation plots presented here encompasses all continents and a wide range of latitudes; it represents regions with markedly different biogeographic history, vegetation types growing on different substrates, and covers large portion of the climatic envelope of global alpine areas (Appendix 2 Figure A2.1). Despite the lack of some remarkable alpine regions, our dataset allowed us to highlight the presence of extra-tropical alpine diversity centres and the importance of historical factors in shaping the current alpine plant richness patterns. We also note that the use of heterogeneous surveys from different collectors may create issues related to different sampling effort among regions. We controlled for sampling effort in two ways. First, we used rarefaction and extrapolation techniques that assumed that the spatial distribution of plots in each region was representative of the regional diversity. Although this assumption is difficult to prove without additional data, we note that our regional samples were selected to capture the local heterogeneity of vegetation types and covered a wide range of elevations in all regions (Appendix 2 Table A2.3), thus increasing the probability that our regional richness estimates correlate with regional species pools. Second, we explicitly quantified the proportion of the alpine area actually sampled in each region, thus allowing interregional comparisons even when the samples covered very different extents, or only a small fraction of the total available alpine area (e.g. Ladakh Range, Pamir Mountains or Southern Cordillera Occidental Peru,).

In addition, we note that taxon concepts may not be consistently applied across all datasets, i.e. they are the result of *lumping* and *splitting* of taxa delimitations that change with time and from place to place (Rouhan and Gaudeul 2014, Wiser 2016). Despite a harmonised species nomenclature cannot fully account for this taxonomic bias (Wiser 2016), it still represents the most effective tool to address taxonomic inflation in macroecological studies (Isaac et al. 2004). Indeed, by correcting misspelt names and merging synonyms, we assume that the main sources of error relevant to the estimation of species richness in different regions were removed, while remaining issues about potential pitfalls in species' geographic distribution (Boyle et al. 2013) are not pertinent to this study.

Conclusions

Overall, we found that the latitudinal distribution of plant species richness in alpine ecosystems is decoupled from the general latitudinal diversity gradient and that it relates to regional idiosyncrasies, rather than macroclimatic gradients. Although our results are conclusive enough to support that current and historical effects of area, isolation and environmental heterogeneity exert an overarching influence on vascular plant richness in

global alpine ecosystems, we are still far from understanding the processes behind such effects. Future alpine research should therefore consider local information about soil biotic and abiotic composition, topographical features, and microclimatic variation at the regional scale. Additionally, further efforts should be oriented toward the collection of plant community data from underrepresented regions. Indeed, this work is the starting point for defining global hotspots of alpine plant diversity and further investigations including patterns of endemism, functional variation and phylogenetic diversity are still needed. This kind of information, together with dynamic regional diversity models accounting for spatiotemporal connectivity, will provide a better understanding of the patterns we have found here, and a tool for the effective conservation of alpine biodiversity in response to climate change.

Chapter 3
Global functional variation in alpine vegetation

Testolin R., Carmona C. P., Attore F., Borchardt P., Bruelheide H., Dolezal J., Finckh M., Haider S., Hemp A., Jandt U., Korolyuk A., Lenoir J., Makunina N., Malanson G. P., Ladislav M., Noroozi J., Nowak A., Peet R. K., Peyre G., Sabatini F. M., Šibík J., Sklenář P., Vassilev K., Virtanen R., Wiser S. K., Zibzeev E. G., Jiménez-Alfaro B.
Global functional variation in alpine vegetation. *Journal of Vegetation Science.* https://doi.org/10.1111/ jvs.13000

Abstract
What are the functional trade-offs of vascular plant species in global alpine ecosystems? How is functional variation related to vegetation zones, climatic groups and biogeographic realms? What is the relative contribution of macroclimate and evolutionary history in shaping the functional variation of alpine plant communities? We compiled a dataset of alpine vegetation with 5,532 geo-referenced plots, 1,933 species and six plant functional traits. We used principal component analysis to quantify functional trade-offs among species and trait probability density to assess the functional dissimilarity of alpine vegetation in different vegetation zones, climatic groups and biogeographic realms. We used multiple regression on distance matrices to model community functional dissimilarity against environmental and phylogenetic dissimilarity, controlling for geographic distance. The first two PCA axes explained 66% of the species' functional variation and were related to the leaf and stem economic spectra, respectively. Trait probability density was largely independent of vegetation zone and macroclimate but differed across biogeographic realms. The same pattern emerged for both species pool and community levels. The effects of environmental and phylogenetic dissimilarities on community functional dissimilarity had similar magnitude, while the effect of geographic distance was negligible. Plant species in alpine areas reflect the global variation of plant function, but with a predominant role

of resource-use strategies. Current macroclimate exerts a limited effect on alpine vegetation, mostly acting at the community level in combination with evolutionary history. Global alpine vegetation is functionally unrelated to the vegetation zones in which it is embedded, exhibiting strong functional convergence across regions.

Introduction

Alpine environments (i.e. high-elevation habitats above the climatic treeline) cover about 3% of land outside Antarctica (Körner et al. 2011, Testolin et al. 2020) and can be found in all continents and at all latitudes (Körner 2003). These habitats include global biodiversity hotspots (Myers et al. 2000) and support about 10,000 plant species worldwide, many of which are endemics (Körner 2003). Globally, the vegetation of alpine environments is dominated by few growth forms (e.g. dwarf shrubs, graminoids, herbaceous rosettes and cushions), reflecting functional adaptations to the characteristics of high-mountain ecosystems, such as low temperatures, short growing season and limited nutrient availability (Körner 1995, 2003, 2020, Dolezal et al. 2016, Stanisci et al. 2020). Some growth forms, however, are more abundant in certain regions (e.g. evergreen dwarf shrubs in boreal ranges, succulents in semi-arid zones, sclerophyllous species in mediterranean-type climates) or are unique to specific areas, such as giant rosettes in tropical mountains (e.g. *Espeletia* and *Dendrosenecio*) (Nagy and Grabherr 2009). Nevertheless, growth forms are poor descriptors of the functional adaptations of alpine vegetation, with several features of alpine plants found to vary widely within a single growth form (Körner 1995), or showed no variation among different growth forms (Körner et al. 2016).

In alpine environments, plants have adapted to low temperatures and low nutrient supply (Nagy and Grabherr 2009). In comparison to lowland species, alpine plants are normally shorter, with smaller leaves and lighter seeds (Körner 2003, Pellissier et al. 2010). These traits increase frost tolerance, photosynthetic efficiency and dispersal success, so they are globally ubiquitous in alpine vegetation (Körner 2003). Yet, considerable variation remains among species from different alpine regions, e.g., differences in leaf traits (Halloy and Mark 1996, Pyankov et al. 1999), suggesting a response to environmental and evolutionary drivers. Most research comparing plants across alpine regions, however, has only focused on individual traits. Assessing how multiple traits vary simultaneously may allow identification of the trade-offs of plant form and function, i.e., the different strategies used by alpine plants for resource acquisition, growth and reproduction (Grime 1974, Díaz et al. 2016, Bruelheide et al. 2018).

Global alpine areas can be grouped according to their macroclimate (Testolin et al. 2020), and they are linked to different vegetation zones (Walter and Box 1976) and biomes characterised by distinct evolutionary history and own species pools (Mucina 2019). Indeed, present-day alpine floras are the result of upward shifts of species undergoing

regional radiations and long-distance migrations associated with the displacement of cold-climate biomes, such as during the Pleistocene glacial cycles (Billings 1974, Hörandl and Emadzade 2011, Jiménez-Alfaro et al. 2021). The historical legacy of ancestral species, which may have belonged to different vegetation zones and biogeographic realms, together with the environmental filtering of the current macroclimate, have determined the diversity of alpine trait pools, i.e. the total set of plant trait values found in an alpine region today.

Factors selecting for favourable combinations of traits are generally scale-dependent (Garnier et al. 2016). At continental scales, trait pools are defined by the interplay of macroclimate and evolutionary history (Moncrieff et al. 2016, Mucina 2019), with the latter constrained by the long-term isolation of major landforms (Chaboureau et al. 2014) and by the phylogenetic origin of species occurring in a biogeographic realm (Holt et al. 2013, Daru et al. 2017, 2018). At the scale of local plant communities, trait pools are further constrained by biotic and abiotic filters that select species assemblages with favourable trait syndromes (Lavorel et al. 1997, Zobel 2016, Mucina 2019). As a consequence, the traits values in communities might deviate from those of trait pools (Grime 2006, Marks and Lechowicz 2006) and depend on local conditions (e.g. soil properties and topoclimate) rather than macroclimate (Bruelheide et al. 2018). However, considering the varied origin of plants across global alpine environments (Billings 1974), an evolutionary mark on functionality might still be detectable at the level of communities (Srivastava et al. 2012). Linking local filtering to evolutionary and biogeographic history remains a major challenge in macroecology and new approaches that incorporate different facets of diversity are required to understand patterns and processes across scales (Pärtel et al. 2016, Ladouceur et al. 2019). Disentangling the effect of macroclimate and evolutionary history might therefore open new prospects for understanding, and possibly predicting, biodiversity patterns in alpine regions.

Here, we provide the first overview of the functional variation of alpine vegetation and an attempt to infer possible drivers across spatial scales. Specifically, we aim to: 1) describe the functional trade-offs of vascular plant species in global alpine ecosystems; 2) assess the functional variation of trait pools and local communities among vegetation zones, climatic groups and biogeographic realms; and 3) quantify the relative contribution of macroclimate and evolutionary history in shaping the functional variation of alpine plant communities.

Material and methods

Study system and data selection

We used data featuring alpine vegetation defined as any vascular plant community above the climatic treeline (Körner 2003). In addition to strictly zonal habitats dominated by

graminoids, forbs, and dwarf shrubs, we also included snow-patch plant communities and vegetation on rocks and screes, as they are also found ubiquitously across the alpine belt. The plot data collected by the authors, compiled from the literature, or stored in the sPlot database (v2.1) (Bruelheide et al. 2019), was first filtered using habitat classifications of the data sources (Appendix 3, Table A3.1), and then further reduced by excluding plots with tree species or incomplete taxonomic identification. We standardised datasets from different sources by identifying a minimum common set of plot attributes including plot size, elevation, and geographic coordinates. Species names were harmonised using the Taxonomic Name Resolution Service (Boyle et al. 2013) (https://tnrs.biendata.org) with default settings. Species cover values coded with discrete scales were transformed to the mean value of the corresponding percentage interval. Subspecies and varieties were merged at the species resolution by summing the respective percentage cover values. At this point, the dataset consisted of 8,419 plots of alpine vascular vegetation with 4,651 plant species recorded.

Each plot was assigned to the vegetation zone dominating the same ecoregion, i.e. montane grasslands and shrublands, temperate broadleaf and mixed forests, temperate coniferous forests, tropical and subtropical moist broadleaf forests, and tundra (Olson et al. 2001). These physiognomic types encompassing large areas are presumed to contribute ancestral clades with potential impact on current alpine trait pools. We also assigned the plots to one of three groups summarizing the climatic variability of global alpine areas, and representing regional alpine biomes in the classification scheme of Testolin et al. (2020): 1) oceanic, characterised by greater precipitation and relative temperature stability; 2) continental, defined by low precipitation and large annual temperature amplitudes; 3) subtropical, encompassing both tropical and subtropical alpine areas, and characterised by low annual precipitation and contrasting diurnal temperature cycles. Single plots falling slightly outside the boundaries of the commonest vegetation zone or climatic group for a given region were manually assigned to those. Finally, each plot was assigned to a biogeographic realm: Afrotropic, Australasia, Nearctic, Neotropic, and Palearctic. Each realm represents a broadly defined geographic region characterised by typical flora and fauna and supposed to have a distinct evolutionary history.

For each species, we extracted the gap-filled trait information from the TRY database (v5.0) (Shan et al. 2012, Fazayeli et al. 2014, Schrodt et al. 2015, Kattge et al. 2020), provided by the sPlot database as species average values (Bruelheide et al. 2019). We selected six plant functional traits: leaf area (one-sided surface of the fresh leaf), specific leaf area (leaf area per leaf dry mass; SLA), leaf dry matter content (leaf dry mass per leaf fresh mass; LDMC), leaf nitrogen (N) (N per leaf dry mass), plant height (maximum total height of the plant), and seed mass (dry mass of the seed). We chose these traits because they are commonly used to characterise tundra and alpine vegetation (Bjorkman et al. 2018, Thomas et al. 2019, Liancourt et al. 2020), and they are fully representative

of plant ecological strategies (Díaz et al. 2016). The gap-filling process employed hierarchical Bayesian modelling to estimate missing trait values based on other traits available in TRY for individuals of the same species (Schrodt et al. 2015). Only traits of those species having at least one measured trait observation were imputed. Of all species that were selected based on trait data availability, 99% had at least one measurement in TRY for leaf area, 96% for SLA, 98% for LDMC, 97% for leaf N, 91% for plant height and 85% for seed mass. The values of plant height, leaf area and seed mass were $\log_{10}$-transformed to reduce skewness. Species for which trait information was not available (n = 2517) were removed. At the community level, we only considered plots with at least 50% cumulative cover of species with trait data. We chose 50% cover as a trade-off between the inclusion of plots for which trait data were scarce versus the representativeness of dominant vegetation in each community. An alternative set of results obtained choosing more conservative thresholds of 75% and 90% cumulative cover of species with trait data (see Results; Appendix 3 Supplementary Text A3.1, Table A3.2) showed minor differences with the results presented here. The final dataset consisted of 5,532 vegetation plots between 0.25 and 400 m^2 in size sampled between 1923 and 2019, with 1,933 species belonging to five vegetation zones, three climatic groups and five biogeographic realms (Figure 3.1). All the following analyses have been carried out using R 3.6.3 (R Core Team 2020).

Functional trade-offs and variation of trait pools

To analyse the relationships among traits of the plant species in our dataset, we performed a principal component analysis (PCA) of the standardised values of the six traits. The loadings of the individual traits were then used to identify the main axes of variation and possible trade-offs of plant strategies (Díaz et al. 2016).

To compare the trait pools across the vegetation zones, climatic groups and biogeographic realms, we employed trait probability densities, a scale-independent framework that implements the concept of the niche hypervolume while accounting for the probabilistic nature of traits (Carmona et al. 2016). This method requires both the mean and the standard deviation of each trait for all the species. As reliable information on the standard deviations was not available, we assumed it to be constant across species and estimated it as 50% of the standard deviation of all species' mean values for each trait (Lamanna et al. 2014, Carmona 2019). Then, we calculated the individual trait pools as the probability densities for each vegetation zone, climatic group and biogeographic realm using the package *TPD* (Carmona 2019), accounting for species frequencies (i.e. the number of plots in each group where a certain species was recorded). We assessed the functional variation of trait pools using kernel density plots and calculated pair-wise functional dissimilarities among trait pools using the *dissim* function of *TPD* package. The significance of the

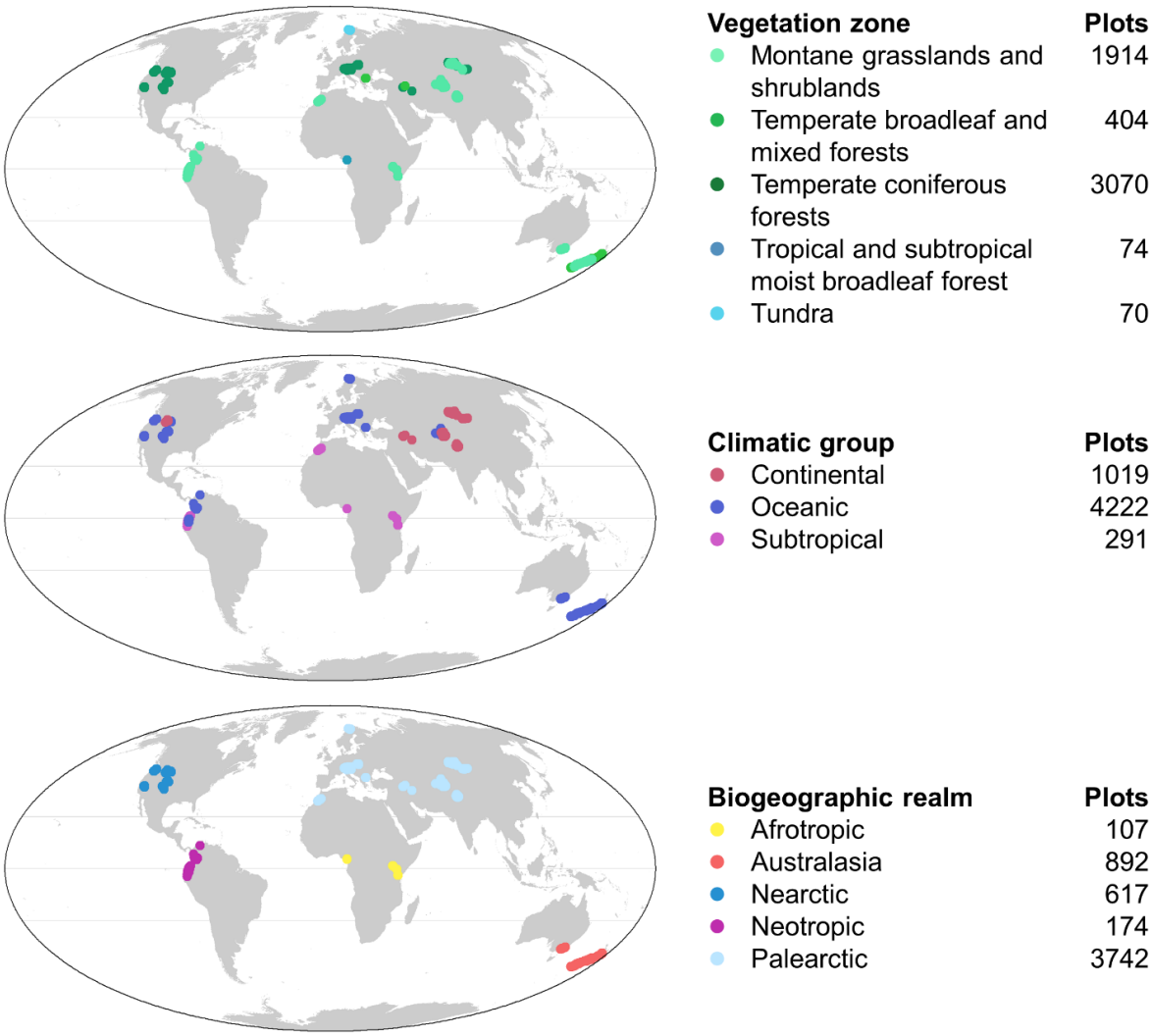

Figure 3.1. Spatial distribution of 5,532 alpine vegetation plots across vegetation zones, climatic groups and biogeographic realms.

pair-wise dissimilarities was evaluated in a null-modelling framework (Geange et al. 2011, Traba et al. 2017) by pooling the observations from each pair, randomizing the species' labels 999 times while keeping the number of species constant for each group and ranking the pair-wise dissimilarity values among the simulated trait probability densities. This allowed us to calculate the Bonferroni-corrected p-values for each comparison as:

$$p = \left(1 - \frac{r_{obs}}{i+1}\right) \times n$$

where r_{obs} is the rank of the observed dissimilarity value among the simulated ones, i is the number of simulations, and n is the number of pair-wise comparisons (Legendre and Legendre 2012, Traba et al. 2017). To assess the overall functional variation among

vegetation zones, climatic groups and biogeographic realms, while excluding potentially redundant information, we calculated multi-trait probability densities by using the first two axes of the PCA of the six traits and repeated the same analyses described above for individual traits.

Functional variation of communities

To analyse the variation in trait values across plant communities, we calculated the multi-trait functional dissimilarities between all vegetation plots as described above, accounting for the cover of the species within each plot. The pair-wise dissimilarities were displayed in the same PCA space as the individual species by calculating the community weighted means of the first two PCA axes for each plot. This allowed the visualisation of the functional variation of plots belonging to different groups. Significant differences among plots belonging to different vegetation zones, climatic groups and biogeographic realms were tested using PERMANOVA (Anderson 2001), implemented by the *adonis* function of the R package *vegan* (Oksanen et al. 2019), with 999 permutations.

To quantify the relative contribution of climate and evolutionary history in determining functional variation among communities, we modelled community functional dissimilarity as a function of environmental and phylogenetic dissimilarity while controlling for geographic distance. Phylogenetic data were provided by the sPlot database based on the phylogeny of Qian & Jin (2016). Species present in our dataset but missing from this phylogeny were added next to a randomly selected congener, if available (Bruelheide et al. 2019). First, we selected the set of species for which both trait and phylogenetic data were available (n = 1,674) and further subset the vegetation plots by keeping those with at least 50% cumulative cover of these species. Thus, we obtained a subset of 5,047 plots and calculated the multi-trait functional dissimilarities between all possible pairs of plots as described above. We also performed alternative selections of plots with 75% and 90% cumulative cover of species with trait and phylogenetic data to assess the effect of a more conservative cumulative cover threshold on the model results (see Results; Appendix 3 Supplementary Text A3.1). Then, we built a set of climatic variables known to affect alpine vegetation (Körner 2003, Moser et al. 2005, Nagy and Grabherr 2009) using data from CHELSA bioclimatic database at ~1 km spatial resolution (Karger et al. 2017). The included variables were mean temperature, precipitation, growing degree days and mean potential evapotranspiration. Each variable was calculated within the time frame of the growing season, defined as days with mean temperature >0.9 °C (Paulsen and Körner 2014). Growing degree days (i.e. the sum of monthly temperatures > 0.9 °C multiplied by the total number of days) were calculated using the *growingDegDays* function of the R package *envirem* (Title and Bemmels 2018). Mean potential evapotranspiration of the growing season was estimated with the *hargreaves* function of the R package *SPEI* (Beguería and Vicente-Serrano 2017), using maximum and minimum monthly values of

temperature and monthly precipitation. The monthly values of potential evapotranspiration obtained were then averaged across months with mean temperature above 0.9 °C. We standardised the four climatic variables and calculated the Euclidean distance among each pair of plots as a measure of environmental dissimilarity.

To account for the evolutionary history of plant species in different communities, we also calculated the pair-wise phylogenetic dissimilarity between plots (Ives and Helmus 2010) with the *pcd* function of the R package *picante* (Kembel et al. 2010). To account for the spatial aggregation of plots and unmeasured regional effects on the estimated functional dissimilarity, we calculated the pair-wise geographical distances between plots. Finally, we modelled functional community dissimilarity against these three distanced-based predictors using multiple regression on distance matrices (MRM) with the *lm* function. Despite our measure of functional dissimilarity is constrained between 0 and 1, our dataset mainly encompassed intermediate levels of functional turnover (Appendix 3 Figure A3.1), allowing us to treat it as approximately linear (Ferrier et al. 2007). Further, a linear modelling approach allowed us to calculate the adjusted R^2 of all the sub-models necessary to perform variance partitioning (Borcard et al. 1992, Swenson 2014).

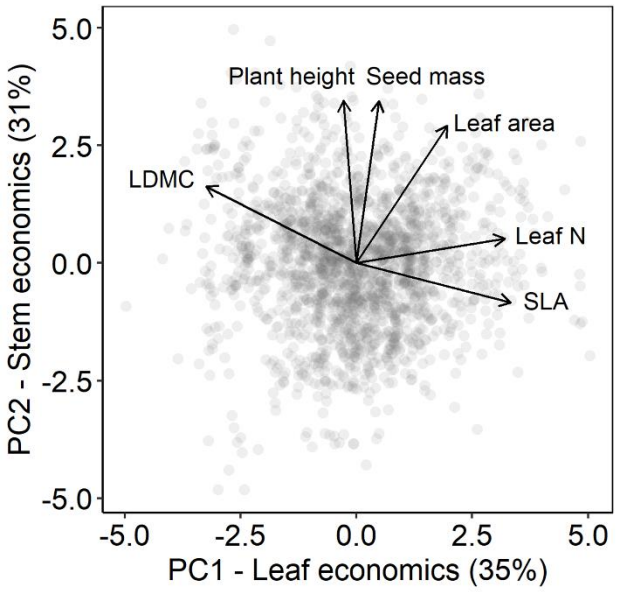

Figure 3.2. Functional variation of 1,933 vascular plant species in global alpine areas along the first two principal components of six traits representing main functional trade-offs. SLA = Specific leaf area; LDMC = Leaf dry matter content.

Results

The first two PCA axes accounted for 66% of the total trait variation among species. The other axes explained less variation than expected by chance and were not considered further. The first axis (PC1; 35% of variation) was mainly related to variations in LDMC, leaf N and SLA, while the second axis (PC2; 31% of variation) was linked to leaf area, plant height and seed mass (Figure 3.2, Appendix 3 Table A3.3).

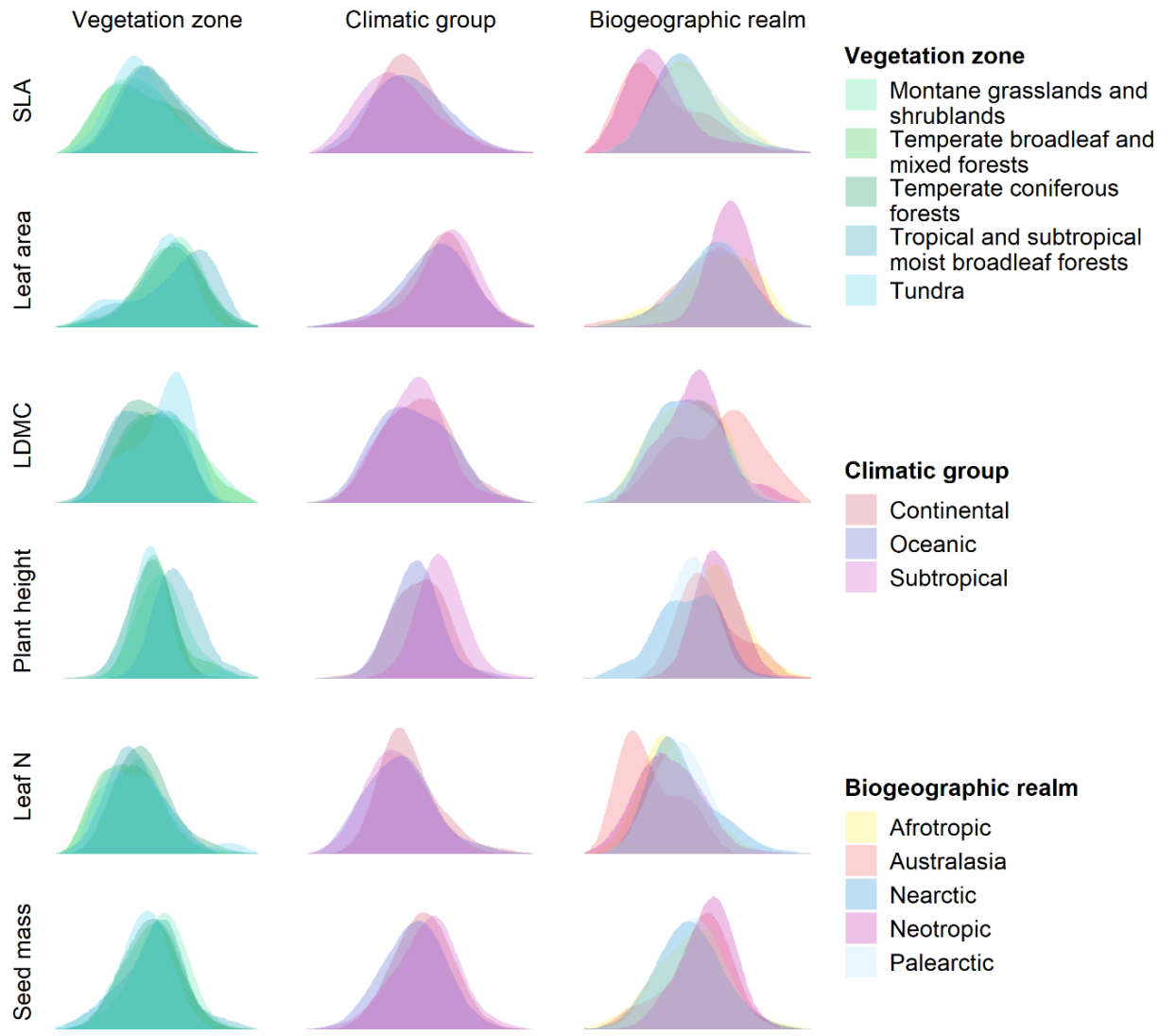

Figure 3.3. Kernel density plots of trait pools estimated using trait probability density for six individual plant functional traits among vegetation zones, climatic groups and biogeographic realms. SLA = Specific leaf area; LDMC = Leaf dry matter content.

When focusing at the level of vegetation zones, we observed negligible differences in trait probability density and low functional dissimilarity among trait pools. The only exception was the alpine vegetation related to tropical and subtropical moist broadleaf forests, which exhibited slightly greater plant height values compared to other vegetation zones (Figure 3.3; Appendix 3 Table A3.4). Among climatic groups, subtropical alpine areas also exhibited greater plant height values when compared to oceanic and continental ones, with minor variation in the distribution of other traits (Figure 3.3; Appendix 3 Table A3.4). However, we observed considerable variability in trait probability density among biogeographic realms. The alpine vegetation of the Australasia and Neotropic realms had

lower SLA compared to that of the others and similar values of plant height to the Afrotropic, which were greater than those of the Palearctic and Nearctic. As for leaf area and seed mass, the Neotropics generally showed higher values compared to the Palearctic and Nearctic, which in turn presented higher leaf N and lower LDMC than Australasia (Figure 3.3; Appendix 3 Table A3.4). Multi-trait patterns seemingly reflected those observed at the single trait level. Among vegetation zones and climatic groups, multi-trait functional dissimilarities were not significant or very modest (Table 3.1). Conversely, among biogeographic realms, Palearctic and Nearctic were similar to one another and differentiated from Neotropic and Australasia, with the Afrotropic pool taking an intermediate position between the two groups.

Table 3.1. Multi-trait pair-wise dissimilarities (Diss) of alpine vegetation between vegetation zones, climatic groups and biogeographic realms. Significant dissimilarities ($P < 0.05$) are in bold.

Vegetation zones	**Diss**
Montane grasslands and shrublands - Temperate broadleaf and mixed forests	0.16^{ns}
Montane grasslands and shrublands - Temperate coniferous forests	$\mathbf{0.27^{**}}$
Montane grasslands and shrublands - Tropical and subtropical moist broadleaf forests	0.29^{ns}
Montane grasslands and shrublands - Tundra	0.27^{ns}
Temperate broadleaf and mixed forests - Temperate coniferous forests	$\mathbf{0.24^{**}}$
Temperate broadleaf and mixed forests - Tropical and subtropical moist broadleaf forests	$\mathbf{0.34^{*}}$
Temperate broadleaf and mixed forests – Tundra	0.23^{ns}
Temperate coniferous forests - Tropical and subtropical moist broadleaf forests	0.28^{ns}
Temperate coniferous forests – Tundra	0.25^{ns}
Tropical and subtropical moist broadleaf forests - Tundra	0.38^{ns}
Climatic groups	
Continental - Oceanic	$\mathbf{0.19^{**}}$
Continental - Subtropical	$\mathbf{0.22^{*}}$
Oceanic - Subtropical	$\mathbf{0.31^{**}}$
Biogeographic realms	
Afrotropic - Australasia	0.40^{ns}
Afrotropic - Nearctic	0.26^{ns}
Afrotropic - Neotropic	0.29^{ns}
Afrotropic - Palearctic	0.23^{ns}
Australasia - Nearctic	$\mathbf{0.47^{**}}$
Australasia - Neotropic	0.36^{ns}
Australasia - Palearctic	$\mathbf{0.45^{**}}$
Nearctic - Neotropic	$\mathbf{0.43^{**}}$
Nearctic - Palearctic	0.13^{ns}
Neotropic - Palearctic	$\mathbf{0.41^{**}}$

Significance codes: ***: $p<0.001$; **: $p< 0.01$; *: $p<0.05$; ns: $p \geq 0.05$.

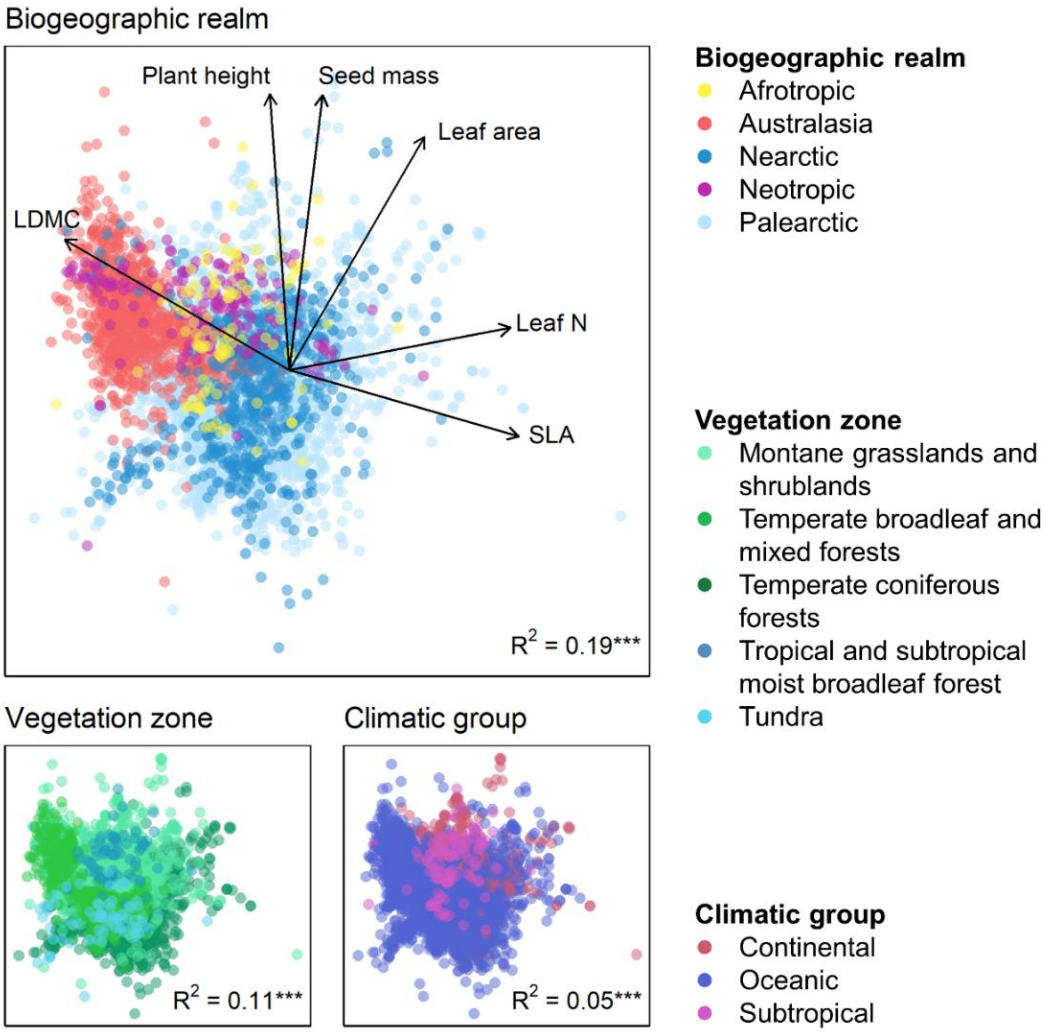

Figure 3.4. Functional variation of alpine plant communities. Each dot represents a vegetation plot, whose position is based on community weighted means of the first two axes of a PCA of six functional traits. The arrows represent the trait loadings on the PCA axes. The total variance of community dissimilarity explained by the groups is reported in the bottom-right corner of each graph. SLA = Specific leaf area; LDMC = Leaf dry matter content. Significance codes: ***: $p<0.001$; **: $p< 0.01$; *: $p<0.05$; ns: $p \geq 0.05$.

Multi-trait dissimilarities of alpine plant communities revealed distinct patterns among biogeographic realms (Figure 3.4) , with Australasian, Afrotropic and Neotropic plots characterised by larger values of LDMC and smaller SLA and leaf N. PERMANOVA showed that biogeographic realms explained 19% of the functional variation (R2 = 0.19, p = 0.001), vegetation zones explained 11% (R2 = 0.11, p = 0.001) and climatic groups explained 5% (R2 = 0.05, p = 0.001). The same patterns emerged when considering more conservative thresholds of cumulative cover of species with trait data (Appendix 3 Supplementary Text A3.1., Figure A3.2).

Finally, the MRM model fit on a subset of plots with available phylogenetic information explained 16.6% of the communities' functional dissimilarity. Environmental and phylogenetic dissimilarities both explained 6.2% individually, while 4% was shared between the two of them. Geographic distance exhibited a marginal effect, explaining only 0.3% (Figure 3.5). Again, adopting more conservative thresholds of cumulative cover of species with trait and phylogenetic data did not significantly affect the results (Appendix 3 Supplementary Text A3.1., Figure A3.3).

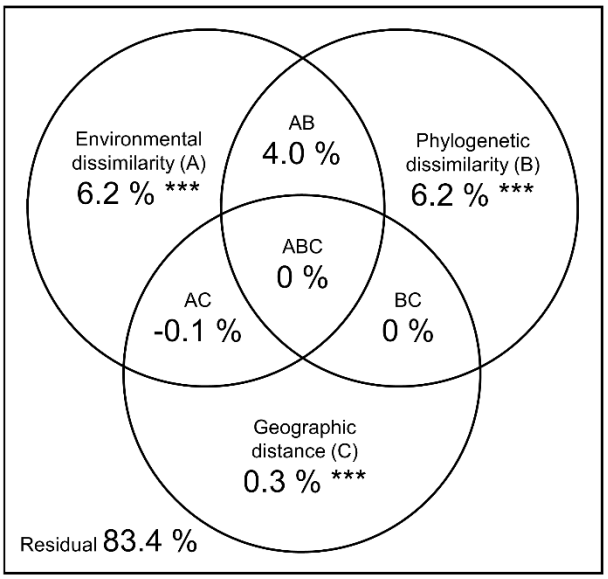

Figure 3.5. Venn diagram of multi-trait functional dissimilarity of alpine vegetation communities displaying variance partitioning among environmental dissimilarity (A), phylogenetic dissimilarity (B), and geographic distance (C). Significance codes: ***: $p<0.001$; **: $p< 0.01$; *: $p<0.05$; ns: $p \geq 0.05$.

Discussion

Functional trade-offs of alpine plant species

We selected six traits linked to resources use, growth and reproduction of plants, and used PCA to describe the functional trade-offs of 1,933 vascular plant species in global alpine ecosystems. PC1 differentiated strategies in terms of investments of nutrients and dry mass in leaves and hence the leaf economics spectrum (Wright et al. 2004). This spectrum discriminates between species, those with high leaf construction costs (high LDMC, low SLA) and low leaf nutrient concentrations (low leaf N) related to slower vegetative development rates versus fast-growing species with high leaf nutrient concentration and cheaper construction costs that promote a quick return of the investments in nutrients and carbon (Wright et al. 2004). PC2 reflected differences in plant size, conforming to the stem economics spectrum (Baraloto et al. 2010) that separates taller plants able to carry larger leaves and seeds (large plant height, leaf area and seed mass) from smaller plants. These results agree with previous analyses of alpine and tundra vascular plants (Dolezal et al. 2016, Thomas et al. 2019) and are consistent with directions of variation in the global spectrum of plant form and function (Díaz et al. 2016). Nevertheless, the

predominance of variation in resource-use strategies rather than size reflects the absence of trees and tall shrubs in alpine vegetation, and the general abundance of prostrate species which are mainly differentiated by local conditions. Small size allows alpine plants to respond to and modify the microclimate near the ground (Geiger et al. 2003) by accumulating heat under the leaf canopy regardless of fluctuations of the macroenvironment (Körner et al. 1989, Körner 2003). Additionally, the main variation observed along PC1 could be explained by the greater variability of leaf construction costs of alpine plants, which depend on local temperature, frost stress and prolonged exposure to light (Körner et al. 1989). Any of these may vary widely even within a single mountain range, hence the greater variation of the related traits (Stanisci et al. 2020).

Variation of alpine trait pools

Trait pools of alpine plants were largely independent of the vegetation zone, suggesting that alpine vegetation is functionally different from the surrounding flora in which it is embedded. Thus, the convergence of growth forms that characterises alpine vegetation (Körner 2003, 2020, Aubert et al. 2014) follows adaptation to similar ecological conditions (Givnish 2010, 2016, Hörandl and Emadzade 2011, Hughes and Atchison 2015). This finding contrasts with the view of alpine areas as elevational *orobiomes* closely related to the *zonobiomes* they originate from (Walter and Box 1976) but agrees with the distinction of alpine ecosystems from other terrestrial biomes (Testolin et al. 2020). Trait pools were also convergent among climatic groups, indicating that macroclimatic differences above the treeline have little influence on the functional features of alpine vegetation, which is consistent with the similar patterns of primary productivity found across global alpine biomes (Testolin et al. 2020).

However, we observed some divergence of trait pools across biogeographic realms. Such functional differences might emerge even among structurally similar plant groups when these are compared across areas with distinct evolutionary histories (Alvarado-Cárdenas et al. 2013). Specifically, we observed a distinction between the trait pool of the Holarctic realm and those of the Neotropic and Australasia, while the trait pool of the Afrotropic realm occupied an intermediate position. This pattern likely reflects different evolutionary histories and adaptations of alpine vegetation in the Northern and Southern Hemispheres (Billings 1974). Indeed, much of the ancestral alpine vascular flora originated during the Miocene (23-5 Ma) from Arcto-Tertiary and Antarcto-Tertiary floras through upward migration and evolution of lowland taxa (Billings 1974). Consequently, Holarctic alpine vegetation shares many species with the Arctic (Billings 1974) and has major links with Afrotropic alpine species (Linder 2014, Carbutt and Edwards 2015). In contrast, a large part of Neotropic alpine plants originated locally through migration and adaptation of Neotropical lowland species (Sklenář et al. 2011), some of which also contributed to Afrotropic lineages (Linder 2014). Finally, the functional similarity of Neotropics and

Australasia probably derived from both migration (Raven and Axelrod 1972) and convergent evolution during the Pliocene (5 Ma) and the Pleistocene (2.5 Ma), when further mountain uplift and repeated glaciations led to the diversification of the respective alpine floras (McGlone et al. 2001, Winkworth et al. 2005, Sklenář et al. 2011, Madriñán et al. 2013).

Functional variation of alpine communities

Communities were not functionally distinct among vegetation zones or climatic groups, while biogeographic realms exhibited greater discriminatory power, as they did for the trait pools. Australasian communities form an isolated group characterised by leaves with high construction costs, which agrees with the greater abundance of sclerophyllous dwarf shrubs in the Australasian alpine flora relative to other global alpine regions (Ballantyne and Pickering 2015). The functional distinctness of Australasian alpine communities from Holarctic and Tropical ones may also reflect differences in trait pools between the two hemispheres and could be related to the long-time isolation (45 – 49 Ma) of Australasian landforms from other biogeographic realms of Gondwanan origin (Raven and Axelrod 1972). Holarctic and Tropical communities, however, were not as functionally distinct as their trait pools, indicating that other processes apart from regional evolutionary history are involved at the local scale. Indeed, although our model highlighted the presence of a phylogenetic signal in functional dissimilarity, environmental dissimilarity explained an equal amount of variance. This is consistent with the process of niche conservatism in highly heterogeneous areas, where the retention of the ancestral niche characteristics could lead to both conservatism and divergence of the realised niche (i.e. the functional characteristics; Pyron et al. 2015). Nevertheless, the negligible effect of geographic distance and the large amount of unexplained variance point to fine-scale environmental factors (e.g. soil properties and topoclimate), disturbance and biotic interactions as the main drivers of community trait composition in alpine ecosystems (Grime 2006, Dolezal et al. 2019).

Assumptions and caveats

Even though we used the largest dataset of alpine vegetation ever collected, our study does not come without uncertainties. First, many mountain regions, including outstanding centres of alpine plant diversity such as the Qinghai-Tibet Plateau and Hengduan Mountains (Favre et al. 2015, Xing and Ree 2017, Muellner-Riehl et al. 2019, Ding et al. 2020), were not represented in our dataset, preventing us to provide a complete global picture of alpine plant functional variation. Still, our plots encompass alpine vegetation in six continents from boreal to tropical latitudes, allowing meaningful global comparisons that could be further refined by the future inclusion of additional alpine regions, especially in the tropical and subtropical belts. Second, when comparing functional dissimilarities

across geographical units and spatial scales, we presumed that the species for which trait data were available were also representative of the dominant vegetation in our study areas. For several tropical species, however, such data were not available, and we had to remove a large number of plots in Africa and South America. Although we recognise that this could have led to the exclusion of unusual combinations of traits and that even rare species can drive trait divergence among communities at the regional scale (Richardson et al. 2012), this is probably less relevant at the global level. Third, we note that our dataset encompasses vegetation plots of very different sizes (0.25 – 400 m^2). As species richness generally increases with area (Lomolino 2000), larger plots might be functionally richer than smaller ones (Smith et al. 2013, Wang et al. 2013), biasing the comparison among plots. However, when accounting for specie abundances – or, in our case, cover – the relationship between functional diversity indices and plot size tends to weaken or disappear because of species dominance and functional redundancy (Karadimou et al. 2016). Therefore, as the trait probability density framework accounts for the distribution of trait values in plant communities, plot size likely had a minor effect in the estimation of functional dissimilarity among alpine communities. Although we collected most of the plot data in alpine vegetation currently available, much effort is still needed to collect data with a consistent sampling protocol, including functional traits and a proper representation of species and vegetation types from disparate global regions.

Conclusions

This study provides the first overview of the global functional trait variation in alpine vegetation. While alpine species exhibit the same trade-offs observed in vascular plants globally, the absence of trees in alpine ecosystems leads to a greater variety of traits related to resource-use strategies rather than size. We found that alpine vegetation is scarcely related to the vegetation zones in which it is embedded and is largely independent of macroclimatic patterns, at least for the traits analysed in this study. However, evolutionary history seemingly affected current trait pools, and phylogenetic constraints and macroclimate equally determine the functional dissimilarity of communities. Overall, our results indicate a strong functional convergence of adult plant traits in global alpine vegetation, with implications at both regional and community level. This finding agrees with the functional convergence observed for regeneration traits in alpine plants across continents (Fernández-Pascual et al. 2020), further supporting a distinct delineation of alpine ecosystems in the context of the global biomes. Yet, other factors not accounted for in this study (e.g. soil properties, topoclimatic gradients) are likely influencing functional traits of alpine vegetation locally. In this respect, future work should be oriented toward the inclusion of additional fine-scale environmental characteristics, as well as trait data from tropical and subtropical species currently underrepresented in global datasets.

Conclusions

In this thesis, I provided a first overview of the diversity patterns of global alpine ecosystems in terms of macroclimate, taxonomic richness and plant functions. The climatic envelope of these environments is characterised by gradients of seasonality and continentality. Yet, these gradients do not affect the patterns of primary productivity, taxonomic richness, or functional variation of global alpine vegetation. Indeed, as alpine climate is independent form that of other biomes regardless of latitude, plant species richness in alpine ecosystems is largely decoupled from the general latitudinal diversity gradient. Likewise, alpine vegetation embedded in different lowland vegetation zones is functionally convergent and – similarly to primary productivity – is largely independent from macroclimatic patterns. However, the diversity of alpine vegetation is strongly related to biogeographic history. Indeed, while the present and historical abundance and heterogeneity of alpine habitats strongly affected large scale patterns of species richness, the functional variation of alpine communities still carries an imprint of the evolutionary origin of their species. Nevertheless, these results also point to other regional idiosyncrasies and fine-scale environmental factors as the main drivers of primary productivity, community species richness and plant functioning in alpine environments.

Overall, despite their global distribution and apparent heterogeneity, alpine environments form a distinct group of functionally convergent biomes, strongly decoupled from lowland environments, and with a varied biogeographic history, whose legacy can still be observed on current diversity patterns which are locally refined by fine-scale factors. Future alpine research should therefore consider local information about soil composition and topoclimate, in combination with the idiosyncrasies driving plant diversity in each mountain region. Further efforts should be also oriented toward the collection of plant community data from regions that were not included in this work. This thesis represents the starting point for improving our understanding of global patterns of alpine ecosystems and for the effective conservation of alpine biodiversity in response to climate change.

References

Agakhanjanz, O. and Breckle, S.-W. 1995. Origin and evolution of the mountain flora in middle asia and neighbouring mountain regions. - In: Chapin III, F. S. and Körner, C. (eds), Arctic and alpine biodiversity: Patterns, causes and ecosystem consequences. Ecological Studies (Analysis and Synthesis). Vol 113. Springer, pp. 63–80.

Agakhanyantz, O. E. and Lopatin, I. K. 1978. Main characteristics of the ecosystems of the Pamirs, USSR. - Arct. Alp. Res. 10: 397.

Alvarado-Cárdenas, L. O. et al. 2013. To converge or not to converge in environmental space: Testing for similar environments between analogous succulent plants of North America and Africa. - Ann. Bot. 111: 1125–1138.

Amatulli, G. et al. 2018. A suite of global, cross-scale topographic variables for environmental and biodiversity modeling. - Sci. Data 5: 1–15.

Anderson, M. J. 2001. A new method for non-parametric multivariate analysis of variance. - Austral Ecol. 26: 32–46.

Anthelme, F. and Dangles, O. 2012. Plant-plant interactions in tropical alpine environments. - Perspect. Plant Ecol. Evol. Syst. 14: 363–372.

Antonelli, A. et al. 2018. Geological and climatic influences on mountain biodiversity. - Nat. Geosci. 11: 718–725.

Aubert, S. et al. 2014. 1914-2014: A revised worldwide catalogue of cushion plants 100 years after Hauri and Schröter. - Alp. Bot. 124: 59–70.

Baker, K. et al. 2019. Decolonizing field ecology. - Biotropica 51: 288–292.

Ballantyne, M. and Pickering, C. M. 2015. Shrub facilitation is an important driver of alpine plant community diversity and functional composition. - Biodivers. Conserv. 24: 1859–1875.

Baraloto, C. et al. 2010. Decoupled leaf and stem economics in rain forest trees. - Ecol. Lett. 13: 1338–1347.

Barrio, I. C. et al. 2013. Alpine ecology in the Iberian Peninsula: What do we know, and what do we need to learn? - Mt. Res. Dev. 33: 437–442.

Barton, K. 2019. MuMIn: Multi-Model Inference. R package version 1.43.15.

Bastin, J.-F. et al. 2017. The extent of forest in dryland biomes. - Science 358: 635–638.

Bastin, J.-F. et al. 2019. The global tree restoration potential. - Science 79: 76–79.

Bates, D. et al. 2015. Fitting linear mixed-effects models using lme4. - J. Stat. Softw. 67: 1-48.

Beguería, S. and Vicente-Serrano, S. M. 2017. SPEI: calculation of the Standardised Precipitation-Evapotranspiration Index. R package version 1.7.

Bell, N. et al. 2018. Spatial patterns of genetic diversity among Australian alpine flora communities revealed by comparative phylogenomics. - J. Biogeogr. 45: 177–189.

Billings, W. D. 1974. Adaptations and origins of alpine plants. - Arct. Alp. Res. 6: 129.

Bjorkman, A. D. et al. 2018. Tundra Trait Team: A database of plant traits spanning the tundra biome. - Glob. Ecol. Biogeogr. 27: 1402–1411.

Borcard, D. et al. 1992. Partialling out the spatial component of ecological variation. - Ecology 73: 1045–1055.

Boyle, B. et al. 2013. The taxonomic name resolution service: an online tool for automated standardization of plant names. - BMC Bioinformatics 14: 16.

Bradley, Z. C. et al. 2017. Observed long-term greening of alpine vegetation - a case study in the French Alps. - Environ. Res. Lett. 12: 114006.

Brand, R. F. et al. 2015. A phytosociology survey and vegetation description of inselbergs in the uKhahlamba-Drakensberg Park World Heritage Site, South Africa. - Koedoe 57: 1–12.

Brand, R. F. et al. 2019. The alpine flora on inselberg summits in the Maloti-Drakensberg Park, KwaZulu-Natal, South Africa. - Bothalia 49: 1–15.

Bruelheide, H. et al. 2018. Global trait–environment relationships of plant communities. - Nat. Ecol. Evol. 2: 1906–1917.

Bruelheide, H. et al. 2019. sPlot – A new tool for global vegetation analyses. - J. Veg. Sci. 30: 161–186.

Brummitt, N. et al. 2020. Areas of plant diversity — What do we know ? - Plants, People, Planet: 1–12.

Bruun, H. H. et al. 2006. Effects of altitude and topography on species richness of vascular plants, bryophytes and lichens in alpine communities. - J. Veg. Sci. 17: 37.

Carbutt, C. 2019. The Drakensberg Mountain Centre: a necessary revision of southern Africa's high-elevation centre of plant endemism. - South African J. Bot. 124: 508-529.

Carbutt, C. and Edwards, T. J. 2015. Reconciling ecological and phytogeographical spatial boundaries to clarify the limits of the montane and alpine regions of sub-Sahelian Africa. - South African J. Bot. 98: 64–75.

Carmona, C. P. 2019. TPD: Methods for Measuring Functional Diversity Based on Trait Probability Density. R package version 1.1.0.

Carmona, C. P. et al. 2016. Traits without borders: integrating functional diversity across scales. - Trends Ecol. Evol. 31: 382–394.

Chaboureau, A. C. et al. 2014. Tectonic-driven climate change and the diversification of angiosperms. - Proc. Natl. Acad. Sci. U. S. A. 111: 14066–14070.

Chao, A. et al. 2014. Rarefaction and extrapolation with Hill numbers: a framework for sampling and estimation in species diversity studies. - Ecol. Monogr. 84: 45–67.

Chase, J. 2012. Historical and contemporary factors govern global biodiversity patterns. - PLoS Biol. 10: 1–2.

Chytrý, M. et al. 2007. Plant species richness in continental southern Siberia: effects of pH and climate in the context of the species pool hypothesis. - Glob. Ecol. Biogeogr. 16: 668–678.

Chytrý, M. et al. 2012. High species richness in hemiboreal forests of the northern Russian

Altai, southern Siberia. - J. Veg. Sci. 23: 605–616.
Chytrý, M. et al. 2019. A modern analogue of the Pleistocene steppe-tundra ecosystem in southern Siberia. - Boreas 48: 36–56.
Cieraad, E. et al. 2014. Southern Hemisphere temperate tree lines are not climatically depressed. - J. Biogeogr. 41: 1456–1466.
Cihlar, J. et al. 1991. Relation between the normalized difference vegetation index and ecological variables. - Remote Sens. Environ. 35: 279–298.
Crisp et al. 2001. Endemism in the Australian flora. - J. Biogeogr. 28: 183–198.
Daru, B. H. et al. 2017. Understanding the processes underpinning patterns of phylogenetic regionalization. - Trends Ecol. Evol. 32: 845–860.
Daru, B. H. et al. 2018. Unravelling the evolutionary origins of biogeographic assemblages. - Divers. Distrib. 24: 313–324.
Development, Q. 2016. Qgis geographic information system. open source geospatial foundation project.
Díaz, S. et al. 2016. The global spectrum of plant form and function. - Nature 529: 167–171.
Ding, W. N. et al. 2020. Ancient orogenic and monsoon-driven assembly of the world's richest temperate alpine flora. - Science 369: 578–581.
Dolezal, J. et al. 2016. Vegetation dynamics at the upper elevational limit of vascular plants in Himalaya. - Sci. Rep. 6: 1–13.
Dolezal, J. et al. 2019. Functionally distinct assembly of vascular plants colonizing alpine cushions suggests their vulnerability to climate change. - Ann. Bot. 123: 569–578.
Dormann, C. F. et al. 2007. Methods to account for spatial autocorrelation in the analysis of species distributional data: A review. - Ecography 30: 609–628.
Evangelista, A. et al. 2016. Changes in composition, ecology and structure of high-mountain vegetation: A re-visitation study over 42 years. - AoB Plants 8: 1–11.
Faber-Langendoen, D. et al. 2016. Classification and description of world formation types. - Gen. Tech. Rep. RMRS-GTR-346. Fort Collins, CO: U.S. Department of Agriculture, Forest Service, Rocky Mountain Research Station.
Farr, T. G. et al. 2007. The shuttle radar topography mission. - Rev. Geophys. 45: 1–33.
Favre, A. et al. 2015. The role of the uplift of the Qinghai-Tibetan Plateau for the evolution of Tibetan biotas. - Biol. Rev. Camb. Philos. Soc. 90: 236–253.
Fazayeli, F. et al. 2014. Uncertainty quantified matrix completion using bayesian hierarchical matrix factorization. - 2014 13th Int. Conf. Mach. Learn. Appl.: 312–317.
Fernández-Palacios, J. M. et al. 2016. Towards a glacial-sensitive model of island biogeography. - Glob. Ecol. Biogeogr. 25: 817–830.
Fernández-Pascual, E. et al. 2020. The seed germination spectrum of alpine plants: a global meta-analysis. - New Phytol. 229: 3573-3586.
Ferrier, S. et al. 2007. Using generalized dissimilarity modelling to analyse and predict patterns of beta diversity in regional biodiversity assessment. - Divers. Distrib. 13: 252–264.

Flantua, S. G. A. et al. 2019. The flickering connectivity system of the north Andean páramos. - J. Biogeogr. 46: 1808–1825.

Flantua, S. G. A. et al. 2020. Snapshot isolation and isolation history challenge the analogy between mountains and islands used to understand endemism. - Glob. Ecol. Biogeogr.: 1–23.

Freeman, B. G. et al. 2018. Expanding, shifting and shrinking: The impact of global warming on species' elevational distributions. - Glob. Ecol. Biogeogr. 27: 1268–1276.

Gao, Q. et al. 2016. Climatic change controls productivity variation in global grasslands. - Sci. Rep. 6: 1–10.

García Molinos, J. et al. 2019. VoCC: An r package for calculating the velocity of climate change and related climatic metrics. - Methods Ecol. Evol. 10: 2195–2202.

Garnier, E. et al. 2016. Plant functional diversity. - Oxford University Press.

Geange, S. W. et al. 2011. A unified analysis of niche overlap incorporating data of different types. - Methods Ecol. Evol. 2: 175–184.

Geiger, R. et al. 2003. The climate near the ground. - Rowman and Littlefield Publishers.

Givnish, T. J. 2010. Giant lobelias exemplify convergent evolution. - BMC Biol. 8: 2–5.

Givnish, T. J. 2016. Convergent evolution, adaptive radiation, and species diversification in plants. - In: Kilman, R. (ed), Encyclopedia of Evolutionary Biology. Academic Press, pp. 362–373.

Gorelick, N. et al. 2017. Google Earth Engine: Planetary-scale geospatial analysis for everyone. - Remote Sens. Environ. 202: 18–27.

Gottfried, M. et al. 2012. Continent-wide response of mountain vegetation to climate change. - Nat. Clim. Chang. 2: 111–115.

Goulden, M. L. and Bales, R. C. 2014. Mountain runoff vulnerability to increased evapotranspiration with vegetation expansion. - Proc. Natl. Acad. Sci. U. S. A. 111: 14071–14075.

Graham, C. H. et al. 2014. The origin and maintenance of montane diversity: integrating evolutionary and ecological processes. - Ecography 37: 711–719.

Grime, J. P. 1974. Vegetation classification by reference to strategies. - Nature 250: 26–31.

Grime, J. P. 2006. Trait convergence and trait divergence in herbaceous plant communities: Mechanisms and consequences. - J. Veg. Sci. 17: 255–260.

Halloy, S. R. P. and Mark, A. F. 1996. Comparative leaf morphology spectra of plant communities in New Zealand, the Andes and the European Alps. - J. R. Soc. New Zeal. 26: 41–78.

Hansen, M. C. et al. 2013. High-resolution global maps of 21st-century forest cover change. - Science 342: 850–853.

Harris, S. A. 2007. Biodiversity of the alpine vascular flora of the N.W. North American Cordillera: the evidence from phyto-geography. - Erdkunde 61: 344–357.

Harrison, X. A. 2014. Using observation-level randomeffects to model overdispersion in count data in ecology and evolution. - PeerJ 2:e616.

Hartig, F. 2020. DHARMa: residual diagnostics for hierarchical (multi-level / mixed) regression models. R package version 0.3.1.

He, X. et al. 2019. Distributional responses to climate change for alpine species of Cyananthus and Primula endemic to the Himalaya-Hengduan Mountains. - Plant Divers. 41: 26–32.

Heaney, L. R. 2000. Dynamic disequilibrium: a long-term, large-scale perspective on the equilibrium model of island biogeography. - Glob. Ecol. Biogeogr. 9: 59–74.

Hengl, T. et al. 2017. SoilGrids250m: global gridded soil information based on machine learning. - PLoS One 12: 1–40.

Hewitt, G. 2000. The genetic legacy of the quaternary ice ages. - Nature 405: 907–913.

Hillebrand, H. 2004. On the generality of the latitudinal diversity gradient. - Am. Nat. 163: 192–211.

Hoegh-Guldberg, O. et al. 2018. Impacts of 1.5^{o} C global warming on natural and human systems. - In: Masson-Delmotte, V., P. et al. (eds), Global Warming of 1.5°C. An IPCC Special Report on the impacts of global warming of 1.5°C above pre-industrial levels and related global greenhouse gas emission pathways, in the context of strengthening the global response to the threat of climate change,. pp. 175–311.

Holben, B. N. 1986. Characteristics of maximum-value composite images from temporal AVHRR data. - Int. J. Remote Sens. 7: 1417–1434.

Holdridge, L. R. 1947. Determination of world plant formations from simple climatic data. - Science 105: 367–368.

Holt, B. G. et al. 2013. An update of Wallace's zoogeographic regions of the world. - Science 339: 74–78.

Holtmeier, F.-K. 2009. Mountain timberlines. Ecology, patchiness, and dynamics. - Springer Netherlands.

Hope, G. S. et al. 1976. The equatorial glaciers of New Guinea. - A.A. Balkema.

Hörandl, E. and Emadzade, K. 2011. The evolution and biogeography of alpine species in Ranunculus (Ranunculaceae): a global comparison. - Taxon 60: 415–426.

Hsieh, T. C. et al. 2016. iNEXT: an R package for rarefaction and extrapolation of species diversity (Hill numbers). - Methods Ecol. Evol. 7: 1451–1456.

Hughes, L. 2000. Biological consequences of global warming: is the signal already apparent? - Trends Ecol. Evol. 15: 56–61.

Hughes, C. E. and Atchison, G. W. 2015. The ubiquity of alpine plant radiations: From the Andes to the Hengduan Mountains. - New Phytol. 207: 275–282.

IPCC 2019. IPCC Special Report on the Ocean and Cryosphere in a Changing Climate. - Intergov. Panel Clim. Chang.

Isaac, N. J. B. et al. 2004. Taxonomic inflation: its influence on macroecology and conservation. - Trends Ecol. Evol. 19: 464–469.

Ives, A. R. and Helmus, M. R. 2010. Phylogenetic metrics of community similarity. - Am. Nat. 176: 128–142.

Jiménez-Alfaro, B. et al. 2014. Biogeographic deconstruction of alpine plant communities

along altitudinal and topographic gradients. - J. Veg. Sci. 25: 160–171.
Jiménez-Alfaro, B. et al. 2021. Postglacial determinants of regional species pools in alpine grasslands. - Glob. Ecol. Biogeogr.
Karadimou, E. K. et al. 2016. Functional diversity exhibits a diverse relationship with area, even a decreasing one. - Sci. Rep. 6: 1–9.
Karger, D. N. et al. 2017. Climatologies at high resolution for the earth's land surface areas. - Sci. Data 4: 170122.
Karger, D. N. et al. 2019. Why tree lines are lower on islands - Climatic and biogeographic effects hold the answer. - Glob. Ecol. Biogeogr. 28: 839–850.
Kattge, J. et al. 2020. TRY plant trait database – enhanced coverage and open access. - Glob. Chang. Biol. 26: 119–188.
Kaufman, L. and Rousseeuw, P. J. 1990. Finding groups in data: An introduction to cluster analysis. - Wiley.
Keil, P. and Chase, J. M. 2019. Global patterns and drivers of tree diversity integrated across a continuum of spatial grains. - Nat. Ecol. Evol. 3: 390–399.
2020. IUCN Global Ecosystem Typology 2.0: Descriptive profiles for biomes and ecosystem functional groups (DA Keith, JR Ferrer-Paris, E Nicholson, and RT Kingsford, Eds.). - IUCN.
Kembel, S. W. et al. 2010. Picante: R tools for integrating phylogenies and ecology. - Bioinformatics 26: 1463–1464.
Kier, G. et al. 2005. Global patterns of plant diversity and floristic knowledge. - J. Biogeogr. 32: 1107–1116.
Koenker, R. 2018. Quantreg: quantile regression. R package version 5.36.
Köppen, W. 1936. Das geographische system der klimate. - In: Koppen, W. and Geiger, G. (eds), Handbuch der Klimatologie. Borntraeger, pp. 1–44.
Körner, C. 1995. Alpine plant diversity: a global survey and functional interpretations. - In: Chapin III, F. S. and Körner, C. (eds), Arctic and alpine biodiversity: patterns, causes and ecosystem consequences. Springer-Verlag, pp. 45–62.
Körner, C. 2003. Alpine plant life. Functional plant ecology of high mountain ecosystems. - Springer-Verlag Berlin Heidelberg.
Körner, C. 2012. Alpine treelines: Functional ecology of the global high elevation tree limits. - Springer.
Körner, C. 2020. Plant adaptations to alpine environments. - In: Encyclopedia of the World's Biomes, Volume 1, Section 2: Mountains (Alpine Systems) - Life at the Top. Elsevier Inc., pp. 355–361.
Körner, C. and Paulsen, J. 2004. A world-wide study of high altitude treeline temperatures. - J. Biogeogr. 31: 713–732.
Körner, C. and Spehn, E. M. 2019. Mountain biodiversity: A global assessment. - Routledge.
Körner, C. et al. 1989. Functional morphology of mountain plants. - Flora 182: 353–383.
Körner, C. et al. 2003. A bioclimatic characterisation of Europe's alpine areas. - In: Nagy,

L. et al. (eds), Alpine biodiversity in Europe. pp. 13–28.
Körner, C. et al. 2011. A definition of mountains and their bioclimatic belts for global comparisons of biodiversity data. - Alp. Bot. 121: 73–78.
Körner, C. et al. 2016. Carbon and nitrogen stable isotope signals for an entire alpine flora, based on herbarium samples. - Alp. Bot. 126: 153–156.
Körner, C. et al. 2017. A global inventory of mountains for bio-geographical applications. - Alp. Bot. 127: 1–15.
Kreft, H. et al. 2008. Global diversity of island floras from a macroecological perspective. - Ecol. Lett. 11: 116–127.
Ladouceur, E. et al. 2019. The functional trait spectrum of European temperate grasslands. - J. Veg. Sci. 30: 777–788.
Lamanna, C. et al. 2014. Functional trait space and the latitudinal diversity gradient. - Proc. Natl. Acad. Sci. U. S. A. 111: 13745–13750.
Lauer, W. 1981. Ecoclimatological conditions of the Paramo belt in the tropical high mountains. - Mt. Res. Dev. 1: 209–221.
Lavorel, S. et al. 1997. Plant functional classifications: from general groups to specific groups based on response to disturbance. - Trends Ecol. Evol. 12: 474–478.
Legendre, P. and Legendre, L. 2012. Numerical ecology. - Elsevier.
Lenoir, J. et al. 2010. Cross-scale analysis of the region effect on vascular plant species diversity in southern and northern european mountain ranges. - PLoS One 5: 6–8.
Lenton, T. M. et al. 2012. First plants cooled the Ordovician. - Nat. Geosci. 5: 86–89.
Liancourt, P. et al. 2020. Plant's-eye view of temperature governs elevational distributions. - Glob. Chang. Biol. 26: 4094–4103.
Liang, Q. et al. 2018. Shifts in plant distributions in response to climate warming in a biodiversity hotspot, the Hengduan Mountains. - J. Biogeogr. 45: 1334–1344.
Linder, H. P. 2014. The evolution of African plant diversity. - Front. Ecol. Evol. 2: 1–14.
Liu, S. et al. 2017. Spatiotemporal dynamics of grassland aboveground biomass on the Qinghai-Tibet Plateau based on validated MODIS NDVI. - Sci. Rep. 7: 1–10.
Loarie, S. R. et al. 2009. The velocity of climate change. - Nature 462: 1052–1055.
Lomolino, M. V. 2000. Ecology's most general, yet protean pattern: the species-area relationship. - J. Biogeogr. 27: 17–26.
Lomolino, M. V et al. 2017. Biogeography: biological diversity across space and time. - Sinauer Associates.
Luteyn, J. L. 1999. Páramos: A cheklist of plant diversity, geographical distribution, and botanical literature (TNYBG Press, Ed.).
MacArthur, R. H. and Wilson, E. O. 1967. The theory of island biogeography. - Princeton University Press.
Madriñán, S. et al. 2013. Páramo is the world's fastest evolving and coolest biodiversity hotspot. - Front. Genet. 4: 1–7.
Maechler, M. et al. 2018. cluster: Cluster analysis basics and extensions. R package version 2.0.7-1.

Marks, C. O. and Lechowicz, M. J. 2006. Alternative designs and the evolution of functional diversity. - Am. Nat. 167: 55–66.

McCormack, J. E. et al. 2009. Sky islands. - In: Gillespie, R. G. and Clague, D. (eds), Encyclopedia of islands. University of Chicago Press, pp. 839–843.

McGill, B. J. et al. 2006. Rebuilding community ecology from functional traits. - Trends Ecol. Evol. 21: 178–185.

McGlone et al. 2001. Endemism, species selection and the origin and distribution of the vascular plant flora of New Zealand. - J. Biogeogr. 28: 199–216.

Metzger, M. J. et al. 2013. A high-resolution bioclimate map of the world: A unifying framework for global biodiversity research and monitoring. - Glob. Ecol. Biogeogr. 22: 630–638.

Monasterio, M. 1986. Adaptive strategies of Espeletia in the Andean desert páramo. - In: Monasterio, M. and Villeumier, F. (eds), High altitude tropical biogeography. Oxford University Press, pp. 49–80.

Moncrieff, G. R. et al. 2016. Revising the biome concept for understanding and predicting global change impacts. - J. Biogeogr. 43: 863–873.

Morueta-Holme, N. et al. 2015. Strong upslope shifts in Chimborazo's vegetation over two centuries since Humboldt. - Proc. Natl. Acad. Sci. U. S. A. 112: 12741–12745.

Moser, D. et al. 2005. Environmental determinants of vascular plant species richness in the Austrian Alps. - J. Biogeogr. 32: 1117–1127.

Mucina, L. 2019. Biome: evolution of a crucial ecological and biogeographical concept. - New Phytol. 222: 97–114.

Muellner-Riehl, A. N. et al. 2019. Origins of global mountain plant biodiversity: testing the 'mountain-geobiodiversity hypothesis.' - J. Biogeogr. 46: 2826–2838.

Müllner, D. 2013. fastcluster: Fast hierarchical, agglomerative clustering routines for R and python. - J. Stat. Softw. 59: 1–18.

Myers, N. et al. 2000. Biodiversity hotspots for conservation priorities. - Nature 403: 853–858.

Nagy, L. and Grabherr, G. 2009. The biology of alpine habitats. - Oxford University Press.

Nagy, L. et al. 2003. Alpine Biodiversity in Europe, Ecological Studies. - Springer-Verlag Berlin Heidelberg.

NASA/METI/AIST/Japan Spacesystems, and U. S. /Japa. A. S. T. 2009. ASTER Global Digital Elevation Model [ASTGTM v002]. NASA EOSDIS Land Processes DAAC. Accessed 2019-01-10.

NASA and JPL 2013. NASA Shuttle Radar Topography Mission Global 1 arc second number [SRTMGL1N_003]. NASA EOSDIS Land Processes DAAC. Accessed 2019-01-10.

Noroozi, J. and Körner, C. 2018. A bioclimatic characterization of high elevation habitats in the Alborz mountains of Iran. - Alp. Bot. 128: 1–11.

Oksanen, J. et al. 2019. vegan: Community Ecology Package. R package version 2.5-6.

Olson, D. M. et al. 2001. Terrestrial ecoregions of the world: a new map of life on earth.

- Bioscience 51: 933–938.
Palpurina, S. et al. 2017. The relationship between plant species richness and soil pH vanishes with increasing aridity across Eurasian dry grasslands. - Glob. Ecol. Biogeogr. 26: 425–434.
Panetta, A. M. et al. 2018. Climate warming drives local extinction: Evidence from observation and experimentation. - Sci. Adv. 4: 1–9.
Pärtel, M. and Zobel, M. 1999. Small-scale plant species richness in calcareous grasslands determined by the species pool, community age and shoot density. - Ecography 22: 153–159.
Pärtel, M. et al. 2016. Macroecology of biodiversity: disentangling local and regional effects. - New Phytol. 211: 404–410.
Pauli, H. et al. 2012. Recent plant diversity changes on Europe's mountain summits. - Science 336: 353–355.
Pauli, H. et al. 2015. The GLORIA field manual – standard Multi-Summit approach, supplementary methods and extra approaches. - GLORIA-Coordination, Austrian Academy of Sciences & University of Natural Resources and Life Sciences.
Paulsen, J. and Körner, C. 2014. A climate-based model to predict potential treeline position around the globe. - Alp. Bot. 124: 1–12.
Pellissier, L. et al. 2010. Plant traits co-vary with altitude in grasslands and forests in the European Alps. - Plant Ecol. 211: 351–365.
Peters, R. H. 1976. Tautology in evolution and ecology. - Am. Nat. 110: 1–12.
Pettorelli, N. et al. 2005. Using the satellite-derived NDVI to assess ecological responses to environmental change. - Trends Ecol. Evol. 20: 503–510.
Pomeroy, J. 2015. Research network to track alpine water. - Nat. 521: 32.
Pyankov, V. I. et al. 1999. Leaf structure and specific leaf mass: The alpine desert plants of the Eastern Pamirs, Tadjikistan. - New Phytol. 143: 131–142.
Pyron, R. A. et al. 2015. Phylogenetic niche conservatism and the evolutionary basis of ecological speciation. - Biol. Rev. 90: 1248–1262.
Qian, H. and Ricklefs, R. E. 2000. Large-scale processes and the Asian bias in species diversity of temperate plants. - Nature 407: 180–182.
Qian, H. and Jin, Y. 2016. An updated megaphylogeny of plants, a tool for generating plant phylogenies and an analysis of phylogenetic community structure. - J. Plant Ecol. 9: 233–239.
Quinn, J. A. 2008. Arctic and Alpine Biomes. - Greenwood Publishing Group.
R Core Team 2020. R: A language and environment for statistical computing.
Rahbek, C. et al. 2019a. Building mountain biodiversity: geological and evolutionary processes. - Science 365: 1114–1119.
Rahbek, C. et al. 2019b. Humboldt's enigma: what causes global patterns of mountain biodiversity? - Science 365: 1108–1113.
Raven, P. H. and Axelrod, D. I. 1972. Plate tectonics and Australasian paleobiogeography. - Science 176: 1379–1386.

Richardson, S. J. et al. 2012. Rare species drive local trait diversity in two geographically disjunct examples of a naturally rare alpine ecosystem in New Zealand. - J. Veg. Sci. 23: 626–639.

Ricklefs, R. E. and He, F. 2016. Region effects influence local tree species diversity. - Proc. Natl. Acad. Sci. U. S. A. 113: 674–679.

Rouhan, G. and Gaudeul, M. 2014. Plant taxonomy: a historical perspective, current challenges, and perspectives. - In: Besse P. (eds) Molecular Plant Taxonomy. Methods in Molecular Biology (Methods and Protocols), vol 1115. Humana Press, Totowa, USA.

Sandel, B. et al. 2011. The influence of late Quaternary climate-change velocity on species endemism. - Science 334: 660–664.

Scherrer, D. and Körner, C. 2011. Topographically controlled thermal-habitat differentiation buffers alpine plant diversity against climate warming. - J. Biogeogr. 38: 406–416.

Schrodt, F. et al. 2015. BHPMF - a hierarchical Bayesian approach to gap-filling and trait prediction for macroecology and functional biogeography. - Glob. Ecol. Biogeogr. 24: 1510–1521.

Shan, H. et al. 2012. Gap filling in the plant kingdom - Trait prediction using hierarchical probabilistic matrix factorization. - Proc. 29th Int. Conf. Mach. Learn.

Shugart, H. H. 2005. Remote sensing detection of high elevation vegetation change. - In: Huber, U. M. et al. (eds), Global change and mountain regions. Advances in global change research, vol 23. Springer, pp. 457–465.

Simpson, B. 1983. An historical phytogeography of the high Andean flora. - Rev. Chil. Hist. Nat. 56: 109–122.

Sklenář, P. et al. 2011. Tropical and temperate: Evolutionary history of páramo flora. - Bot. Rev. 77: 71–108.

Sklenář, P. et al. 2014. Island biogeography of tropical alpine floras. - J. Biogeogr. 41: 287–297.

Smith, A. B. et al. 2013. Characterizing scale-dependent community assembly using the functional-diversity-area relationship. - Ecology 94: 2392–2402.

Srivastava, D. S. et al. 2012. Phylogenetic diversity and the functioning of ecosystems. - Ecol. Lett. 15: 637–648.

Stanisci, A. et al. 2020. Functional composition and diversity of leaf traits in subalpine versus alpine vegetation in the Apennines. - AoB Plants 12: 1–11.

Steinbauer, M. J. et al. 2016. Topography-driven isolation, speciation and a global increase of endemism with elevation. - Glob. Ecol. Biogeogr. 25: 1097–1107.

Steinbauer, M. J. et al. 2018. Accelerated increase in plant species richness on mountain summits is linked to warming. - Nature 556: 231–234.

Swenson, N. G. 2014. Functional and Phylogenetic Ecology in R. - Springer.

Testolin, R. et al. 2020. Global distribution and bioclimatic characterization of alpine biomes. - Ecography 43: 779–788.

Thomas, H. J. D. et al. 2019. Traditional plant functional groups explain variation in economic but not size-related traits across the tundra biome. - Glob. Ecol. Biogeogr. 28: 78–95.

Title, P. O. and Bemmels, J. B. 2018. ENVIREM: an expanded set of bioclimatic and topographic variables increases flexibility and improves performance of ecological niche modeling. - Ecography 41: 291–307.

Traba, J. et al. 2017. Realised niche changes in a native herbivore assemblage associated with the presence of livestock. - Oikos 126: 1400–1409.

Visser, V. et al. 2014. Mechanisms driving an unusual latitudinal diversity gradient for grasses. - Glob. Ecol. Biogeogr. 23: 61–75.

Vonlanthen, C. M. et al. 2006. Alpine vascular plant species richness: the importance of daily maximum temperature and pH. - Plant Ecol. 184: 13–25.

Wade, L. K. and McVean, D. N. 1969. Mt Wilhelm studies I. The alpine and subalpine vegetation. - Australian National University, Department of Biogeography.

Walter, H. 1973. Die Vegetation der Erde: in ökologischer Betrachtung: Band I: Die tropischen und subtropischen Zonen. - Gustav Fischer.

Walter, H. and Box, E. 1976. Global classification of natural terrestrial ecosystems. - Vegetatio 32: 75–81.

Wang, Z. et al. 2009. Temperature dependence, spatial scale, and tree species diversity in eastern Asia and North America. - Proc. Natl. Acad. Sci. U. S. A. 106: 13388-13392.

Wang, X. et al. 2013. Phylogenetic and functional diversity area relationships in two temperate forests. - Ecography 36: 883–893.

Weigelt, P. et al. 2013. Bioclimatic and physical characterization of the world's islands. - Proc. Natl. Acad. Sci. U. S. A. 110: 15307–15312.

Weigelt, P. et al. 2016. Late quaternary climate change shapes island biodiversity. - Nature 532: 99–102.

Whittaker, R. H. 1975. Communities and Ecosystems. - Macmillan Publishing Co.

Whittaker, R. J. et al. 2008. A general dynamic theory of oceanic island biogeography. - J. Biogeogr. 35: 977–994.

Whittaker, R. J. et al. 2017. Island biogeography: taking the long view of natures laboratories. - Science 885: 1-7.

Winkworth, R. C. et al. 2005. Evolution of the New Zealand mountain flora: Origins, diversification and dispersal. - Org. Divers. Evol. 5: 237–247.

Wiser, S. K. 2016. Achievements and challenges in the integration, reuse and synthesis of vegetation plot data. - J. Veg. Sci. 27: 868–879.

WMO 2020. Global annual to decadal climate ppdate. Target years: 2020 and 2020-2024. Executive summary.: 1–16.

Wood, S. 2011. Fast stable restricted maximum likelihood and marginal likelihood estimation of semiparametric generalized linear models. - J. R. Stat. Soc. Ser. B 73: 3–36.

Wright, D. H. 1983. Species-energy theory: an extension of species-area theory. - Oikos

41: 496–506.
Wright, I. J. et al. 2004. The worldwide leaf economics spectrum. - Nature 428: 821–827.
Xing, Y. and Ree, R. H. 2017. Uplift-driven diversification in the Hengduan Mountains, a temperate biodiversity hotspot. - Proc. Natl. Acad. Sci. U. S. A. 114: 3444–3451.
You, J. et al. 2018. Response to climate change of montane herbaceous plants in the genus Rhodiola predicted by ecological niche modelling. - Sci. Rep. 8: 1–12.
Zobel, M. 2016. The species pool concept as a framework for studying patterns of plant diversity. - J. Veg. Sci. 27: 8–18.

Appendix 1

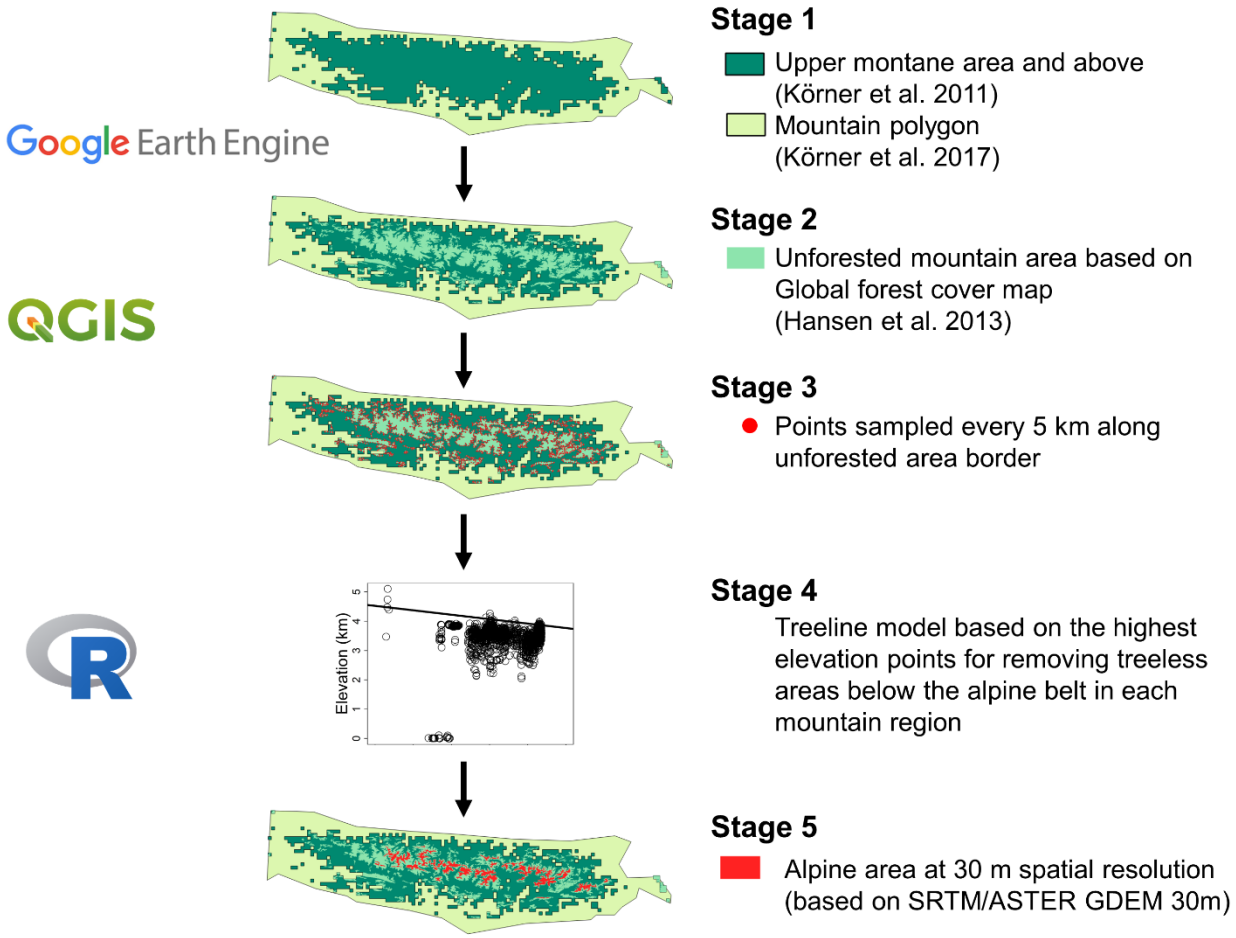

Figure A1.1. Schematic representation of the workflow for modelling the extent of alpine areas based on high-resolution forest cover and mountain inventory data exemplified for a single mountain region.

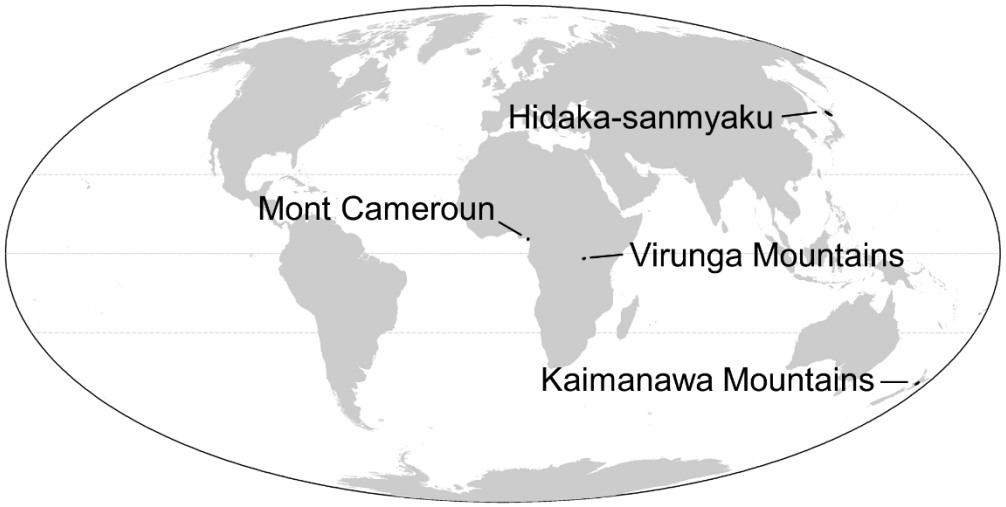

Figure A1.2. Distribution of mountain regions that, despite hosting an alpine belt, were excluded due to the spatial resolution of the present study.

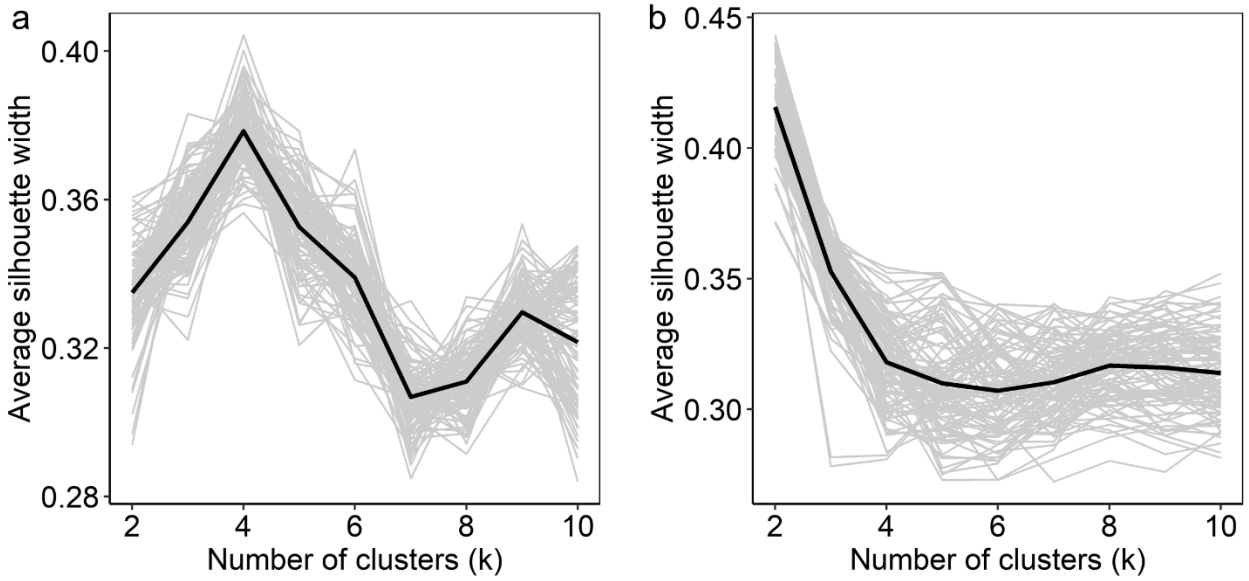

Figure A1.3. Average silhouette widths at different k for (a) the CLARA algorithm and (b) the hierarchical clustering with Ward2 method. The grey lines represent the average widths for each of the 100 random samples. The black line represents the mean of the average.

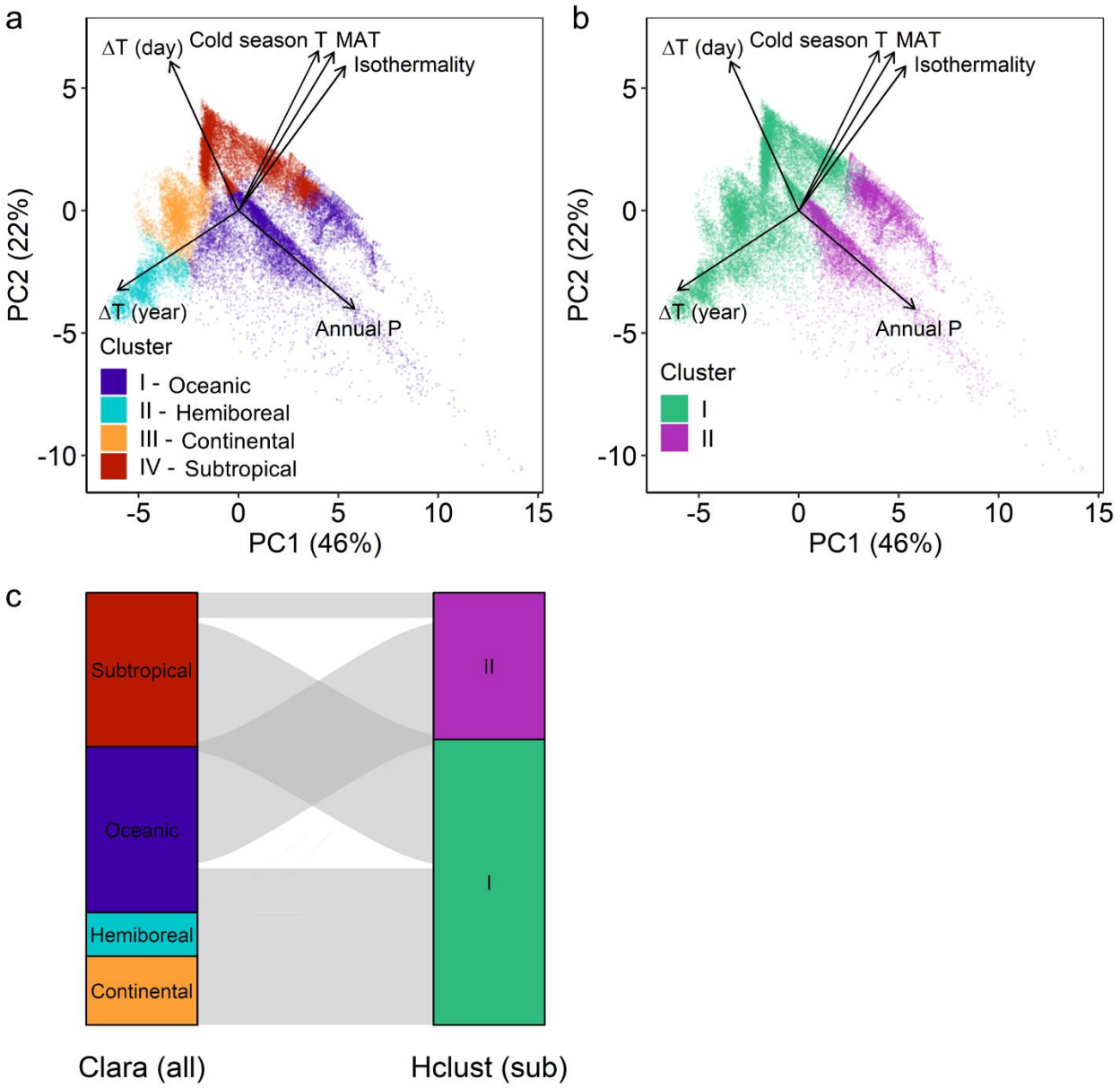

Figure A1.4. Comparison between the hierarchical clustering output of a subsample of 30,000 climatic records and the corresponding clusters defined by the CLARA algorithm at the same locations based on the whole data set. The top panel contains the biplots of the principal component analysis of 19 climatic variables. The arrows indicate the loadings of selected climatic variables (correlation > 0.3 with one of the two axes). Points are coloured according to the clusters as defined by CLARA (a) and the hierarchical clustering (b). Variables names' abbreviations and symbols (MAT: Mean annual temperature, P: Precipitation, T: temperature, Δ: Difference). (c) Alluvial plot representing the correspondence between the two clustering algorithms on the subset. The panels are coloured according to the clusters as reported in (a) and (b).

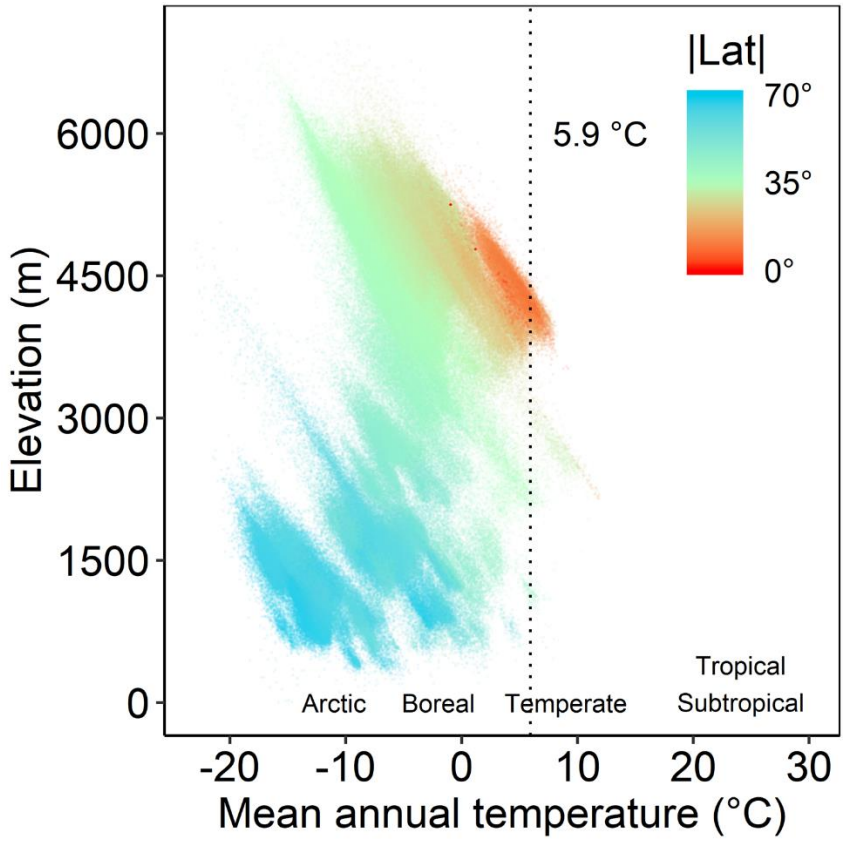

Figure A1.5. Elevation of alpine areas along the temperature gradient. The names at the bottom of the plot indicate major biomes according to Whittaker and are placed close to their mean temperature value. The dotted line represents the 99th percentile of the distribution of temperature values. To improve readability, the figure is based on a random subset of 500,000 30 arc-second cells in alpine areas. Points are colored according to their distance from the equator (|Lat|).

Table A1.1. List of mountain regions for which no or few points were available to model treeline elevation. The mountain regions whose model was used to estimate the former, as well as the model predictors are also provided.

Continent	Mountain ranges	Model	Predictors
Asia	Anyemaqen Shan	Himalaya	Northness + Latitude
	Chola Shan		
	Daban Shan		
	Danghe Nanshan		
	Datong Shan		
	Karakoram		
	Lenglong Ling		
	Ningjing Shan		
	Pamir Mountains		
	Qaidam Shan		
	Qinghai Nanshan		
	Shule Nanshan		
	Tanggula Shan		
	Tergun Daba Shan		
	Tibetan Plateau (Xizang Gaoyuan)		
	Tulai Nanshan		
	Tulai Shan		
	Yema Nanshan		
	Yema Shan		
	Zoulang Nanshan		
	Ferganskiy Khrebet	Khrebet Terskey Alatau	Northness
	Khrebet Kokshaal-Tau		
	Dahei Shan Karlik Shan	Bogda Shan	Northness
	Gichgeniyn Nuruu	Altai Mountains	Northness
	Hangayn Nuruu		
	Horh Uul		
	Agri Dagi	Kuzey Anadolu Daglari / Pontus Mountains	Northness
	Ala Daglari		
	Erciyas Dagi		
	Hakkari Daglari		
	Kuh haye Sabalan		
	Suphan Dagi		
	Eren Habirga Shan	Horo Shan	Northness
	Tien Shan-02	Tien Shan-01	Northness
South America	Altiplano	Cordillera Oriental Peru Bolivia Chile + Cordillera Frontal	Northness + Latitude
	Cordillera de los Frailes		
	Central Volcanic Zone		
	Cerro de Ansilta		
	Cordillera de Lipez		
	Cordillera de Oliva		
	Cordillera de Ollita		
	Cordillera Domeyko		
	Cordillera Frontal		

	Cordillera Occidental Peru Bolivia Chile		
	Cordillera Oriental (Argentina)		
	Cordillera Oriental Peru Bolivia		
	Sierra de Famatina		
	Sierra de la Punilla		
	Sierra de Tatul		
	Sierra del Nevado		
	Sierra Fiambala		
	Sierra Tigre		
	Sierra Tontal		
	Sierra Ambato	Sierra del Alconquija	Northness
	Sierra de Velasco		

Appendix 2

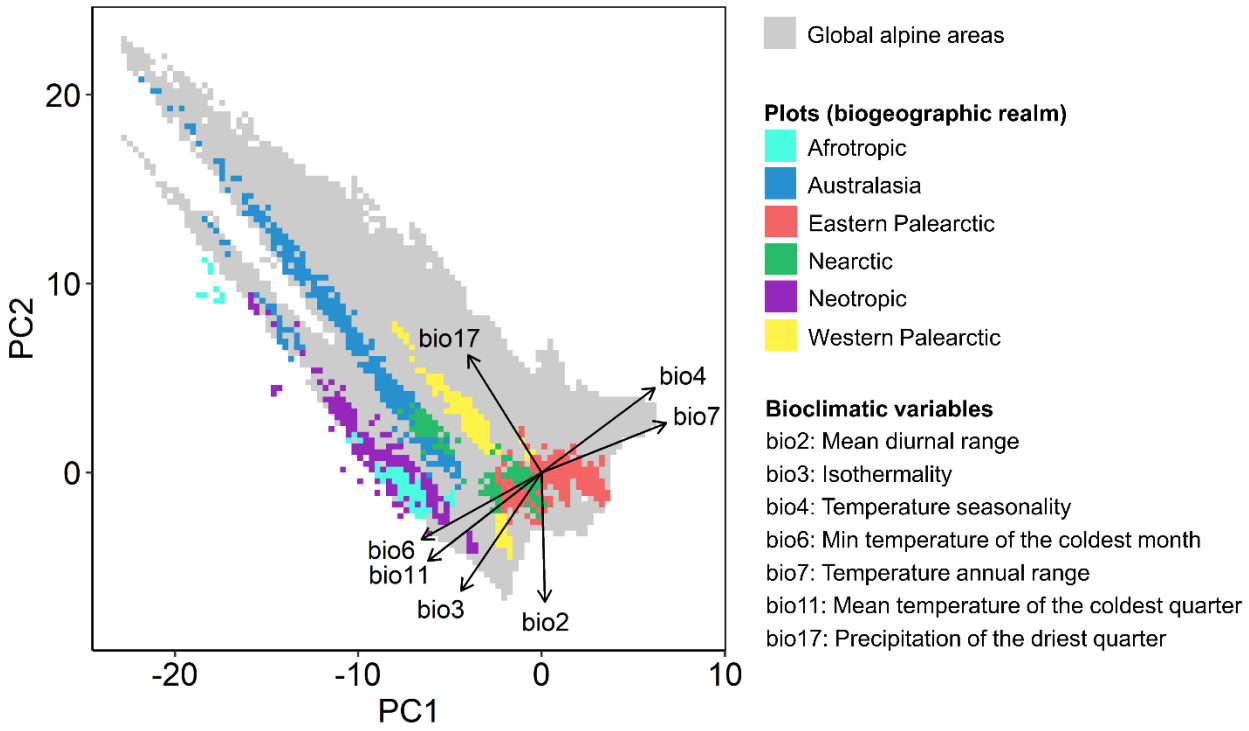

Figure A2.1. Climatic space of vegetation plots against global alpine climatic envelope. The climatic space and envelope are based on a principal component analysis of 19 bioclimatic variables (see Testolin et al., 2020 for information on the delineation of global alpine areas and their bioclimatic characterization). The climatic envelope of global alpine areas also includes the nival belt and unvegetated mountain tops. The arrows indicate the loadings of selected climatic variables (correlation > 0.3 with one of the two axes). Plots are coloured according to biogeographic realms.

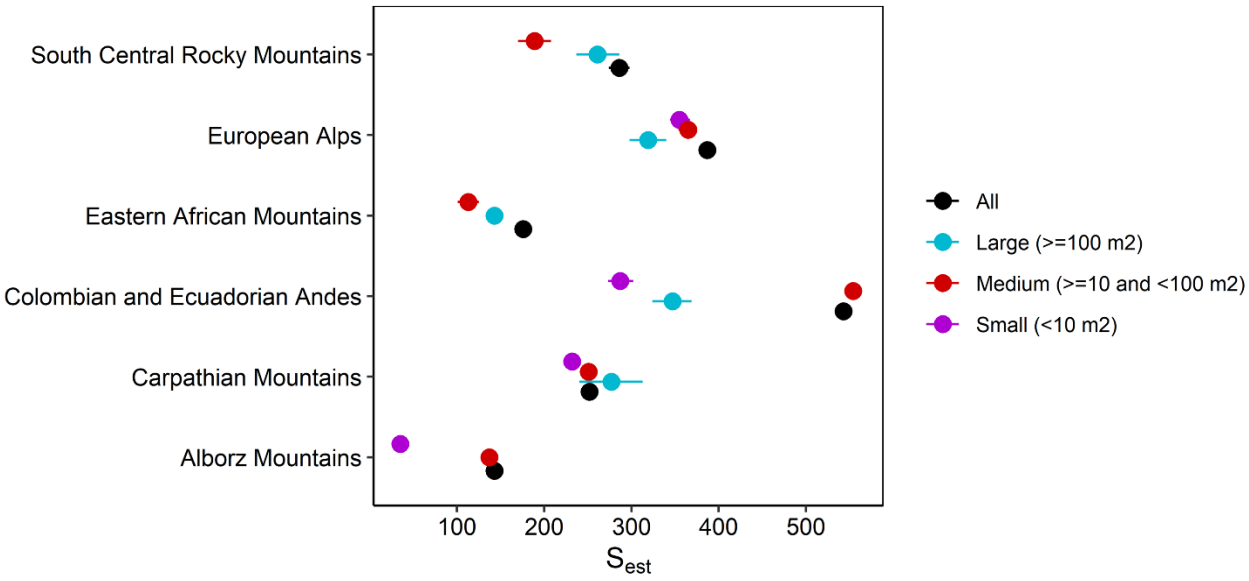

Figure A2.2. Sensitivity analysis of the estimations of regional richness to plot size. Estimates of regional richness (S_{est}) for regions where at least 60 plots of different size classes were available are reported. The dots represent the regional richness estimates. The error bars represent the 95% confidence intervals.

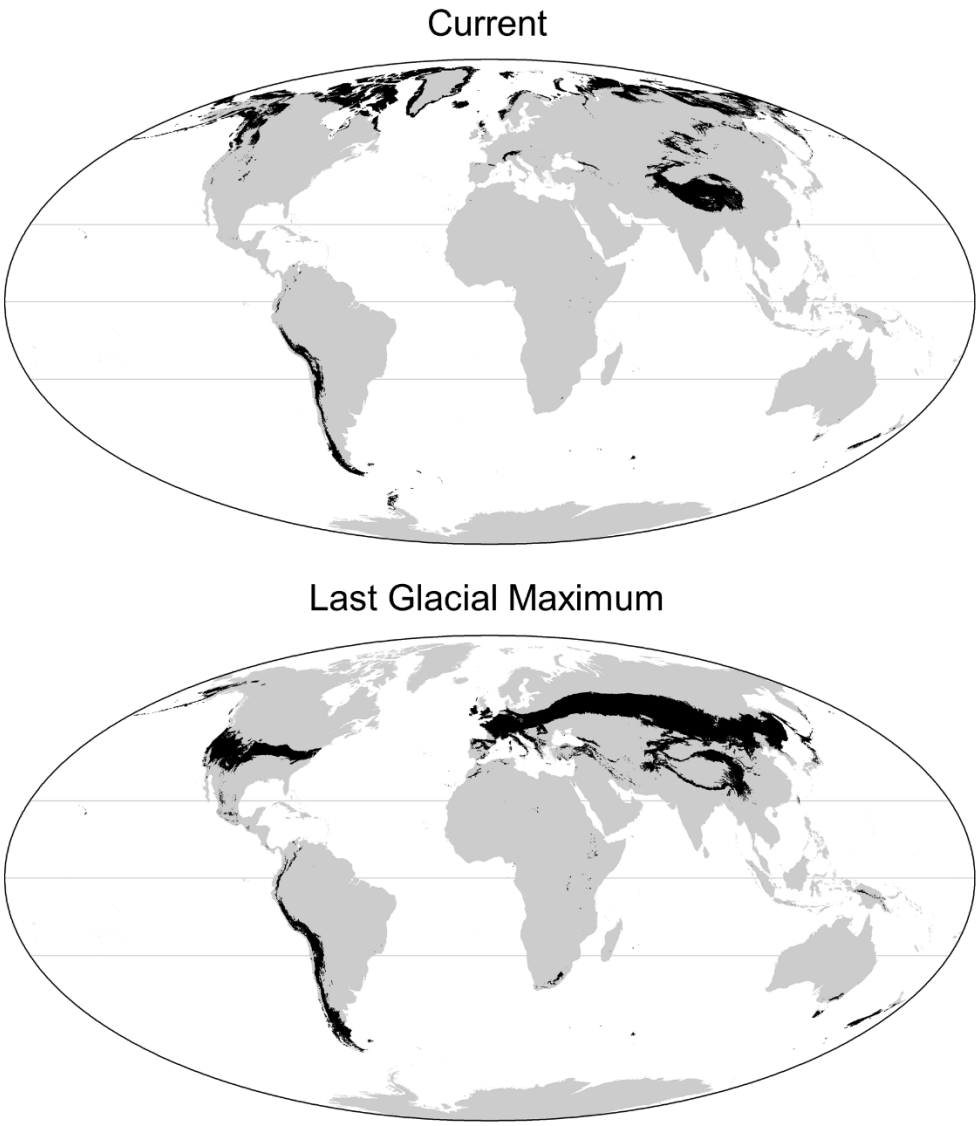

Figure A2.3. Extent of current and Last Glacial Maximum alpine areas. The areas are defined as the portion of land with mean temperature of the growing season between 3.5 and 6.4 °C, or with length of the growing season between 1 and 3 months.

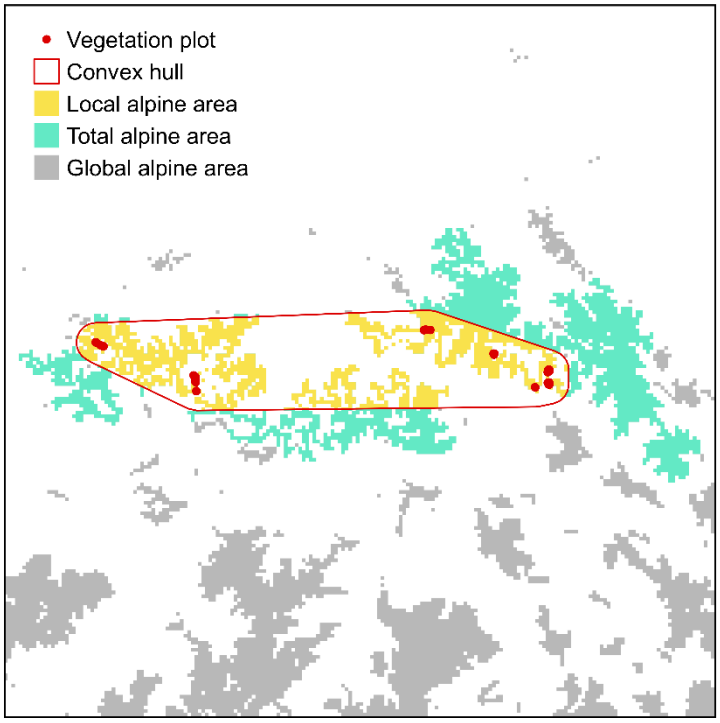

Figure A2.4. Estimation of local and total alpine areas. The extent of the convex hull is based on the spatial distribution of the plots in a certain region (here displayed for Southern Cordillera Oriental Peru). The local area is defined as the extent of alpine area contained within the hull. The total alpine area is defined as the continuous extent of all alpine patches intersected by the hull and reflects the total extent of alpine habitats available to species dispersal.

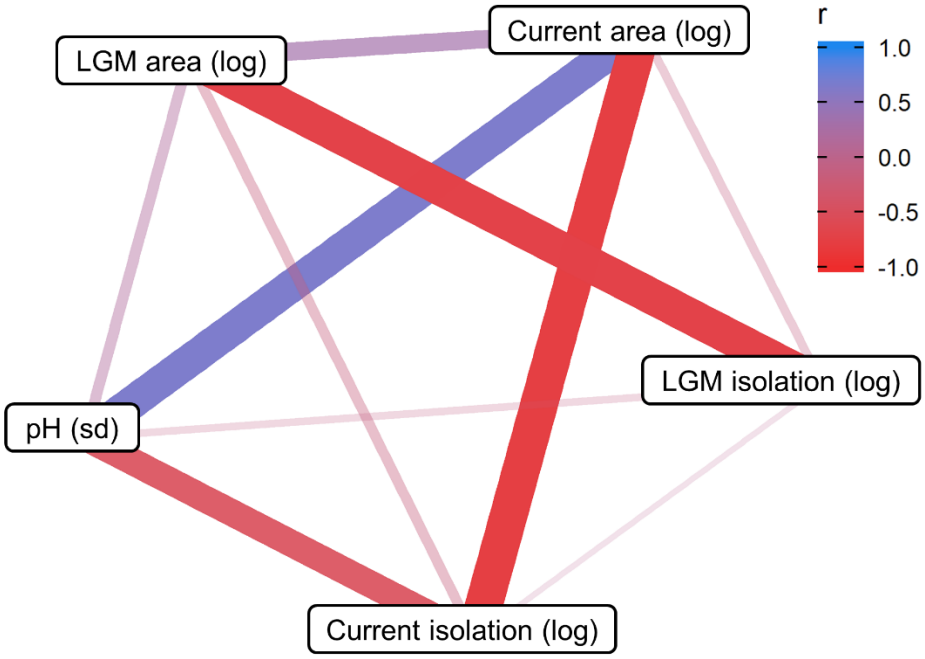

Figure A2.5. Correlations of predictors of regional species richness. r is the Pearson's correlation coefficient. The colour of the lines indicates the strength and the sign of the correlations. The width of the lines indicates the strength of the correlations.

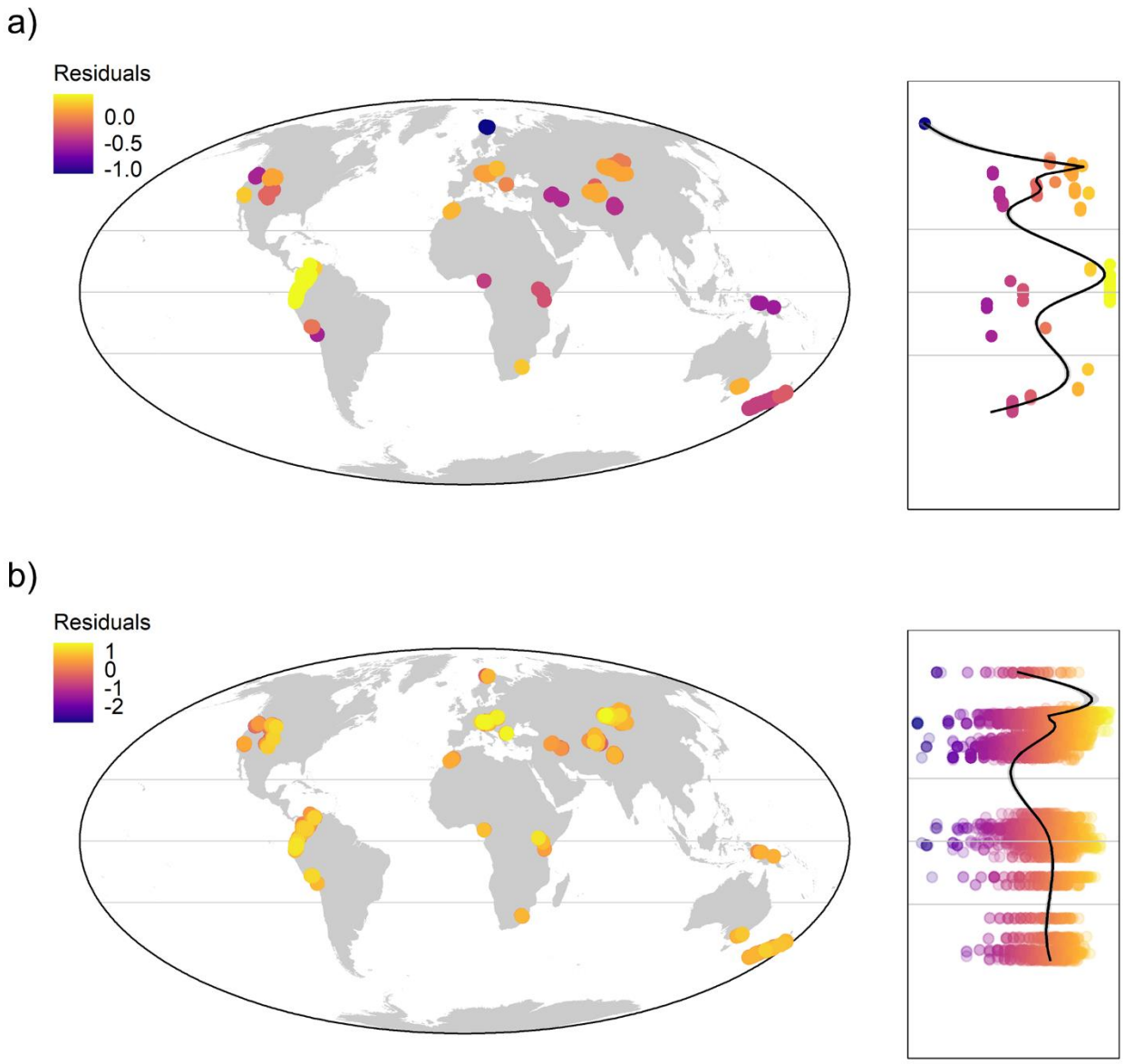

Figure A2.6. Latitudinal patterns of species richness after controlling for local alpine area or plot size. Species richness is expressed as residuals of units of number of species from an ordinary least-squares regression of a) log(regional richness) on log(current local alpine area), and b) log(community richness) on log(plot size). The scatterplots to the right represent the latitudinal trends. The horizontal grey lines in the maps and the scatterplots represent the equator and the tropics. The black lines represent a GAM fit.

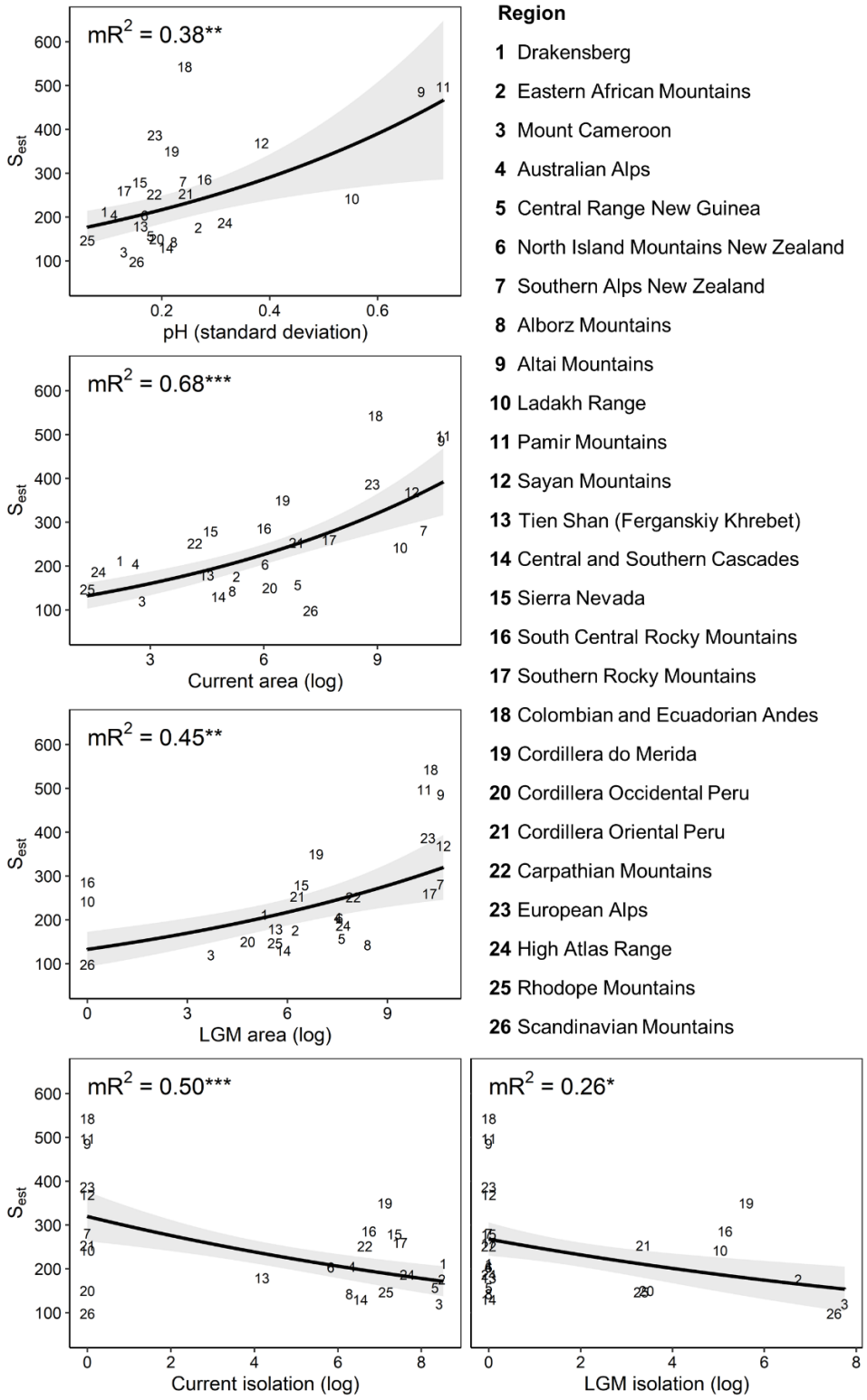

Figure A2.7. Single-predictor models of regional species richness. The numbers represent the regional plant species richness estimated for 180 plots (Sest). Black lines represent the individual GLMM fits. The grey bands are the 95% bootstrap confidence intervals. Marginal R2 (mR2) and model significance are reported. Significance codes: < 0.001 (***); < 0.01 (**); < 0.05 (*).

Table A2.1. Data sources and main habitat types sampled for each mountain region. This description refers to the original data before further filtering process. GIVD code refers to the official name of the database if it has been registered in the Global Index of Vegetation Databases (https://www.givd.info/). For the data provided via sPlot (the Global Vegetation Database http://idiv.de/en/splot), including those provided by the European Vegetation Archive (http://euroveg.org/eva-database), the custodians of individual databases (most of them among the authors) were contacted directly to perform data selection according to the habitats described below (habitat names follow the conventions of each region).

Realm	Name	Ecoregion	Mountains
Afrotropic	Drakensberg	Drakensberg alti-montane grasslands and woodlands	Drakensberg
	Eastern African Mountains	East African montane moorlands	(Great Rift Valley): Kilimanjaro, Mount Elgon
	Mount Cameroon	Mount Cameroon and Bioko montane forests	Mount Cameroon
Australasia	Australian Alps	Australian Alps montane grasslands	Snowy Mountains
	Central Range New Guinea	Central Range sub-alpine grasslands	Bismarck Range, Pegunungan Maoke
	North Island Mountains New Zealand	North Island temperate forests	Kaimanawa Mountains, Kaweka Range, Ruahine Range, Tararua Range
	Southern Alps New Zealand	South Island montane grasslands	(Southern Alps New Zealand): Cameron Mountains, Eyre Mountains, Garvie Mountains, Hector Mountains, Humboldt Mountains, Kaherekoan Mountains, Kaikoura Ranges, Livingstone Mountains, Olivine Range, Princess Mountains, Puketeraki Range, Richmond Range, Rolleston Range, Seaward Kaikoura Range, Spenser Mountains, Takitimu Mountains, Young Range
Eastern Palearctic	Alborz Mountains	Elburz Range forest steppe	Alborz Mountains, Küh-e haye Sabalan, Küh-e Sahand
	Altai Mountains	Altai alpine meadow and tundra	Altai Mountains, Khrebet Listvyaga
	Ladakh Range	Karakoram-West Tibetan Plateau alpine steppe	(Hindukush-Himalaya): Himalaya, Karakorum, Ladakh Range
	Pamir Mountains	Pamir alpine desert and tundra	Alayskiy Khrebet, Gissarskiy Khrebet, Pamir Mountains, Zeravshanskiy Khrebet
	Sayan Mountains	Sayan Alpine meadows and tundra	Kuroyskiy Khrebet, Nagor'ye Sangilen, Tannu Ola, Vostochnyy Sayan,
	Western Tien Shan	Tian Shan montane steppe and meadows	(Tien Shan): Ferganskiy Khrebet

Nearctic	Central and Southern Cascades	Central and Southern Cascades forests	Cascade Range
	Sierra Nevada	Sierra Nevada forests	Sierra Nevada
	South Central Rocky Mountains	South Central Rockies forests	(Rocky Mountains): Absaroka Range, Anaconda Range, Bitterroot Range, Madison Range, Pioneer Mountains, Tobacco Root Mountains
	Southern Rocky Mountains	Colorado Rockies forests	(Rocky Mountains): Flat Tops, Front Range, Sangre de Christo Mountains, San Juan Mountains
Neotropic	Colombian and Ecuadorian Andes	Northern Andean páramo	(Cordillera de los Andes): Cordillera Central Colombia, Cordillera Central Ecuador, Cordillera Oriental Colombia Venezuela, Cordillera Occidental Colombia, Sierra de Perija
	Cordillera de Mérida	Cordillera de Merida páramo	(Cordillera de los Andes): Cordillera de Merida
	Southern Cordillera Occidental Peru	Central Andean Puna	(Cordillera de los Andes): Cordillera Occidental Peru Bolivia Chile
	Southern Cordillera Oriental Peru	Central Andean wet Puna	(Cordillera de los Andes): Cordillera Oriental Peru Bolivia
Western Palearctic	Central and Eastern Alps	Alps conifer and mixed forests	European Alps
	High Atlas Range	Mediterranean High Atlas juniper steppe	(Atlas): Anti-Atlas Range, High Atlas Range
	Northern Scandes	Scandinavian Montane Birch forest and grasslands	Scandinavian Mountains
	Rila	Rhodope montane mixed forests	Rila
	Western Carpathians	Carpathian montane forests	Carpathian Mountains

[1] Wesche, K. (2002) The high-altitude environment of Mt. Elgon (Uganda, Kenya): Climate, vegetation, and the impact of fire. Ecotropical Monographs.

Table A2.2. Details on the delimitation of alpine regions. Plots were grouped based on the approximate extent of ecoregions and named after the main mountain range. Ecoregion names are based on Olson et al. (2001). Mountain names are based in Körner et al. (2017). The names of large-scale mountain ranges encompassing all the others within the same region are reported in brackets.

Realm	Name	Ecoregion	Mountains
Afrotropic	Drakensberg	Drakensberg alti-montane grasslands and woodlands	Drakensberg
	Eastern African Mountains	East African montane moorlands	(Great Rift Valley): Kilimanjaro, Mount Elgon
	Mount Cameroon	Mount Cameroon and Bioko montane forests	Mount Cameroon
Australasia	Australian Alps	Australian Alps montane grasslands	Snowy Mountains
	Central Range New Guinea	Central Range sub-alpine grasslands	Bismarck Range, Pegunungan Maoke
	North Island Mountains New Zealand	North Island temperate forests	Kaimanawa Mountains, Kaweka Range, Ruahine Range, Tararua Range
	Southern Alps New Zealand	South Island montane grasslands	(Southern Alps New Zealand): Cameron Mountains, Eyre Mountains, Garvie Mountains, Hector Mountains, Humboldt Mountains, Kaherekoan Mountains, Kaikoura Ranges, Livingstone Mountains, Olivine Range, Princess Mountains, Puketeraki Range, Richmond Range, Rolleston Range, Seaward Kaikoura Range, Spenser Mountains, Takitimu Mountains, Young Range
Eastern Palearctic	Alborz Mountains	Elburz Range forest steppe	Alborz Mountains, Küh-e haye Sabalan, Küh-e Sahand
	Altai Mountains	Altai alpine meadow and tundra	Altai Mountains, Khrebet Listvyaga
	Ladakh Range	Karakoram-West Tibetan Plateau alpine steppe	(Hindukush-Himalaya): Himalaya, Karakorum, Ladakh Range
	Pamir Mountains	Pamir alpine desert and tundra	Alayskiy Khrebet, Gissarskiy Khrebet, Pamir Mountains, Zeravshanskiy Khrebet
	Sayan Mountains	Sayan Alpine meadows and tundra	Kuroyskiy Khrebet, Nagor'ye Sangilen, Tannu Ola, Vostochnyy Sayan,
	Western Tien Shan	Tian Shan montane steppe and meadows	(Tien Shan): Ferganskiy Khrebet
Nearctic	Central and Southern Cascades	Central and Southern Cascades forests	Cascade Range
	Sierra Nevada	Sierra Nevada forests	Sierra Nevada

	South Central Rocky Mountains	South Central Rockies forests	(Rocky Mountains): Absaroka Range, Anaconda Range, Bitterroot Range, Madison Range, Pioneer Mountains, Tobacco Root Mountains
	Southern Rocky Mountains	Colorado Rockies forests	(Rocky Mountains): Flat Tops, Front Range, Sangre de Christo Mountains, San Juan Mountains
Neotropic	Colombian and Ecuadorian Andes	Northern Andean páramo	(Cordillera de los Andes): Cordillera Central Colombia, Cordillera Central Ecuador, Cordillera Oriental Colombia Venezuela, Cordillera Occidental Colombia, Sierra de Perija
	Cordillera de Mérida	Cordillera de Merida páramo	(Cordillera de los Andes): Cordillera de Merida
	Southern Cordillera Occidental Peru	Central Andean Puna	(Cordillera de los Andes): Cordillera Occidental Peru Bolivia Chile
	Southern Cordillera Oriental Peru	Central Andean wet Puna	(Cordillera de los Andes): Cordillera Oriental Peru Bolivia
Western Palearctic	Central and Eastern Alps	Alps conifer and mixed forests	European Alps
	High Atlas Range	Mediterranean High Atlas juniper steppe	(Atlas): Anti-Atlas Range, High Atlas Range
	Northern Scandes	Scandinavian Montane Birch forest and grasslands	Scandinavian Mountains
	Rila	Rhodope montane mixed forests	Rila
	Western Carpathians	Carpathian montane forests	Carpathian Mountains

Table A2.3. Description of the dataset used in the analyses including, for each region, the number (N) of plots, longitudinal, latitudinal and elevational ranges of the plots, the gradient length of the DCA1 axis expressed in standard deviations of species turnover, the local alpine area and its percentage with respect of the total alpine area of the region.

Realm	Region	N plots	Longitudinal range (°) [min-max]	Latitudinal range (°) [min-max]	Elevational range (m) [min-max (sd)]	DCA1 Length	Local alpine area (1000 * km^2) [(% of total)]
Afrotropic	Drakensberg	91	28.89 – 29.35	-29.08 – -28.74	3020 – 3156 (45)	4.5	0.009 (100)
	Eastern African Mountains	238	34.47 – 37.45	-3.13 – 1.22	3200 – 4710 (272)	3.9	0.196 (100)
	Mount Cameroon	115	9.11 – 9.17	4.14 – 4.22	2151 – 4037 (540)	6.0	0.016 (100)
Australasia	Australian Alps	157	146.64 – 148.39	-37.18 – -36.15	1600 – 2230 (147)	5.8	0.014 (91)
	Central Range New Guinea	91	137.1 – 145.06	-5.8 – -4.04	3810 – 4480 (177)	4.9	0.993 (82)
	North Island Mountains New Zealand	67	175.23 – 176.4	-40.93 – -39.12	1402 – 1882 (77)	3.6	0.42 (98)
	Southern Alps New Zealand	743	166.83 – 173.77	-46.14 – -41.43	1067 – 2185 (163)	3.7	27.682 (97)
Eastern Palearctic	Alborz Mountains	524	46.49 – 52.11	35.85 – 38.31	3014 – 4799 (271)	6.6	0.176 (99)
	Altai Mountains	544	85.8 – 95.91	46.42 – 50.36	1880 – 3221 (218)	6.9	43.792 (79)
	Ladakh Range	452	77.59 – 79.05	32.48 – 34.07	3700 – 5822 (364)	8.6	14.722 (1)
	Pamir Mountains	175	68.17 – 74	37.62 – 39.72	2316 – 4092 (349)	9.9	46.279 (3)
	Sayan Mountains	314	88.86 – 100.73	50 – 52.66	2201 – 2678 (106)	5.7	19.999 (34)
	Western Tien Shan	74	72.83 – 73.05	41.33 – 41.58	2405 – 3063 (189)	3.6	0.089 (77)
Nearctic	Central and Southern Cascades	239	-121.87 – -121.44	45.34 – 46.57	1801 – 2690 (166)	6.0	0.122 (98)
	Sierra Nevada	153	-119.5 – -118.85	37.51 – 38.04	2695 – 3749 (167)	6.0	0.099 (99)
	South Central Rocky Mountains	136	-113.27 – -109.38	44.64 – 46.05	2804 – 3356 (144)	4.9	0.404 (98)
	Southern Rocky Mountains	153	-107.81 – -105.41	36.52 – 40.62	3292 – 4021 (149)	5.5	2.267 (100)
Neotropic	Colombian and Ecuadorian Andes	1534	-79.32 – -72.29	-3.72 – 10.34	2591 – 4851 (417)	9.3	7.679 (99)
	Cordillera de Mérida	74	-72.08 – -70.47	7.95 – 9.1	3076 – 4400 (353)	8.4	0.659 (77)
	Southern Cordillera Occidental Peru	85	-70.77 – -70.53	-16.2 – -16.1	4111 – 4690 (132)	4.9	0.473 (0.1)
	Southern Cordillera Oriental Peru	168	-73.07 – -72.02	-13.29 – -13.14	4062 – 4824 (171)	6.2	0.956 (38)
Western Palearctic	Central and Eastern Alps	684	9.61 – 14.75	46.17 – 47.56	1710 – 3000 (190)	6.9	7.111 (87)
	High Atlas Range	125	-7.63 – -5.59	30.7 – 31.96	2415 – 3955 (404)	7.9	0.005 (100)
	Rila	267	23.31 – 23.73	42.16 – 42.21	1870 – 2805 (139)	4.3	0.004 (100)
	Northern Scandes	76	19.25 – 21.3	69.04 – 69.55	760 – 1316 (109)	5.3	1.39 (65)
	Western Carpathians	1649	18.99 – 20.27	48.88 – 49.25	1450 – 2425 (149)	5.5	0.065 (100)

Table A2.4. GLMMs of regional species richness. For each individual and multivariate model, the scaled coefficients, z-values and p-values of the fixed effects are reported.

Predictor	Coef ± se	z	*p*	mR^2	AICc	Moran's I (*p*)
Null model	-	-	-	-	67	-0.01 (ns)
Individual models - Environment						
Mean temperature of the growing season (mean)	-0.07 ± 0.10	-0.70	ns	-	-	-
Mean temperature of the growing season (sd)	0.08 ± 0.09	0.88	ns	-	-	-
Precipitation of the growing season (mean)	-0.09 ± 0.10	-0.95	ns	-	-	-
Precipitation of the growing season (sd)	0.12 ± 0.08	1.48	ns	-	-	-
Evapotranspiration of the growing season (mean)	0.05 ± 0.10	0.51	ns	-	-	-
Evapotranspiration of the growing season (sd)	0.15 ± 0.09	1.71	ns	-	-	-
Growing degree days (mean)	-0.08 ± 0.10	-0.84	ns	-	-	-
Growing degree days (sd)	0.02 ± 0.09	0.21	ns	-	-	-
pH (mean)	0.06 ± 0.09	0.59	ns	-	-	-
pH (sd)	0.24 ± 0.08	3.06	**	0.38	61	-0.01 (ns)
Topographic position index	-0.08 ± 0.10	-0.83	ns	-	-	-
Terrain ruggedness index	0.04 ± 0.10	0.41	ns	-	-	-
Individual models – Geography and history						
Velocity of climate change	-0.03 ± 0.10	-0.32	ns	-	-	-
Current area (log)	0.33 ± 0.07	4.63	***	0.68	54	-0.05 (ns)
LGM area (log)	0.26 ± 0.08	3.21	**	0.45	61	-0.01 (ns)
Current isolation (log)	-0.26 ± 0.08	-3.48	***	0.50	61	-0.01 (ns)
LGM isolation (log)	-0.20 ± 0.09	-2.19	*	0.26	65	-0.04 (ns)
Biogeographic realm	-	-	ns	-	-	-0.08 (ns)
Multivariate model – Local area						
Current area (log)	0.27 ± 0.07	3.82	***	0.79	52	-0.07 (ns)
LGM area (log)	0.16 ± 0.07	2.30	*			
Multivariate model – Isolation						
Current isolation (log)	-0.25 ± 0.07	-3.59	***	0.67	58	0.01 (ns)
LGM isolation (log)	-0.17 ± 0.07	-2.30	*			

Significance codes: < 0.001 (***); < 0.01 (**); < 0.05(*).

Table A2.5. GLMMs of community species richness. The scaled coefficients, z-values and p-values of the fixed effects are derived from a weighted average of 999 models fit to 999 random subsets of vegetation plots. The average AICc, mR^2 and cR^2 are reported. The average AICc of the corresponding null model with the same random effects structure is reported in brackets.

Random effects	**OLRE + .05° + .1°**			**OLRE + .05° + .1° + Reg**		
Fixed effects	**Coef ± se**	**z**	**p**	**Coef ± se**	**z**	**p**
Mean temperature of the growing season	0.01 ± 0.03	0.59	ns	0.04 ± 0.03	2.39	*
Evapotranspiration of the growing season	0.13 ± 0.05	4.67	***	0.06 ± 0.06	1.82	ns
pH	-0.12 ± 0.05	5.1	***	-0.07 ± 0.05	2.78	*
Topographic position index	-0.01 ± 0.02	1.05	ns	-0.01 ± 0.02	1.17	ns
Terrain ruggedness index	0.02 ± 0.02	1.35	ns	0.02 ± 0.02	1.61	ns
Velocity of climate change	0.10 ± 0.05	4.1	***	0.04 ± 0.13	0.59	ns
Current area (log)	0.00 ± 0.05	0.03	ns	0.05 ± 0.15	0.60	ns
LGM area (log)	0.19 ± 0.05	7.32	***	0.13 ± 0.19	1.37	ns
Biogeographic realm						
Eastern Palearctic	-0.09 ± 0.20	0.84	ns	-0.10 ± 0.46	0.44	ns
Western Palearctic	-0.07 ± 0.18	0.77	ns	-0.05 ± 0.46	0.21	ns
Nearctic	-0.44 ± 0.22	3.89	***	-0.30 ± 0.49	1.20	ns
Australasia	-0.04 ± 0.18	0.38	ns	0.10 ± 0.44	0.46	ns
Neotropic	-0.00 ± 0.18	0.01	ns	0.20 ± 0.45	0.85	ns
Plot size	0.14 ± 0.03	8.05	***	0.15 ± 0.04	7.24	***
AICc	16991 (*null model*: 17244)			16869 (*null model*: 16929)		
mR^2	0.22			0.26		
cR^2	0.58			0.65		

Random effects: OLRE (Observation Level Random Effect. Accounts for overdispersion); .05° + .1° (Group plots belonging to the same 0.05- and 0.1-degree cell, corresponding to about 5 and 10 km. Account for spatial autocorrelation); Reg (Groups plots belonging to the same region. Accounts for the idiosyncratic effect of regions). Significance codes: < 0.001 (***); < 0.01 (**); < 0.05(*).

Appendix 3

Supplementary Text A3.1.

The results reported in the main text are based on the selection of plots with at least 50% cumulative cover of species with trait data. We chose such percentage as a trade-off between inclusion of plots for which trait data were scarce versus the representativeness of dominant vegetation in each community. To assess the robustness of our results against the choice of more conservative cumulative cover thresholds, we repeated part of the analyses on two selections of plots with at least 75% and 90% cumulative cover of species with trait data. This led to a decrease in the number of available plots (75% threshold: 4,196 plots with 1,693 species; 90% threshold: 3,064 plots with 1,340 species), especially in certain groups (Table A3.2), which prevented meaningful comparisons of the trait pools. Therefore, we limited our sensitivity analysis to the patterns and drivers of functional variation among plant communities (see Methods).

Different choices of cumulative cover thresholds did not significantly affect the results and the same patterns emerged as when choosing a 50% threshold (see Results). Regardless of the threshold used, multi-trait dissimilarities of plant communities revealed no distinct patterns among different vegetation zones or climatic groups while, among biogeographic realms, Australasian communities were quite distinct from the others. (Figure A3.2). Vegetation zones explained 8-11% of the functional variation, climatic groups explained 4%, and biogeographic realms explained 11-16%. The lower explanatory power of biogeographic realms compared to the main results obtained using the 50% threshold can be explained by the lower number Australasian plots in the more conservative samples, which are mainly represented by Holarctic communities.

The selected plots were further subset by only keeping those with at least 75% or 90% cumulative cover of species with both phylogenetic and trait data. This led to a further reduction in the number of plots available for the analyses (75% threshold: 3,732 plots with 1,383 species; 90% threshold: 2,447 plots with 1,074 species). However, the model results obtained using both subsets were similar to one another and consistent to those reported in the main text for the 50% threshold. The MRM model explained 12.9-16.4% of the communities' functional dissimilarity. Environmental and phylogenetic dissimilarities individually explained 4.9-7.2% and 4.5-5.6% of the variance, respectively, while 3.5-3.6% was shared between the two. Geographic distance exhibited a marginal effect, explaining only 0.1-0-2% (Figure A3.3).

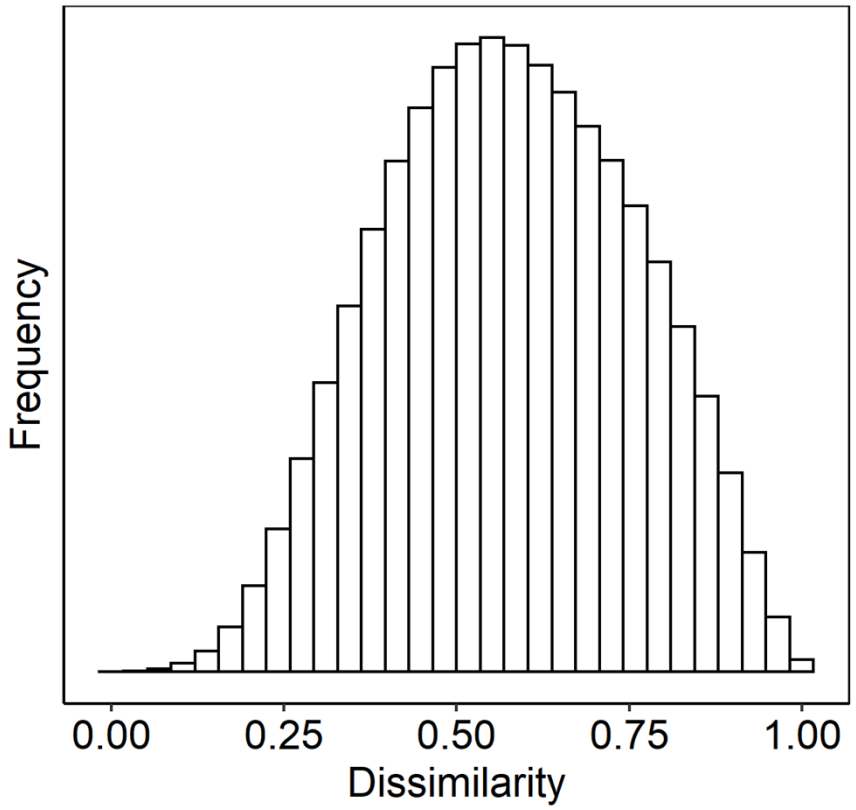

Figure A3.1. Distribution of multi-trait pair-wise functional dissimilarity values among alpine vegetation plots.

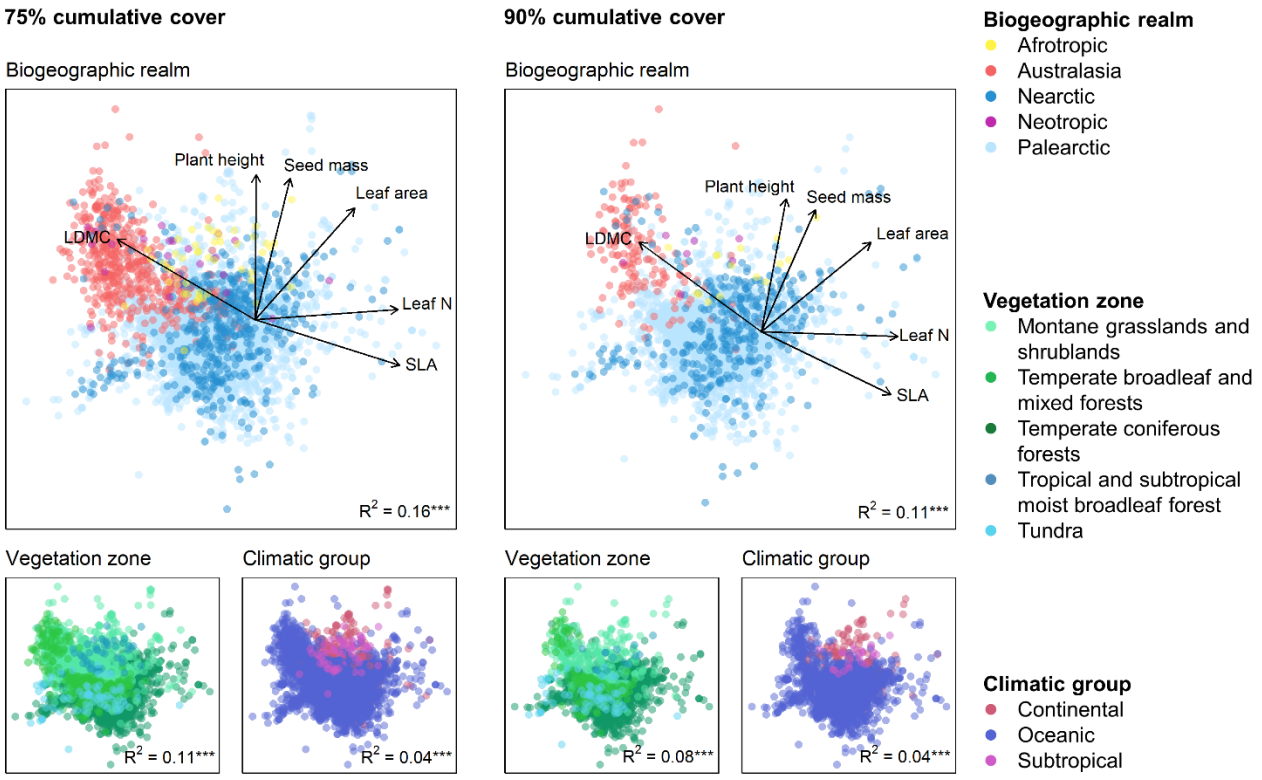

Figure A3.2. Functional variation of alpine plant communities. The two panels represent the results obtained by selecting vegetation plots with at least 75% and 90% cumulative cover threshold of species with trait data. Each dot represents a vegetation plot, whose position is based on community weighted means of the first two axes of a PCA of six functional traits. The arrows represent the trait loadings on the PCA axes. The total variance of community dissimilarity explained by the groups (PERMANOVA) is reported in the bottom-right corner of each graph. SLA = Specific leaf area; LDMC = Leaf dry matter content. Significance codes: ***: $p<0.001$; **: $p< 0.01$; *: $p<0.05$; ns: $p \geq 0.05$.

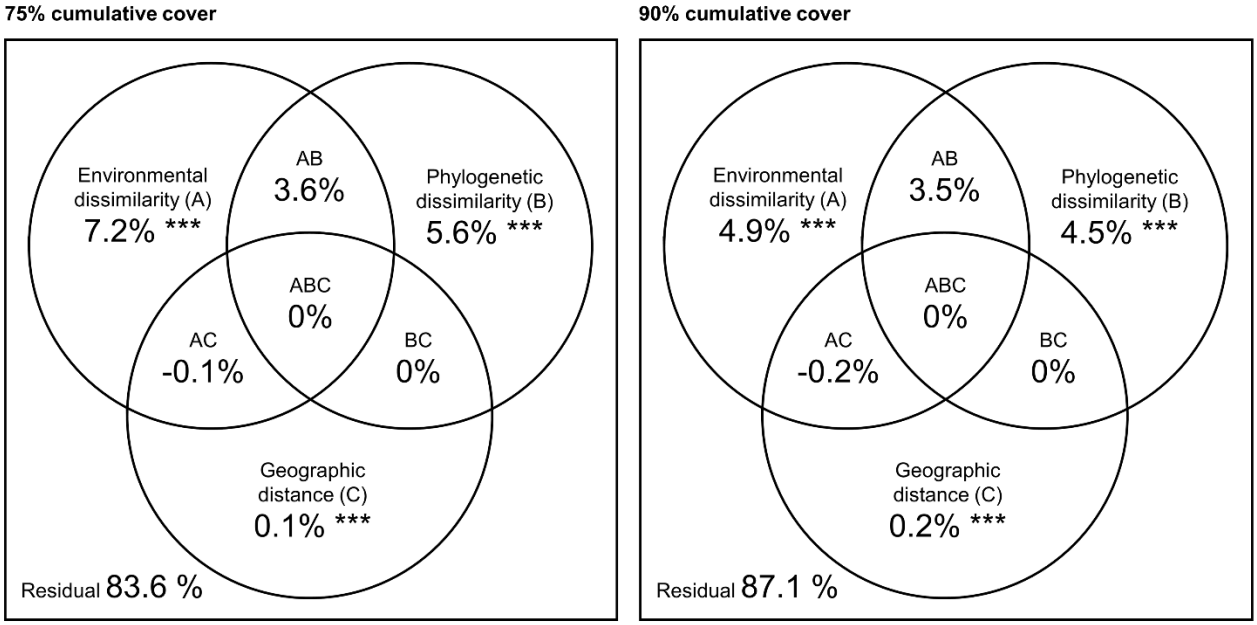

Figure A3.3. Venn diagrams of multi-trait functional dissimilarity of alpine vegetation communities displaying variance partitioning among environmental dissimilarity (A), phylogenetic dissimilarity (B), and geographic distance (C). The two panels represent the results obtained by selecting vegetation plots with at least 75% and 90% cumulative cover threshold of species with trait and phylogenetic data. Significance codes: ***: $p<0.001$; **: $p< 0.01$; *: $p<0.05$; ns: $p \geq 0.05$.

Table A3.1. Data sources and main habitat types for each alpine vegetation dataset. This description refers to the original data before further filtering process. GIVD code refers to the official name of the database if it has been registered in the Global Index of Vegetation Databases (https://www.givd.info/). For the data provided via sPlot (the Global Vegetation Database http://idiv.de/en/splot), including those provided by the European Vegetation Archive (http://euroveg.org/eva-database), the custodians of individual databases (most of them among the authors) were contacted directly to perform data selection according to the habitats described below (habitat names follow the conventions of each region).

Continent	Region	Data description
Africa	Eastern African Mountains	Source: Afroalpine vegetation database (GIVD: AF-00-010; Custodian: Petr Sklenar) via sPlot + personal data from P. Sklenar and Karsten Wesche. Habitats: Aberdare Range: "Alpine bush and shrubland" (Erica arborea - Hebenstretia angolensis community, Senecio jacksonii - Euryops brownei community) and "Alpine grassland" (Alchemilla cyclophylla communities). Mount Elgon: "Alchemilla Dendrosenecio Afroalpine communities" and "Tussock grasslands".
	Eastern African Mountains	Source: personal database of Andreas Hemp for Kilimanjaro. Habitats: "Helichrysum scrub".
	High Atlas Range	Source: Vegetation Database of Southern Morocco (GIVD: AF-MA-001; Custodian: Manfred Finckh) Habitats: Manual selection of dominant "Alpine shrublands" mainly dominated by thorny cushion shrubs.
	Mount Cameroon	Source: Personal database of Jiri Dolezal Habitats: Alpine vegetation, excluding ruderal vegetation, water bodies and bogs.
Asia	Alborz Mountains	Source: Vegetation Database of Iran (GIVD: AS-IR-001; Custodian: Jalil Noroozi) via sPlot. Habitats: "Alpine grasslands", "Alpine rocky vegetation", "Alpine scree vegetation", "Snowbed communities".
	Altai Mountains	Source: personal database of Andrey Korolyuk. Habitats: "Cryophytic steppes", "Grass tundra", "Scrub and semi scrub tundra", "Subalpine and alpine meadows". Plots located at the border of tundra and steppe belts were removed.
	Altai Mountains	Source: personal database of Eugeny Zibzeev and Natalia Makunina Habitats: "Alpine meadows", "Dwarf shrub tundra", "Shrub tundra", "Grass tundra", "Petrophytic communities" and "Snowbed communities".
	Ladakh Range	Source: Personal database of Jiri Dolezal Habitats: Alpine vegetation manually selected from the database, excluding ruderal vegetation, water bodies and bogs.
	Pamir Mountains	Source: Personal database of Arkadiusz Nowak Habitats: Selection of "Alpine screes", "Alpine steppes", "Alpine forb" and "Alpine semi-desert" vegetation above the treeline.
	Sayan Mountains	Source: personal database of Eugeny Zibzeev and Natalia Makunina Habitats: "Alpine meadows", "Dwarf shrubs tundra", "Shrub tundra", "Grass tundra", "Petrophytic communities" and "Snowbed communities".
	Western Tien Shan	Source: Vegetation Database of South-Western Kyrgyzstan (GIVD: AS-KG-001; Custodian: Peter Borchardt) and personal database of Arkadiusz Nowak Habitats: "Alpine meadows" (selected from the database by using the regional treeline) together with "Alpine screes", "Alpine steppes", "Alpine forb" and "Alpine semi-desert" vegetation.

Oceania	Australian Alps	Source: personal database of Keith McDougall. Habitats: “Gravelly pavement herb fields” (community 10), “Snowpatch herbfields” (communities 12, 13), “Closed alpine grasslands” (communities 17, 18, 19), “High altitude grasslands & open heathlands” (communities 20, 21, 22, 24, 25, 26, 27, 28), “Short alpine heathlands”, (communities 39, 40), “High altitude closed heathlands” (communities 46, 47).
	North Island Mountains New Zealand	Source: New Zealand National Vegetation Databank (GIVD: AU-NZ-001; Custodian: Susan Wiser) via sPlot. Habitats: Selected from the database by using the regional treeline to include only alpine vegetation named as “Herbfield”, “Indigenous grassland”, “Indigenous shrubland (incl subshrubs)” and “Tussock grassland”.
	Southern Alps New Zealand	Source: New Zealand National Vegetation Databank (GIVD: AU-NZ-001; Custodian: Susan Wiser) via sPlot. Habitats: Selected from regional treeline to include only alpine vegetation identified as “Herbfield”, “Indigenous grassland”, “Indigenous shrubland (incl subshrubs)” and “Tussock grassland”.
Europe	West Carpathians	Source: European Vegetation Archive (various custodians) via sPlot. Habitats: “Temperate acidophilous alpine grassland” (E4.3b), “Arctic-alpine calcareous grassland” (E4.4a), “Shrub tundra” (F1.1a), “Subarctic and alpine dwarf Salix scrub” (F2.1) and “Alpine and subalpine ericoid heath” (F2.2a).
	Central and Eastern Alps	Source: European Vegetation Archive (various custodians) via sPlot. Habitats: Based on EUNIS expert-system classification and regional treeline, selecting “Vegetated snow-patch” (E4.1), “Temperate acidophilous alpine grassland” (E4.3b), “Arctic-alpine calcareous grassland” (E4.4a), “Shrub tundra” (F1.1a) and “Alpine and subalpine ericoid heath” (F2.2a).
	Rila	Source: European Vegetation Archive (various custodians) via sPlot. Habitats: “Vegetated snow-patch” (E4.1), “Temperate acidophilous alpine grassland” (E4.3b), “Alpine and subalpine calcareous grassland of the Balkan and Apennines” (E4.4b), “Shrub tundra” (F1.1a) and “Alpine and subalpine Juniperus scrub” (F2.2b).
	Northern Scandes	Source: The Nordic Vegetation Database (GIVD: EU-00-018; Custodian: Jonathan Lenoir) via sPlot. Habitats: “Vegetated snow-patch” (E4.1), “Boreal and arctic acidophilous alpine grassland” (E4.3a), “Shrub tundra (F1.1a, b), “Subarctic and alpine dwarf Salix scrub” (F2.1) and Alpine and subalpine ericoid heath (F2.2a).
North America	Central and Southern Cascades	Source: VegBank, the vegetation plot archive of the ESA (GIVD: NA-US-002; Custodian: Robert Peet) via sPlot. Habitats: manually selected from the database based on treeline elevation and community composition, then assigned to “Alpine” and “Open vegetation - probably alpine” habitats.
	Sierra Nevada	Source: VegBank, the vegetation plot archive of the ESA (GIVD: NA-US-002; Custodian: Robert Peet) via sPlot. Habitats: manually selected from the database based on treeline elevation and community composition, then assigned to “Alpine” and “Open vegetation - probably alpine” habitats.
	Sierra Nevada	Source: Personal database of George Malanson Habitats: “Alpine grasslands” and “Alpine scrub”, excluding wetlands. Archived at ir.uiowa.edu.

	South Central Rocky Mountains	Source: VegBank, the vegetation plot archive of the ESA (GIVD: NA-US-002; Custodian: Robert Peet) via sPlot. Habitats: manually selected from the database based on treeline elevation and community composition, then assigned to “Alpine” and “Open vegetation - probably alpine” habitats.
	South Central Rocky Mountains	Source: Personal database of George Malanson Habitats: “Alpine grasslands” and “Alpine scrub”, excluding wetlands. Archived at ir.uiowa.edu.
	Southern Rocky Mountains	Source: VegBank, the vegetation plot archive of the ESA (GIVD: NA-US-002; Custodian: Robert Peet) via sPlot. Habitats: manually selected from the database based on treeline elevation and community composition, then assigned to “Alpine” and “Open vegetation - probably alpine” habitats.
	Southern Rocky Mountains	Source: Personal database of George Malanson Habitats: “Alpine grasslands” and “Alpine scrub”, excluding wetlands. Archived at ir.uiowa.edu.
South America	Colombian and Ecuadorian Andes	Source: VegParamo (GIVD: SA-00-002; Custodian: Gwendolyn Peyre) via sPlot. Habitats: Paramo and Superparamo, including grass-like habitats, rocky and scree afroalpine vegetation.

Table A3.2. Number of plots belonging to different vegetation zones, climatic groups and biogeographic realms selected according to two cumulative cover thresholds of species with trait data.

	75% threshold (number of plots)	**90% threshold (number of plots)**
Vegetation zone		
Montane grasslands and shrublands	931	294
Temperate broadleaf and mixed forests	299	174
Temperate coniferous forests	2849	2514
Tropical and subtropical moist broadleaf forests	47	15
Tundra	70	67
Climatic group		
Continental	507	188
Oceanic	3597	2845
Subtropical	92	31
Biogeographic realm		
Afrotropic	49	15
Australasia	522	155
Nearctic	503	356
Neotropic	26	7
Palearctic	3096	2531

Table A3.3. Correlations of single traits with the first two PCA axes. SLA = Specific leaf area; LDMC = Leaf dry matter content.

Traits	PC1	PC2
SLA	0.55	-0.14
Leaf area	0.33	0.49
LDMC	-0.54	0.27
Plant height	-0.05	0.58
Leaf N	0.53	0.09
Seed mass	0.08	0.57

Table A3.4. Pair-wise dissimilarity of alpine vegetation trait pools between vegetation zones, climatic groups and biogeographic realms for 6 plant functional traits.

	SLA	Leaf area	LDMC	Plant height	Leaf N	Seed mass
Vegetation zones						
Montane grasslands and shrublands - Temperate broadleaf and mixed forests	0.08^{ns}	0.09^{ns}	0.04^{ns}	0.12^{ns}	0.06^{ns}	0.13^{*}
Montane grasslands and shrublands - Temperate coniferous forests	0.18^{**}	0.05^{ns}	0.19^{**}	0.20^{**}	0.15^{**}	0.15^{**}
Montane grasslands and shrublands - Tropical and subtropical moist broadleaf forests	0.23^{*}	0.20^{**}	0.17^{ns}	0.25^{**}	0.10^{ns}	0.10^{ns}
Montane grasslands and shrublands - Tundra	0.11^{ns}	0.19^{**}	0.17^{ns}	0.24^{**}	0.09^{ns}	0.25^{**}
Temperate broadleaf and mixed forests - Temperate coniferous forests	0.17^{**}	0.05^{ns}	0.16^{**}	0.10^{ns}	0.21^{**}	0.04^{ns}
Temperate broadleaf and mixed forests - Tropical and subtropical moist broadleaf forests	0.21^{ns}	0.22^{ns}	0.15^{ns}	0.36^{**}	0.12^{ns}	0.09^{ns}
Temperate broadleaf and mixed forests - Tundra	0.16^{ns}	0.12^{ns}	0.17^{ns}	0.13^{ns}	0.09^{ns}	0.13^{ns}
Temperate coniferous forests - Tropical and subtropical moist broadleaf forests	0.06^{ns}	0.20^{ns}	0.06^{ns}	0.45^{**}	0.12^{ns}	0.11^{ns}
Temperate coniferous forests - Tundra	0.15^{ns}	0.16^{ns}	0.24^{**}	0.08^{ns}	0.17^{**}	0.10^{ns}
Tropical and subtropical moist broadleaf forests - Tundra	0.21^{ns}	0.30^{ns}	0.22^{ns}	0.48^{**}	0.11^{ns}	0.18^{ns}
Climatic groups						
Continental - Oceanic	0.10^{**}	0.07^{ns}	0.07^{ns}	0.09^{ns}	0.14^{**}	0.11^{**}
Continental - Subtropical	0.17^{**}	0.09^{ns}	0.08^{ns}	0.31^{**}	0.16^{**}	0.08^{ns}
Oceanic - Subtropical	0.12^{ns}	0.14^{ns}	0.11^{ns}	0.39^{**}	0.05^{ns}	0.16^{**}
Biogeographic realms						
Afrotropic - Australasia	0.36^{*}	0.11^{ns}	0.31^{ns}	0.23^{ns}	0.31^{ns}	0.14^{ns}
Afrotropic - Nearctic	0.06^{ns}	0.12^{ns}	0.04^{ns}	0.41^{**}	0.11^{ns}	0.07^{ns}
Afrotropic - Neotropic	0.40^{**}	0.25^{ns}	0.13^{ns}	0.07^{ns}	0.08^{ns}	0.23^{ns}
Afrotropic - Palearctic	0.03^{ns}	0.12^{ns}	0.04^{ns}	0.43^{**}	0.18^{**}	0.07^{ns}
Australasia - Nearctic	0.34^{**}	0.04^{ns}	0.33^{**}	0.24^{**}	0.40^{**}	0.19^{ns}
Australasia - Neotropic	0.13^{ns}	0.27^{**}	0.30^{ns}	0.25^{**}	0.27^{ns}	0.12^{ns}
Australasia - Palearctic	0.34^{**}	0.05^{ns}	0.30^{**}	0.22^{**}	0.43^{**}	0.16^{**}
Nearctic - Neotropic	0.36^{**}	0.26^{**}	0.12^{ns}	0.40^{**}	0.14^{ns}	0.27^{**}
Nearctic - Palearctic	0.07^{ns}	0.02^{ns}	0.03^{ns}	0.17^{*}	0.09^{ns}	0.06^{ns}
Neotropic - Palearctic	0.38^{**}	0.25^{**}	0.13^{ns}	0.41^{**}	0.18^{**}	0.22^{**}

SLA = Specific leaf area; LDMC = Leaf dry matter content. Significance codes: ***: $p<0.001$; **: $p< 0.01$; *: $p<0.05$; ns: $p \geq 0.05$.

Author contributions

Chapter 1: Global distribution and bioclimatic characterization of alpine biomes. R.T and B.J.-A. conceived the study and developed the methodology. R.T. analysed the data and produced the outputs. R.T and B.J.-A wrote the first manuscript draft, substantially integrated F.A. B.J.-A supervised the study. All the authors discussed the methodology and commented various versions of the manuscript.

Chapter 2: Global patterns and drivers of alpine plant species richness. R. T. and B. J.-A. conceived the study and developed the methodology. P. B., R. F. B, J. D., M. F., A. H., M. K., A. Y. K., J. L., N. M., G. P. M., D. M.-T., J. N., A. N., R. K. P., G. P., J. Š., P. S., S. P. S., K. V., R. V., W. W., S. K. W. and E. G. Z. provided the vegetation plot data. F. M. S. and H. B. facilitated access to the sPlot database. R.T. analysed the data and produced the outputs. R.T and B.J.-A wrote the first manuscript draft. B.J.-A supervised the study. All the authors discussed the methodology and commented on various versions of the manuscript.

Chapter 3: Global functional variation in alpine vegetation. R. T., B. J.-A., L. M., and C. P. C. conceived the study and developed the methodology. P. B., J. D., M. F., A. H., A. Y. K., J. L., N. M., G. P. M., J. N., A. N., R. K. P., G. P., J. Š., P. S., K. V., R. V., S. K. W. and E. G. Z. provided the vegetation plot data. F. M. S. and H. B. facilitated access to the sPlot database. R.T. analysed the data and produced the outputs. R.T and B.J.-A wrote the first manuscript draft. B.J.-A supervised the study. All the authors discussed the methodology and commented on various versions of the manuscript.

Online resources

The data and code used in this thesis are available at the following online repositories:

Chapter 1: Global distribution and bioclimatic characterization of alpine biomes
https://dx.doi.org/10.6084/m9.figshare.11710002

Chapter 2: Global patterns and drivers of alpine plant species richness
https://dx.doi.org/10.6084/m9.figshare.14191268

Chapter 3: Global functional variation in alpine vegetation
https://dx.doi.org/10.6084/m9.figshare.14040152